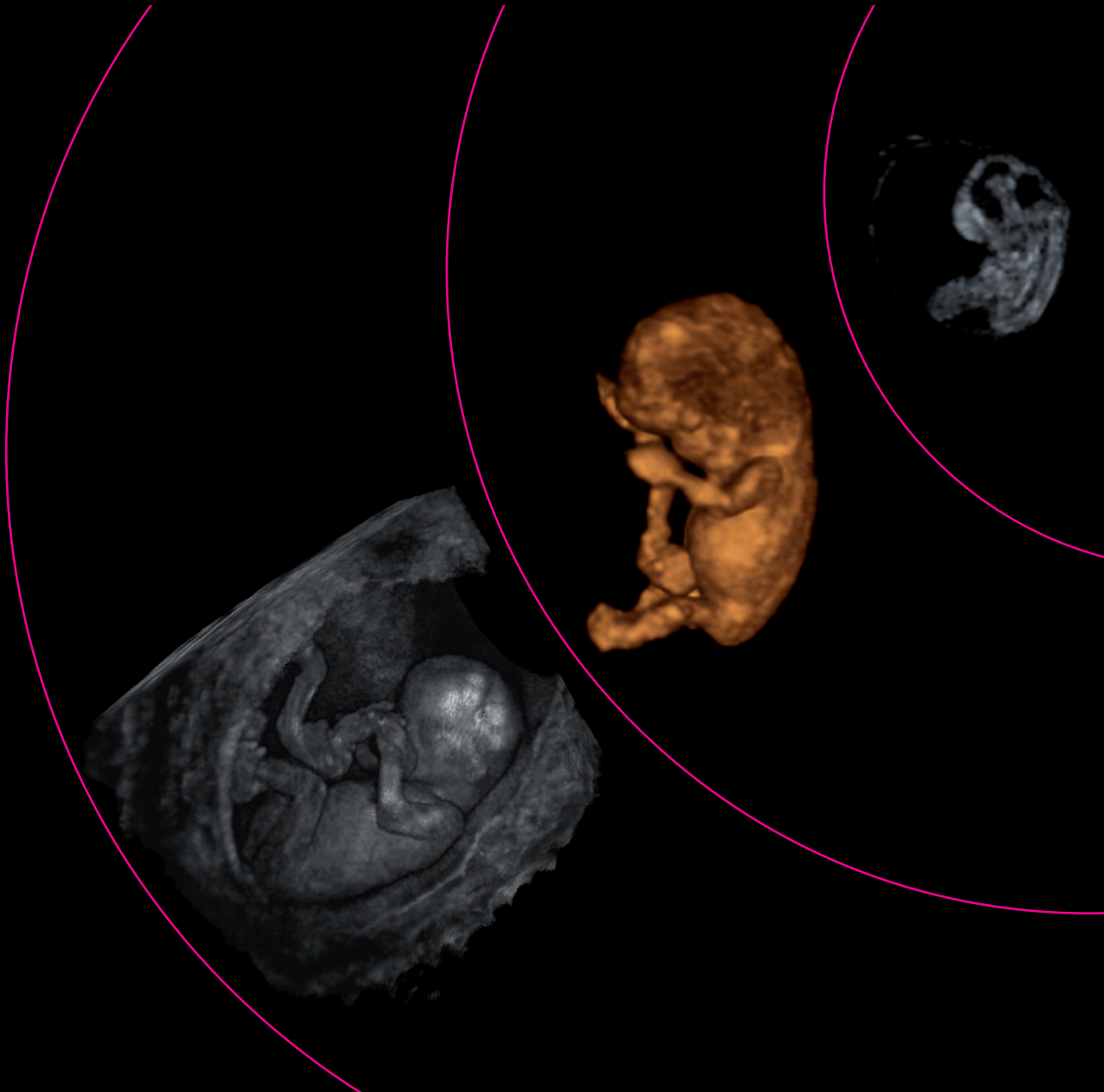


Normal and Abnormal Embryonic Development in Virtual Reality

Leonie Baken



Normal and Abnormal Embryonic Development in Virtual Reality

Leonie Baken

Normal and Abnormal Embryonic Development in Virtual Reality
Thesis, Erasmus University Rotterdam, The Netherlands

The printing of this thesis has been financially supported by the Department of Obstetrics and Gynaecology and the Department of Bioinformatics, Erasmus MC Rotterdam, MPluz, BMA Mosos, Chipsoft, ABN Amro.



Cover design: Leonie Baken
Lay-out: Ridderprint
Printing: Ridderprint

ISBN/EAN: 978-90-5335-946-4
2014© Leonie Baken

No part of this thesis may be reproduced, stored in a retrieval system or transmitted in any form or by any means, without written permission of the author or, when appropriate, of the publishers of the publications.

Normal and Abnormal Embryonic Development in Virtual Reality

Normale en abnormale embryonale ontwikkeling in virtuele realiteit

Proefschrift

ter verkrijging van de graad van doctor aan de
Erasmus Universiteit Rotterdam
op gezag van de rector magnificus

Prof.dr. H.A.P. Pols

en volgens besluit van het College voor Promoties.
De openbare verdediging zal plaatsvinden op
dinsdag 9 december 2014 om 13:30 uur

door
Leonie Baken
geboren te Delft



Promotiecommissie

Promotoren: Prof.dr. E.A.P. Steegers
Prof.dr. P.J. van der Spek

Overige leden: Prof.dr. R.M.W. Hofstra
Prof.dr. D. Tibboel
Prof.dr. D. Oepkes

Copromotoren: Dr. N. Exalto
Dr. A.H.J. Koning

Paranimfen: Vera van den Berg
Jenny Zuidgeest

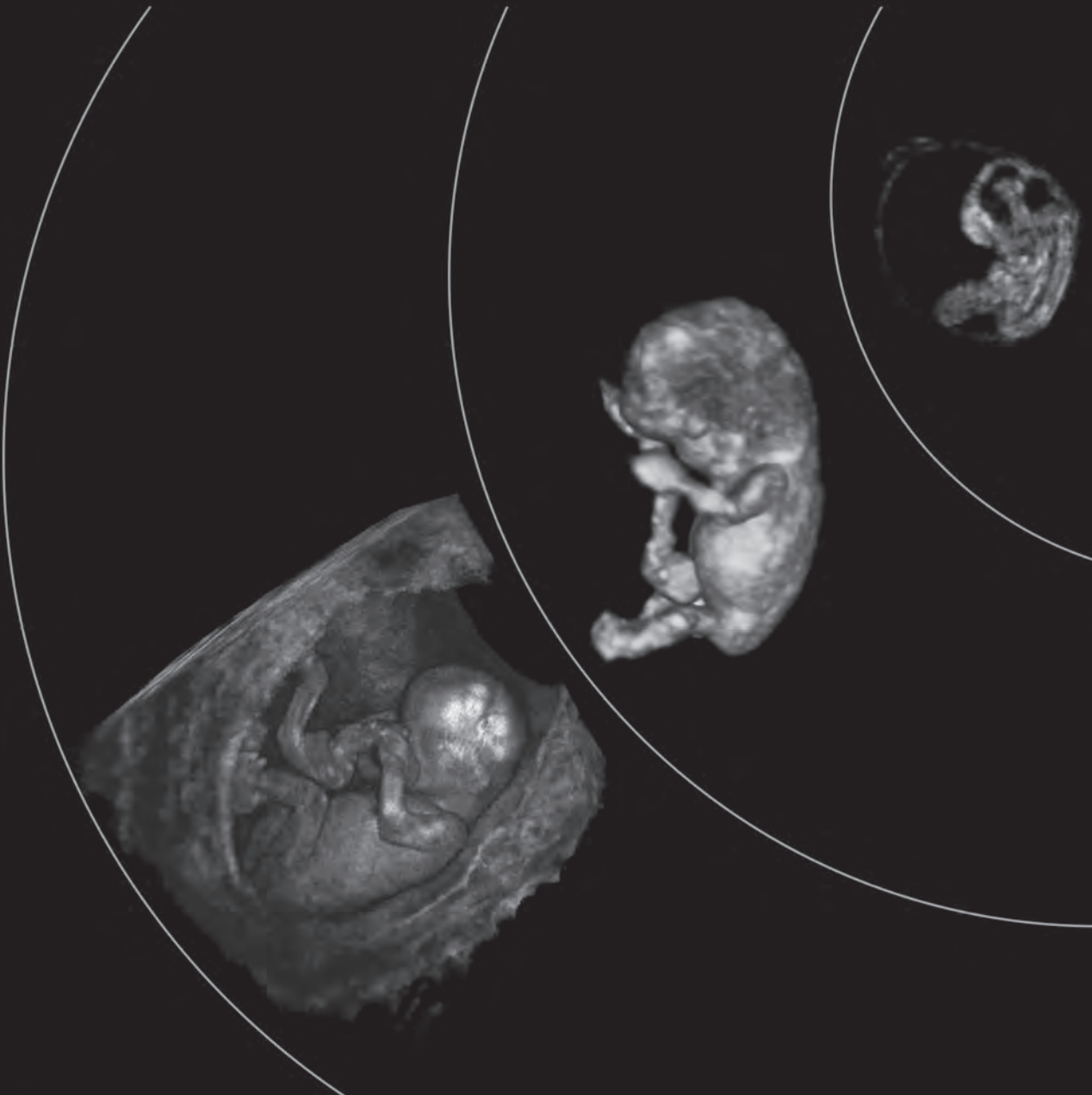
Voor mijn ouders.

Table of Contents

Chapter 1	General Introduction	9
1.1	Introduction	11
1.2	The I-Space Virtual Reality System	19
Chapter 2	New Perspectives on the Virtual Reality Approach	27
2.1	Design and Validation of a 3D Virtual Reality Desktop System for Early Pregnancy Evaluation	29
2.2	First-Trimester Detection of Surfaces Abnormalities: a Comparison of Two- and Three-Dimensional Ultrasound and Three-Dimensional Virtual Reality Ultrasound	45
Chapter 3	Automated Embryonic Volume Measurements in the Detection of Abnormal Embryonic Development	59
3.1	First-Trimester Crown-Rump Length and Embryonic Volume of Fetuses with Structural Congenital Abnormalities measured in Virtual Reality	61
3.2	Crown-Rump Length and Embryonic Volume in Miscarriages measured in Virtual Reality	73
Chapter 4	Biometry and Volumetry in Aneuploid Pregnancies	85
4.1	First-Trimester Hand Measurements in Euploid and Aneuploid Human Fetuses using Virtual Reality	87
4.2	First-Trimester Crown-Rump Length and Embryonic Volume of Aneuploid Fetuses in Virtual Reality	103
Chapter 5	Diagnostic Applicability of the Third Dimension in Embryos and Fetuses with Structural Congenital Abnormalities	113
5.1	Diagnostic Techniques and Criteria for First-Trimester Conjoined Twin Documentation: a Review of the Literature illustrated by Three Recent Cases	115
5.2	First-Trimester Diagnosis of Thrombocytopenia-Absent Radius Syndrome using Virtual Reality	133
5.3	Differentiation of Early First-Trimester Cranial Neural Tube Defects	141
Chapter 6	General Discussion	153
Chapter 7	Summary / Samenvatting	161
Chapter 8	Addendum	169
	Authors and Affiliations	171
	List of Abbreviations	173
	PhD Portfolio	175
	Word of Thanks / Dankwoord	177

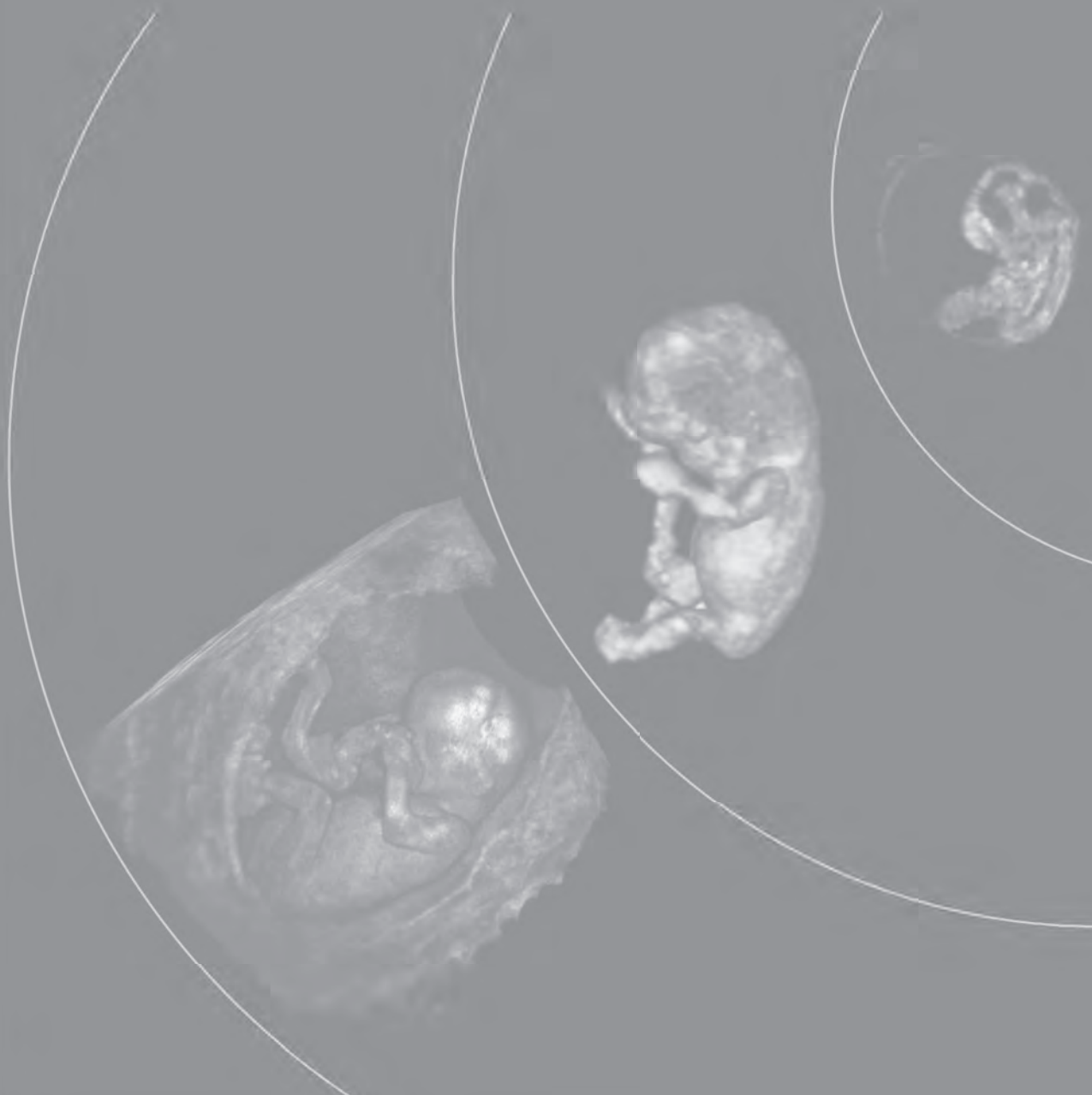
CHAPTER 1

General Introduction



1.1

Introduction



Rationale

Until recently, prenatal care and research focused mainly on fetal growth in the second and third trimester of pregnancy. However, growth and development rates are highest in early pregnancy. This also makes the first-trimester a vulnerable period in which complications of pregnancy might originate.

The past years of research have provided obstetricians with new insights in the early pregnancy and especially in the periconception period.¹ The periconception period comprises gametogenesis, placentation and embryogenesis. The well recognized fetal origins (or Barker's) hypothesis postulates that conditions or exposures during the periconception period influence pregnancy outcome, health during adult life and even future generations.²

First-trimester growth is documented by crown-rump length (CRL) measurements and is used for pregnancy dating. Thereby, it is assumed that first-trimester growth is uniform. We now know that multiple factors, like maternal characteristics and lifestyle, are associated with embryonic and fetal growth.³⁻⁸ In Figure 1 several factors associated with either an increased or a decreased CRL are shown. The study of Mook-Kanamori *et al.* demonstrated that first-trimester growth restriction is associated with an increased risk of adverse pregnancy outcomes.⁶ Recently it was found that impaired first-trimester growth is associated with an adverse cardiovascular risk profile in school age children.⁹

Developmental adaptations to a suboptimal environment, also called fetal programming, arise mainly through the mechanism of epigenetics. Epigenetics is defined by Callinan and Feinberg as "the study of heritable changes other than those in the DNA sequence"; for example DNA methylation and histone modification.¹⁰ An example of an environmental factor leading to epigenetic changes that persist throughout life, is shown in a study on prenatal exposure to famine during the Dutch Hunger

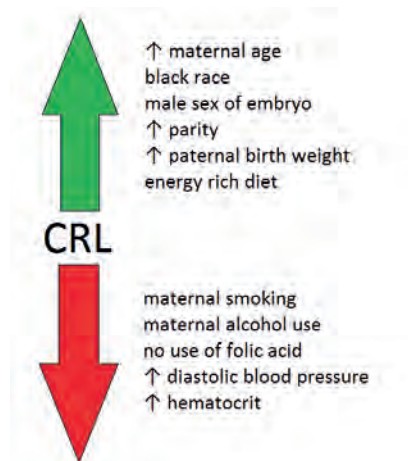


Figure 1: Factors associated with either an increased or a decreased crown-rump length (CRL) during the first-trimester of pregnancy.

Winter in World War II.¹¹ In this study, six decades after the event, an association of lower methylation of a specific gene (IGF2 DMR) and prenatal exposure to famine was found.

These new insights highlight the importance of the early pregnancy period, the recognition of which is essential to improve perinatal outcome. Physicians should acknowledge the importance of embryonic health, both in research and in clinical practice.

Ultrasound

Ultrasound provides an excellent, safe, technical opportunity through which invaluable information about early pregnancy can be obtained. Until the mid-80's first-trimester ultrasound scans were limited to establishing localization of the pregnancy, diagnosing non-viable pregnancies, detecting multiple pregnancies, and estimating gestational age more accurately. With the introduction of high resolution ultrasound and transvaginal ultrasound much more information can now be obtained. Routine first-trimester ultrasound scans are increasingly being offered to pregnant women in most developed countries. Although the mid-trimester scan is considered the standard screening moment for congenital abnormalities, the advances in ultrasound technology will contribute to the shift towards an earlier anomaly scan. Several studies demonstrate that a significant proportion of structural congenital abnormalities can consistently be diagnosed in the first-trimester.¹²⁻¹⁶ Clinical effectiveness of first-trimester screening for these abnormalities is, however, still at debate due to the wide range of detection rates that have been reported.¹⁷ Though, it should be beared in mind that with ongoing technological development and further refinement of already established screening tools the screening for congenital abnormalities will continue to evolve and move towards early pregnancy.

Early detection of 'abnormal' pregnancies

Most future parents want to know about any abnormal development or congenital abnormalities as early as possible.¹⁸⁻²⁰ An earlier prenatal diagnosis of (major) congenital abnormalities may also result in improved management: the possibility of scheduling additional ultrasound scans (before the limits of legal termination), the option for an earlier and safer termination of pregnancy²¹ and in some cases intrauterine treatment.^{22, 23} Furthermore, the future parents are counseled and can prepare themselves for the birth of a child with congenital abnormalities. In case of a normal screening earlier reassurance and reduced anxiety are favorable outcomes.

Three-dimensional ultrasound and Virtual Reality

Advances in computer technology made it possible to create three-dimensional (3D) reconstructions of ultrasound scans starting in the 1980's. Nowadays 3D ultrasound is used in selected cases for the detection of fetal malformations, mainly malformations of the face, limbs, thorax, spine, and central nervous system.²⁴ The embryonic period is especially well visualized using 3D ultrasound due to the

relative large amount of amniotic fluid. However, the third dimension of these so called 3D ultrasounds is not used to its optimum. 3D ultrasounds are usually evaluated on a computer screen, which is a two-dimensional medium.

Truly benefitting from all three dimensions is possible using a stereoscopic display or virtual reality (VR) system. A VR system immerses the viewer(s) in a virtual environment that allows for true depth perception and interaction with the 'hologram'. VR might revolutionize the assessment of 3D data, such as 3D ultrasound and MRI scans.

Clinicians and researchers, when using this VR approach, should be familiar with normal embryonic growth and development before any attempt is made to diagnose early structural congenital abnormalities or abnormal growth patterns. Therefore, normal embryonic growth and development in VR was previously studied extensively in the theses of Verwoerd-Dikkeboom²⁵ and Rousian²⁶. As a logical next step, in this thesis the use of VR in the assessment of abnormal growth and development is described.

Outline of this thesis

This thesis focuses on the transition from studying physiology to studying abnormal embryonic and fetal development using VR.

This thesis consists of six parts. A general introduction on the thesis and the I-Space virtual reality system is provided in **chapter 1**. **Chapter 2** describes the new concepts of the VR approach that have been introduced. In **chapter 3**, two studies regarding the relationship of embryonic volume and adverse pregnancy outcome are presented. The use of embryonic volume measurements as a measure of growth restriction is described in pregnancies in which a structural congenital abnormality was diagnosed in the first-trimester of pregnancy (chapter 3.1) and in pregnancies that will subsequently end in a miscarriage (chapter 3.2). **Chapter 4** presents data on newly introduced, non-standard biometric measurements of embryonic and fetal development. Their role in detecting aneuploid pregnancies is discussed. Finally, **chapter 5** provides insight in the diagnostic opportunities of VR in the first-trimester diagnosis of specific structural congenital abnormalities. In **chapter 6**, the general discussion is presented.

The research objectives can be summarized as follows:

- Chapter 2: To investigate new concepts of the virtual reality approach.
- Chapter 3: To determine the role of automated embryonic volume measurements in the detection of abnormal embryonic development.
- Chapter 4: To analyze (non-standard) biometry and volumetry in aneuploid pregnancies.
- Chapter 5: To determine the diagnostic applicability of the third dimension in embryos and fetuses with structural congenital abnormalities.

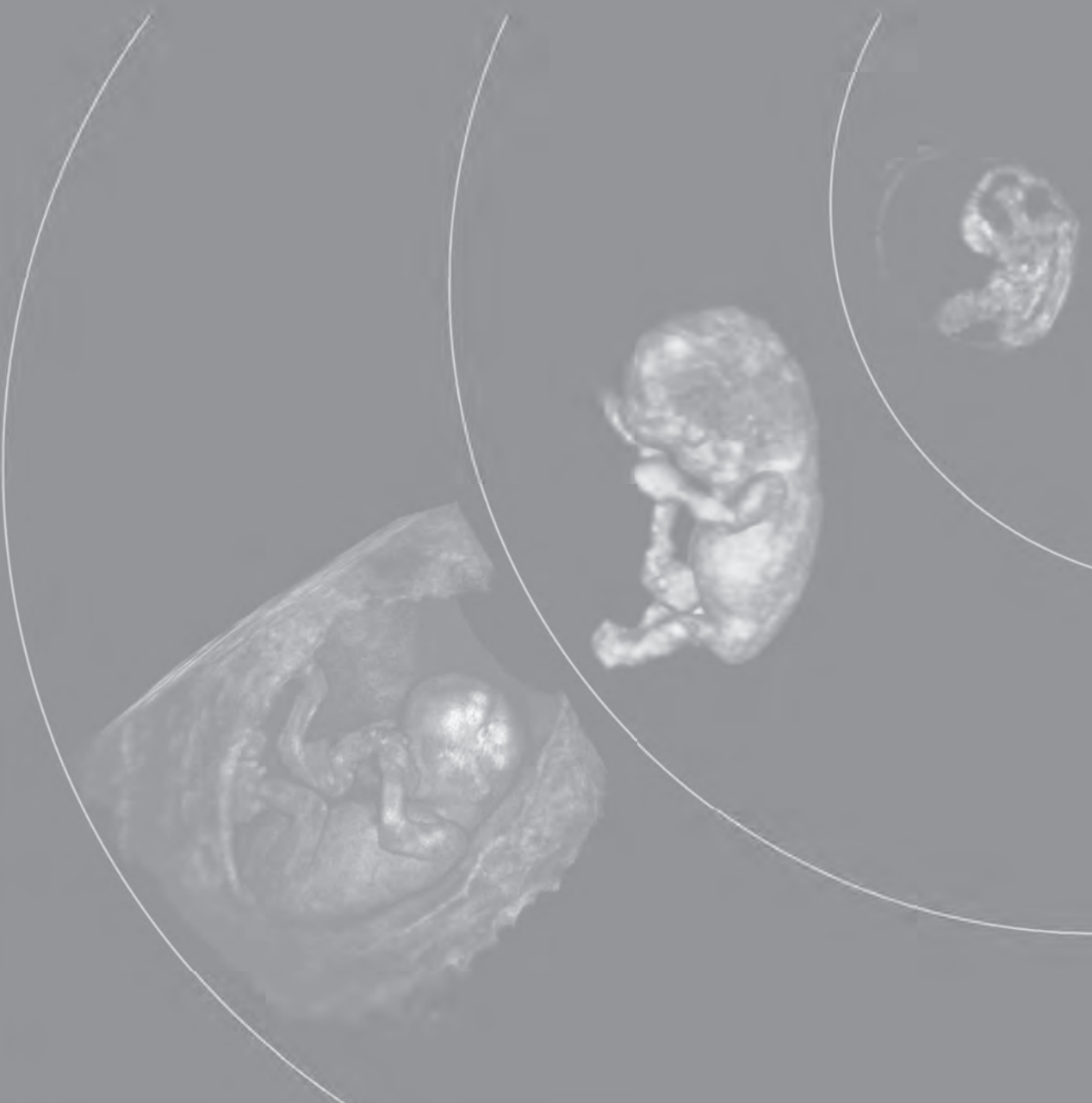
References

1. Steegers-Theunissen RP, Twigt J, Pestinger V, *et al.* The periconceptional period, reproduction and long-term health of offspring: the importance of one-carbon metabolism. *Hum Reprod Update* 2013; 19(6):640-55.
2. Barker DJ. The origins of the developmental origins theory. *J Intern Med* 2007; 261(5):412-7.
3. van Uiter EM, van der Elst-Otte N, Wilbers JJ, *et al.* Periconception maternal characteristics and embryonic growth trajectories: the Rotterdam Predict study. *Hum Reprod* 2013; 28(12):3188-96.
4. Bouwland-Both MI, Steegers-Theunissen RP, Vujkovic M, *et al.* A periconceptional energy-rich dietary pattern is associated with early fetal growth: the Generation R study. *BJOG* 2013; 120(4):435-45.
5. Bukowski R, Smith GC, Malone FD, *et al.* Human sexual size dimorphism in early pregnancy. *Am J Epidemiol* 2007; 165(10):1216-8.
6. Mook-Kanamori DO, Steegers EA, Eilers PH, *et al.* Risk factors and outcomes associated with first-trimester fetal growth restriction. *JAMA* 2010; 303(6):527-34.
7. Bottomley C, Daemen A, Mukri F, *et al.* Assessing first-trimester growth: the influence of ethnic background and maternal age. *Hum Reprod* 2009; 24(2):284-90.
8. Ben-Haroush A, Melamed N, Oron G, *et al.* Early first-trimester crown-rump length measurements in male and female singleton fetuses in IVF pregnancies. *J Matern Fetal Neonatal Med* 2012; 25(12):2610-2.
9. Jaddoe VW, de Jonge LL, Hofman A, *et al.* First-trimester fetal growth restriction and cardiovascular risk factors in school age children: population based cohort study. *BMJ* 2014; 348:g14.
10. Callinan PA, Feinberg AP. The emerging science of epigenomics. *Hum Mol Genet* 2006; 15 Spec No 1:R95-101.
11. Heijmans BT, Tobi EW, Stein AD, *et al.* Persistent epigenetic differences associated with prenatal exposure to famine in humans. *Proc Natl Acad Sci USA* 2008; 105(44):17046-9.
12. Sonek J. First-trimester ultrasonography in screening and detection of fetal anomalies. *Am J Med Genet C Semin Med Genet* 2007; 145C(1):45-61.
13. Katorza E, Achiron R. Early pregnancy scanning for fetal anomalies—the new standard? *Clin Obstet Gynecol* 2012; 55(1):199-216.
14. Iliescu D, Tudorache S, Comanescu A, *et al.* Improved detection rate of structural abnormalities in the first-trimester using an extended examination protocol. *Ultrasound Obstet Gynecol* 2013; 42(3):300-9.
15. Donnelly JC, Malone FD. Early fetal anatomical sonography. *Best Pract Res Clin Obstet Gynaecol* 2012; 26(5):561-73.
16. Becker R, Wegner RD. Detailed screening for fetal anomalies and cardiac defects at the 11-13-week scan. *Ultrasound Obstet Gynecol* 2006; 27(6):613-8.
17. Borrell A, Robinson JN, Santolaya-Forgas J. Clinical value of the 11- to 13+6-week sonogram for detection of congenital malformations: a review. *Am J Perinatol* 2011; 28(2):117-24.
18. Kornman LH, Wortelboer MJ, Beekhuis JR, *et al.* Women's opinions and the implications of first- versus second-trimester screening for fetal Down's syndrome. *Prenat Diagn* 1997; 17(11):1011-8.
19. de Graaf IM, Tijmstra T, Bleker OP, *et al.* Women's preference in Down syndrome screening. *Prenat Diagn* 2002; 22(7):624-9.

20. Mulvey S, Wallace EM. Women's knowledge of and attitudes to first and second trimester screening for Down's syndrome. *BJOG* 2000; 107(10):1302-5.
21. Chasen ST, Kalish RB. Can early ultrasound reduce the gestational age at abortion for fetal anomalies? *Contraception* 2013; 87(1):63-6.
22. Biard JM, Johnson MP, Carr MC, *et al.* Long-term outcomes in children treated by prenatal vesicoamniotic shunting for lower urinary tract obstruction. *Obstet Gynecol* 2005; 106(3):503-8.
23. Adzick NS, Thom EA, Spong CY, *et al.* A randomized trial of prenatal versus postnatal repair of myelomeningocele. *N Engl J Med* 2011; 364(11):993-1004.
24. Timor-Tritsch IE, Platt LD. Three-dimensional ultrasound experience in obstetrics. *Curr Opin Obstet Gynecol* 2002; 14(6):569-75.
25. Verwoerd-Dikkeboom CM. Virtual Embryoscopy [Thesis]. Rotterdam: Erasmus University Rotterdam; 2009.
26. Rousian M. Embryonic Development in Virtual Reality [Thesis]. Rotterdam: Erasmus University Rotterdam; 2011.

1.2

The I-Space Virtual Reality System



The I-Space virtual reality (VR) system discussed in this thesis is situated at the department of Bioinformatics at the Erasmus MC, University Medical Center Rotterdam. In 2004 the Erasmus MC was the first medical center to install such a system for both research and clinical applications.

The I-Space is a CAVETM-like¹ VR system where the researcher stands in a small room that provides a three-dimensional (3D) virtual environment. Eight projectors are directed to the three walls and the floor of this small room. The CAVE, an acronym for Cave Automatic Virtual Environment and inspired by Plato's cave allegory, was developed as an alternative to head mounted displays, also known as VR helmets. Advantages of a CAVE system over a head mounted display, are a marked reduction in 'simulator sickness' as well as the possibility of multiple viewers experiencing the virtual world together.

Because our eyes are separated by a 4-6 centimeter distance humans are able to see depth. Due to this difference in position, each eye has a slightly different viewpoint. The two different viewpoints are processed by the brain and the difference is interpreted as depth. Stereoscopic imaging, as used in the I-Space VR system, relies on the same principle. Two slightly different images are projected, one for each eye. By wearing stereoscopic glasses, the left eye image is only seen by the left eye and the same applies for the right eye.

The images in the I-Space are generated by eight Barco SIM5 DLP projectors that are directed to the four projection screens (2.60 by 1.95 meters) forming the three walls and the floor of a small room. Infrared cameras are installed in four corners of the room to enable head and hand tracking. Using the

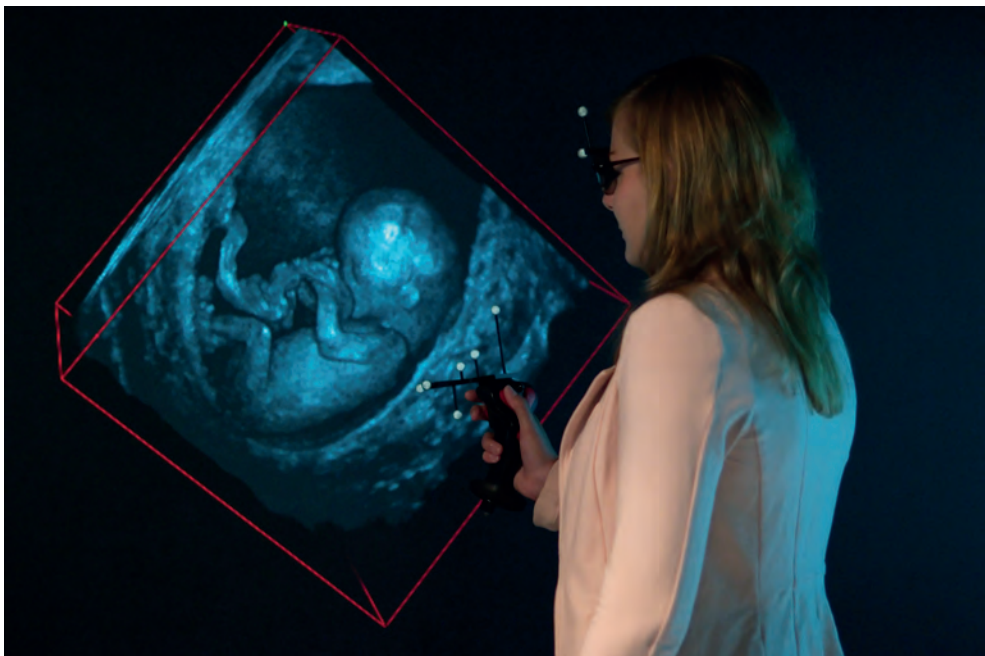


Figure 1: Picture of observer (LB) in the I-Space. The user is wearing the tracking glasses and holding the wireless pointer. An embryo of twelve weeks gestation is projected.

information of the tracking system, the user is provided with the correct perspective, allowing him to walk around and interact with the stereoscopic projected image, which we will call a 'hologram' (Figure 1). The wireless four-button plus hat switch joystick is used to operate the V-Scope volume rendering application², designed by Anton Koning, for interaction and manipulation of the volumetric dataset. Using the joystick, it is possible to rotate, translate and enlarge the hologram. A clipping plane makes it possible to "cut" the hologram in any direction. Furthermore, V-Scope offers several other tools, e.g. a virtual eraser to create a better view of the object of interest and tools to perform several biometric and volumetric measurements.

Most 3D imaging modalities can be visualized using V-Scope in the I-Space. In addition to the 3D ultrasound datasets featured in this thesis, datasets from computed-tomographic (CT), magnetic resonance imaging (MRI), positron emission tomography (PET) and similar modalities can be used. Several other departments in the Erasmus MC are using the I-Space in both research and clinical practice.³⁻⁶

V-Scope measurement tools used in this thesis

Biometric measurements can be easily performed in the I-Space by placing two or more measuring points (calipers) in the dataset. This can be used for standard, routinely used, biometric measurements like the crown-rump length (Figure 2). Non-standard measurements can also been performed using this tool; measurements of the width of the hips, knees, elbows and the length of the ear and foot

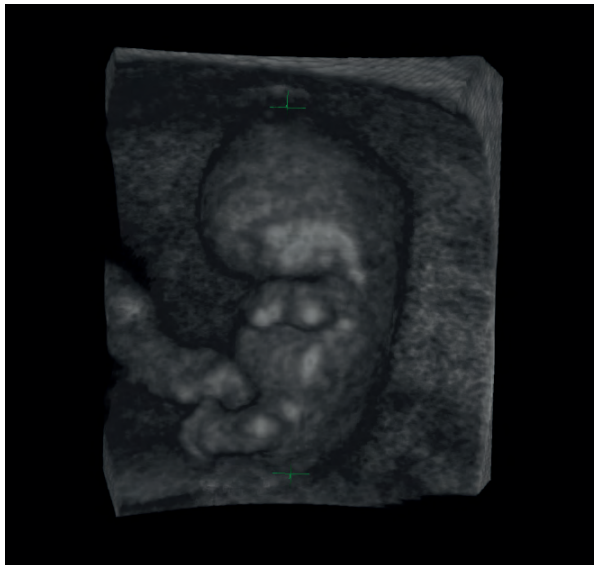


Figure 2: A picture of a nine weeks old embryo. Calipers are placed from crown to rump to measure crown-rump length.

were published earlier⁷ and in this thesis non-standard measurements of the hand are described (chapter 4.1). By placing multiple calipers the length of an irregular structure, e.g. the umbilical cord⁸ or the hand (chapter 4.1), can be traced and measured. The depth perception and intuitive interaction with the volume enable the measurement of complex structures, and allow precise verification of the accurate positioning of the calipers.

The V-Scope application implements semi-automatic volume measurements in 3D datasets. In contrast to two-dimensional (length) measurements, 3D measurements take into account all three dimensions, and therefore are assumed to reflect growth more accurately. The semi-automatic algorithm of V-Scope is based on a region growing approach with both grey level and neighborhood variation thresholds. The user selects the thresholds and places a seed point in the structure of interest. The algorithm will then segment the structure of interest starting from the seed point by adding voxels, i.e. 3D pixels, until voxels exceeding one of the thresholds are reached (Figure 3). Prior to a volume measurement all connecting structures that fall within the threshold values have to be erased in order to limit the segmentation to the structure of interest. Both hypoechoic and hyperechoic structures can be measured using the segmentation algorithm. If the structure of interest consists of both hypoechoic and hyperechoic structures, as does an embryo, the segmentation has to take place in two steps, by first segmenting the hyperechoic parts and later filling in the hypoechoic spaces. Due to the depth perception and simple 3D interaction offered by the I-Space the user can quickly check whether the segmentation is correct. If not, additional seed points can be placed, the volume can be manually grown or shrunk and a brush function can be used to add or delete voxels from the segmentation.

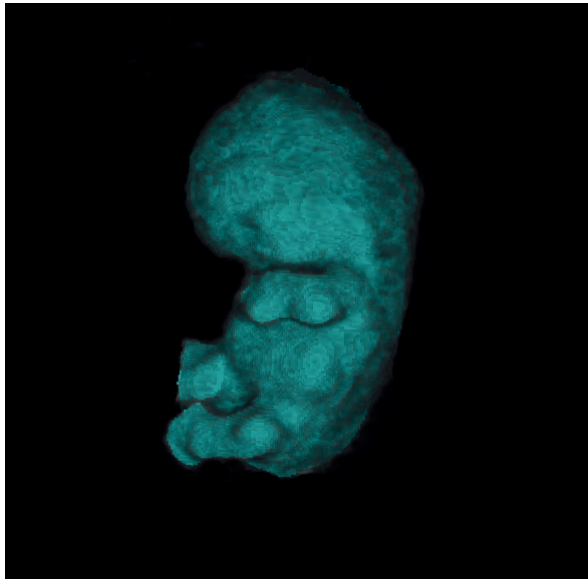


Figure 3: The same embryo as seen in Figure 2 of which an embryonic volume measurement is shown.

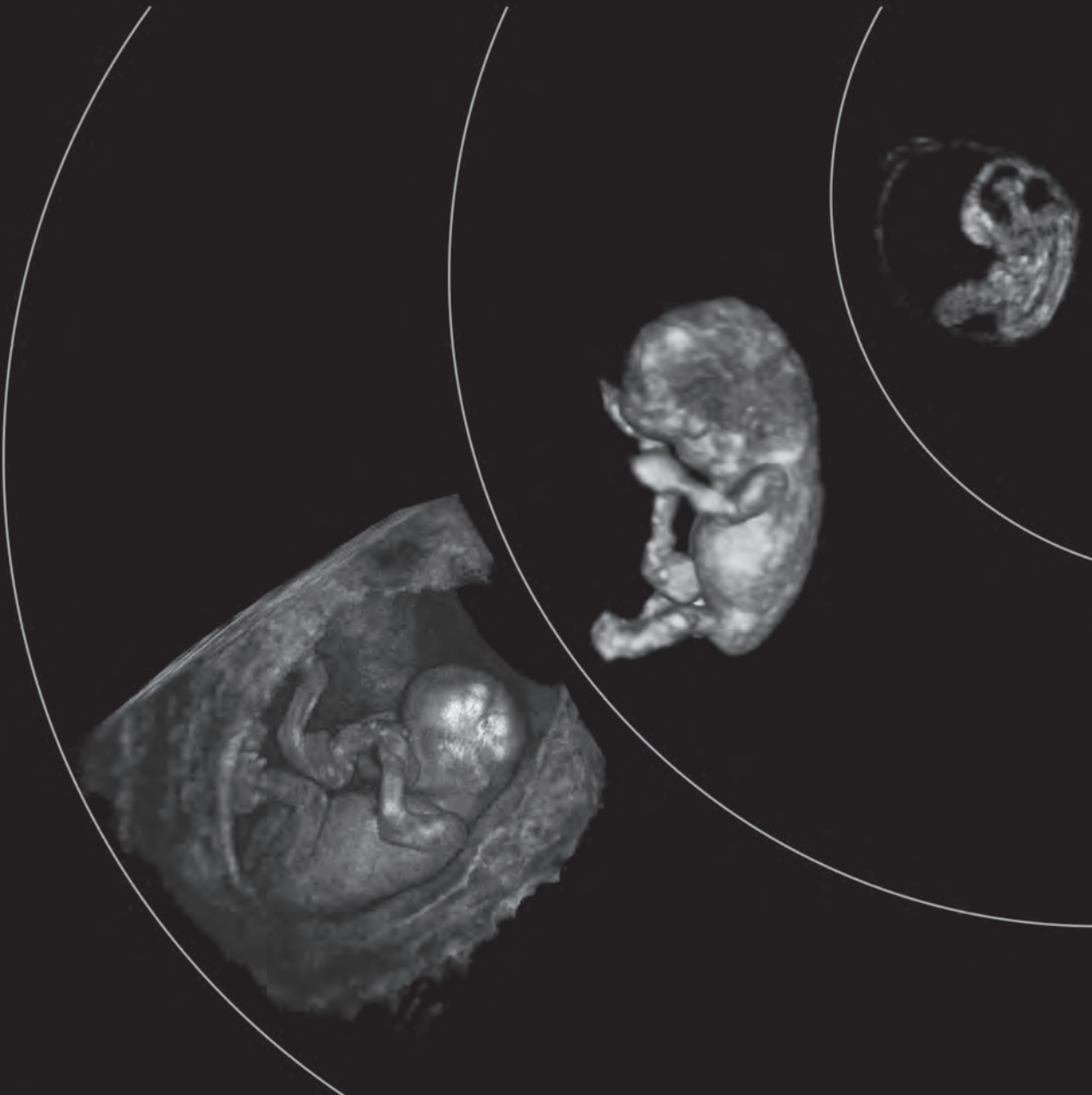
In conclusion, the I-Space VR system offers a new and promising way of visualizing early pregnancy. Growth and development can be accurately monitored *in vivo* by using biometry, volumetry and by studying morphology.

References

1. Cruz-Neira C, Sandin DJ, DeFanti TA. Surround-screen projection-based virtual reality: the design and implementation of the CAVE (tm). *Proceedings of the 20th Annual Conference on Computer Graphics and Interactive Techniques* 1993;135-142.
2. Koning AH, Rousian M, Verwoerd-Dikkeboom CM, Goedknecht L, Steegers EA, van der Spek PJ. V-scope: design and implementation of an immersive and desktop virtual reality volume visualization system. *Stud Health Technol Inform* 2009;142:136-138.
3. van Adrichem LN, van Vlimmeren LA, Cadanova D, Helders PJ, Engelbert RH, van Neck HJ, Koning AH. Validation of a simple method for measuring cranial deformities (plagiocephalometry). *J Craniofac Surg* 2008;19:15-21.
4. Meuffels DE, Potters JW, Koning AH, Brown CH, Jr., Verhaar JA, Reijman M. Visualization of postoperative anterior cruciate ligament reconstruction bone tunnels: reliability of standard radiographs, CT scans, and 3D virtual reality images. *Acta Orthop* 2011;82:699-703.
5. Bol Raap G, Koning AH, Scohy TV, ten Harkel AD, Meijboom FJ, Kappetein AP, van der Spek PJ, Bogers AJ. Virtual reality 3D echocardiography in the assessment of tricuspid valve function after surgical closure of ventricular septal defect. *Cardiovasc Ultrasound* 2007;5:8.
6. van den Bosch AE, Koning AH, Meijboom FJ, McGhie JS, Simoons ML, van der Spek PJ, Bogers AJ. Dynamic 3D echocardiography in virtual reality. *Cardiovasc Ultrasound* 2005;3:37.
7. Verwoerd-Dikkeboom CM, Koning AH, Hop WC, Rousian M, Van Der Spek PJ, Exalto N, Steegers EA. Reliability of three-dimensional sonographic measurements in early pregnancy using virtual reality. *Ultrasound Obstet Gynecol* 2008;32:910-916.
8. Rousian M, Verwoerd-Dikkeboom CM, Koning AH, Hop WC, van der Spek PJ, Steegers EA, Exalto N. First-trimester umbilical cord and vitelline duct measurements using virtual reality. *Early Hum Dev* 2011;87:77-82.

CHAPTER 2

New Perspectives on the Virtual Reality Approach

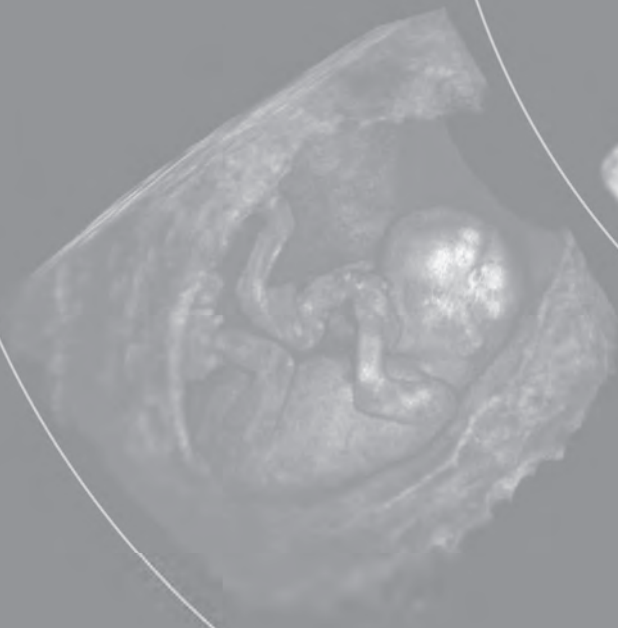
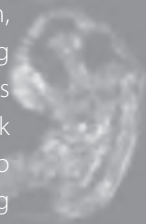


2.1

Design and Validation of a 3D Virtual Reality Desktop System for Early Pregnancy Evaluation

Journal of Clinical Ultrasound 2014; Jul 9 [Epub ahead of print]

L. Baken,
I.M.A. van Gruting
E.A.P. Steegers
P.J. van der Spek
N. Exalto
A.H.J. Koning



Abstract

Purpose. To design and validate a desktop virtual reality (VR) system, for presentation and assessment of volumetric data, based on commercially-of-the-shelf (COTS) hardware as an alternative to a fully immersive CAVETM-like I-Space VR system.

Methods. We designed a desktop VR system, using a three-dimensional (3D) monitor and a 6 degrees-of-freedom (6DOF) tracking system. A personal computer uses the V-Scope (Erasmus MC, Rotterdam, The Netherlands) volume rendering application, developed for the I-Space, to create a hologram of volumetric data. Inter- and intraobserver reliability for crown-rump length (CRL) and embryonic volume (EV) measurements are investigated using Bland-Altman plots and intraclass correlation coefficients (ICC). Time required for the measurements was recorded.

Results. Comparing the I-Space and the desktop VR system, the mean difference for CRL is -0.34% (limits of agreement (LoA) -2.58 to 1.89, $\pm 2.24\%$) and for EV -0.92% (LoA -6.97 to 5.13, $\pm 6.05\%$). Intra- and interobserver ICCs of the desktop VR system were all > 0.99 . Measurement times were longer on the desktop VR system compared to the I-Space, but the differences were not statistically significant.

Conclusions. A user friendly desktop VR system can be put together using COTS hardware at an acceptable price. This system provides a valid and reliable method for embryonic length and volume measurements and can be used in clinical practice.

Introduction

The introduction of three-dimensional (3D) imaging modalities such as computed tomography (CT), magnetic resonance imaging (MRI), and 3D ultrasound (US) made it possible to non-invasively study internal details of the human body in all three dimensions. In the 90's 3D ultrasound was introduced in the field of prenatal diagnostics. The advantages of 3D ultrasound in the diagnosis of congenital abnormalities are unequivocal and it is mainly used for the anatomical evaluation of the developing face, limbs, thorax, and spine.

Although a great step forward, in most cases 3D datasets are still presented either as slices, or as 3D reconstructions on flat two-dimensional (2D) computer screens, or on paper. These media do not offer depth perception, nor do they allow natural 3D interaction. Although physicians can gather much information from these imaging modalities, it is well known that humans are better at understanding three-dimensional relations when they are viewed on three-dimensional displays.

The I-Space, a CAVETM-like¹ virtual reality (VR) system at the department of Bioinformatics of the Erasmus MC in Rotterdam, is a stereoscopic projection system that allows optimal presentation and assessment of data in all three dimensions (Figure 1). A hologram of the 3D volume can be created by the V-Scope² volume rendering software (Erasmus MC, Rotterdam, The Netherlands) developed at our department of Bioinformatics. The hologram can be manipulated with the use of a wireless joystick;



Figure 1: Image of the I-Space VR-system. Three-dimensional datasets are projected on the three walls and the floor of the room using eight projectors. An embryo of ten weeks and four days gestational age is visualized in the I-Space. The observer wears stereoscopic glasses and handles a wireless joystick to interact with the dataset.

the hologram can be sized, turned, and clipped. The V-Scope software makes it possible to accurately measure length and volume.

In our center the I-Space is used in a wide range of medical fields. Virtual reality is used by the department of plastic and reconstructive surgery in evaluating cranial deformities³ and by the department of orthopedic surgery in evaluating postoperative results.⁴ The department of cardiology did several studies to investigate the added value of VR in the assessment of 3D echocardiography.^{5,6} Through research of the department of obstetrics and gynecology it has been proven that the I-Space is a powerful tool for early prenatal research⁷⁻¹⁰ and diagnostics.^{11,12} However, the relatively high cost (approximately US\$ 500,000) and the necessity of a separate room of at least 40m²/400 sq. ft. are an obstacle for wide spread integration in daily clinical practice. To enable routine use of a VR system it is necessary to have the functionality of the I-Space and V-Scope in the form of a desktop system to facilitate clinical use in the consulting room.

The primary aim of this study is to explore the necessary characteristics of a desktop VR system, and to investigate how such system can be put together at an acceptable price and in such a way that it takes up a limited amount of (desk) space and integrates well with the normal work flow. The secondary aim is to establish to which degree the much smaller desktop system can provide the same high standard of performance in the accuracy of measurements performed and to establish the time that is required for these measurements compared to the I-Space. As a proof of concept we will compare the desktop VR system to the I-Space using embryonic length and volume measurements.

Material and Methods

Design

As a successful volume rendering application for the I-Space² had already been developed, a desktop VR system capable of running this with little or no adaptation would be preferable over either using a different application, or having to develop a completely new one from scratch. Although 'portable' versions of the CAVE-concept are commercially available, e.g. the ImmersaDesk, these are too large to be considered as a desktop system. An extensive literature and Internet search is performed to investigate the availability of a 3D VR desktop system that can run V-Scope and that complies with our requirements.

The envisioned system should meet the following criteria to enable easy integration in routine daily (prenatal) care:

- Small foot print, as desk and floor space tends to be limited in most hospitals.
- Low price (below US\$ 25,000/20,000 euro), as ultrasound equipment is relatively cheap (compared to CT or MRI scanners).
- As similar to the I-Space as possible, to limit the effort needed in software development and to allow us to build on our experiences with the I-Space.
- Easy to install, use, and maintain. To be accepted by clinicians the system should be easy to use and should not require special IT-skills to operate.

These aspects also interact. Ease-of-use and similarity to the I-Space interface means the desktop system needs to offer the same interaction model as the I-Space. Therefore, ideally it should be a single-handed six degrees-of-freedom (6DOF) pointing device with at least four buttons and a dual-axis joystick/hat switch to mimic the wireless joystick used in the I-Space.

Should no such system be commercially available, a desktop VR system using commercially-off-the-shelf (COTS) components will have to be custom built.

Validation

Patient and Ultrasound Scan selection

From January 1st 2009 until December 31st 2009 a total of 112 patients with uncomplicated singleton pregnancies were included in an ongoing study on embryonic growth and development. The collected data of these patients were also used in other studies.¹³⁻¹⁵ In this group 3D US scans were performed weekly between 6+0 and 12+6 weeks gestation using a 3.7-9.3 MHz transvaginal probe of the GE Voluson E8 expert system (GE Medical systems, Zipf, Austria). A total of 595 different 3D datasets had been collected for general study purposes of the department. The scans were saved as Cartesian volumes and transferred to the I-Space and the desktop VR system. The procedures of the study received ethics approval from the medical ethical committee of the Erasmus MC (METC Erasmus MC MEC 2004-227).

Since this study focuses on validity and reliability, only volumes with acceptable image quality were included. In addition, volumes in which parts of the embryo were missing, and volumes with shadowing and movement artifacts were excluded.

For a more convenient sample size a random subset was subsequently chosen using a free online random number generator. A total of 5 US datasets per gestational week were selected, resulting in 30 3D US volumes of 30 different patients (gestational age ranged from 7+0 to 12+6 weeks) that remained for analysis.

Measurements

To optimize the image quality the gray scale and opacity of the data were adjusted in the I-Space and on the desktop 3D VR system when necessary. The volumes were enlarged, rotated, and cropped where necessary to provide the best view of the embryo.

For measuring the crown-rump length (CRL, the length of the embryo or fetus from crown to rump excluding the limbs), the calipers were placed from crown to caudal rump in the mid-sagittal plane. The embryo's hologram was turned to verify correct position of the calipers. The previously mentioned V-Scope software includes a region-growing segmentation algorithm to semi-automatically measure volumes of a structure of interest. The segmentation algorithm combines a region-growing approach with a neighborhood variation threshold, originally proposed for MRI data.¹⁶ Upper and lower grey level threshold and the standard deviation threshold of the voxels neighborhood are determined by

the researcher. After placing a seed point the algorithm will grow a region until a tissue interface is reached.¹⁵

The measurements in the I-Space VR system and on the 3D VR Desktop system were performed by a single examiner (I.v.G). A second series of measurements on the 3D VR Desktop system were performed by the same examiner (I.v.G) to calculate intraobserver reliability. These measurements were performed one week later than the first series to avoid recollection bias. For interobserver reliability another operator (L.B.) performed the same measurements once on the 3D VR Desktop system. Observer 1 (I.v.G.) had recently started to perform measurements in the I-Space. Observer 2 had two years of experience measuring CRL and embryonic volume (EV) in the I-Space. Both observers were blinded to each other's results as well as to the gestational age of the embryo. The 3D US volumes were presented in a different order for both imaging techniques to avoid recognition of the datasets. The time per measurement was recorded.

Statistical Analysis

Data analysis was performed using SPSS (Release 19.0 for Windows) and R (Release 2.15.1 for Windows). The validity of the 3D VR desktop system was studied by comparing measurements made using this system to the same measurements performed in the already validated Barco (Kortrijk, Belgium) I-Space system. For testing this agreement mean differences and limits of agreement as described by Bland and Altman^{17,18} were calculated. For the Bland-Altman plots the relative difference in percentages was chosen, because the size of the embryo increases over time and so will the absolute differences. Therefore, uniform limits of agreement cannot support this relationship between difference and magnitude. Although acceptable limits of agreement are subjective and differ for various clinical decisions, one can say that a mean relative difference less than $\pm 2.5\%$ and limits of agreement smaller than $\pm 10\%$ would support the validity of the system.

Apart from agreement, the repeatability of measurements has to be assessed by testing the intra- and interobserver reliability. Intraclass-correlation coefficients (ICC) were calculated and values above 0.90 indicate a good correlation.

The mean time per measurement (CRL and EV) was calculated for both techniques. The Wilcoxon signed-rank test was used to test for statistical significance. A *p*-value < 0.05 was considered to be statistically significant.

Results

Design

Over the years many solutions have been proposed for stereoscopic display systems for medical applications, ranging from simple workstations with 3D monitors to the very expensive Dextroscope¹⁹, but none have attained any widespread acceptance. Despite an extensive literature and Internet search no suitable commercially available desktop-system that would support the V-Scope application could be found. It was therefore decided to custom build a desktop VR system out of COTS components.

In order to satisfy the low costs and small footprint requirements a 24" passive stereoscopic monitor (Miracube G240M, Pavonine Korea Inc., Incheon, Korea) was selected as the 3D display device. A passive stereo display has the advantage that the glasses are very cheap and no special graphics hardware is required to create the stereoscopic images (Figure 2). An auto-stereoscopic display was not considered as this type of display tends to have a very limited viewing angle, requiring the user to sit in a stable and fixed position, directly in front of the display.

As the new 3D VR desktop system should ideally possess the same interaction model as the I-Space, a single-handed 6DOF pointing device with at least four buttons and a dual-axis joystick/hat switch is preferred. Although this particular joystick was available separately, and could be used on a desktop system, it is rather unwieldy and too expensive for the system that's being build. As a suitable pointing device with buttons could not be found, it was decided to initially use a simple marker for pointing, tracked by an infrared optical tracking system (Atracsys beMerlin, Atracsys LCC, Le Mont-sur-Lausanne, Switzerland) and a stationary 6DOF mouse (3Dconnexion SpaceExplorer, 3Dconnexion, Boston, MA) to orient the dataset. While this changes the interaction model slightly, it better fits a desktop system and is also more flexible.

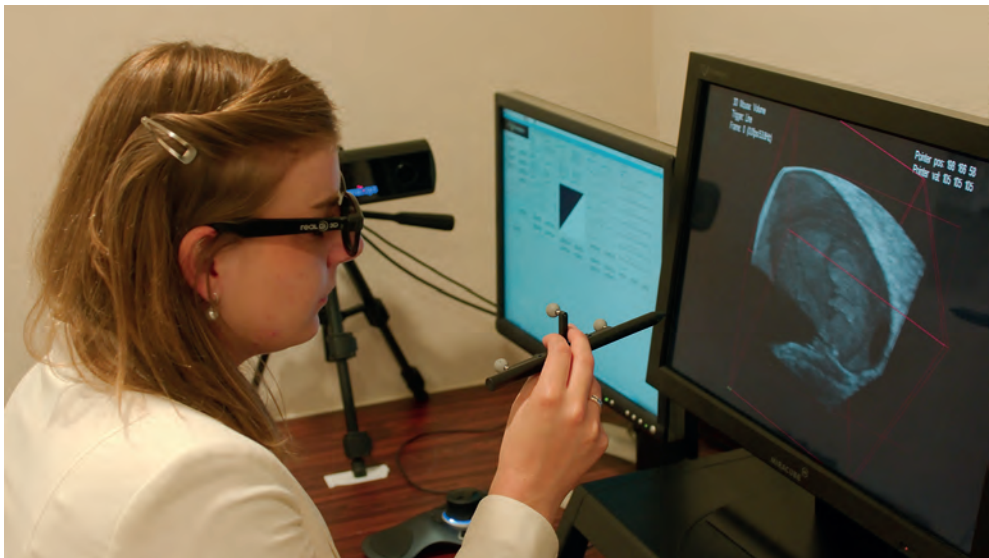


Figure 2: Image of an observer using our three-dimensional (3D) virtual reality desktop system. An embryo of nine weeks and three days gestational age is projected on the 3D monitor. The observer wears stereoscopic glasses to obtain depth perception from the 3D monitor. The observer is holding the 6DOF pointing device. In combination with the 6DOF mouse, which is on the left of the observer, and the tracking system interaction with the dataset is possible. The second, two-dimensional, computer monitor displays the menu containing all measurement tools.

Validation

Scatter plots comparing the I-Space and the 3D VR desktop system measurements of the two parameters (CRL and EV) are presented (see supplemental Figure 1). Bland-Altman plots of the mean relative difference between the measurements are given in Figure 3. The mean relative differences, comparing the two techniques, for the CRL and EV are -0.34% and -0.92%, respectively and showed no statistical difference ($p=0.109$ and 0.114 , respectively). The limits of agreement for the CRL are -2.58 to 1.89 ($\pm 2.24\%$) and for the EV from -6.97 to 5.13 ($\pm 6.05\%$) (Table 1).

Table 2a shows data for the two measurements by the same observer (intraobserver reliability). No significant differences were found. Table 2b shows the data of the two different operators (interobserver reliability). No significant differences were found for the CRL measurements. A significant mean difference of -1.52% was found for the EV measurements ($p=0.046$). The ICCs are all >0.99 for both

Table 1: Agreement between measurements using I-Space and 3D VR desktop system of two biometric parameters.

Parameter	n	Mean difference (%) [*]	95% CI for mean difference (%)	p	Limits of agreement [#]	ICC	95% CI for ICC
CRL	30	-0.34	-0.77 to 0.08	0.109	-2.58 to 1.89	1.000	0.999 to 1.000
EV	30	-0.92	-2.07 to 0.23	0.114	-6.97 to 5.13	0.999	0.998 to 1.000

* Mean difference = I-Space minus 3D VR Desktop system divided by mean of two systems in percentages

Limits of agreement = mean difference \pm 1.96 SD

Table 2: Intraobserver agreement between measurements using 3D VR desktop system of two biometric parameters (A). Interobserver agreement between measurements using 3D VR desktop system of two biometric parameters (B).

A

Parameter	n	Mean difference (%) [*]	95% CI for mean difference (%)	p	Limits of agreement [#]	ICC	95% CI for ICC
CRL	30	-0.05	-0.52 to 0.43	0.838	-2.53 to 2.44	1.000	1.000 to 1.000
EV	30	-0.20	-1.22 to 0.82	0.695	-5.55 to 5.15	1.000	0.999 to 1.000

B

Parameter	n	Mean difference (%) [§]	95% CI for mean difference	p	Limits of agreement [#]	ICC	95% CI for ICC
CRL	30	-0.06	-0.60 to 0.48	0.828	-2.89 to 2.78	1.000	0.999 to 1.000
EV	30	-1.52	-3.01 to -0.03	0.046	-9.35 to 6.31	0.999	0.997 to 0.999

* Mean difference = second measurement minus first measurement divided by mean of two measurements in percentages

Limits of agreement = mean difference \pm 1.96 SD

§ Mean difference = measurements of the second examiner (LB) minus measurement of the first examiner (lvG) divided by mean of two measurements in percentages

CRL= crown-rump length, EV= embryonic volume, 95% CI = 95% confidence interval, ICC = intraclass correlation coefficient

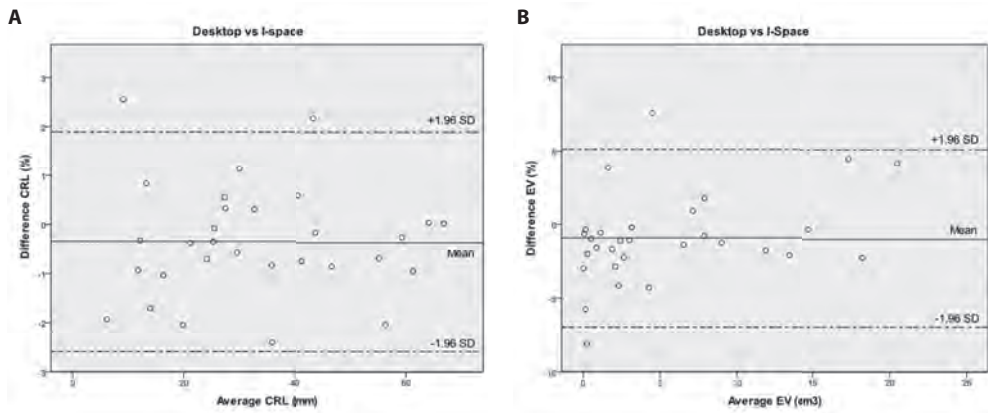


Figure 3: Bland-Altman plots comparing I-Space en 3D VR Desktop system measurements: (A) crown-rump length (CRL) and (B) embryonic volume (EV). The solid line represents the mean percentage difference and the broken lines the limits of agreement, calculated as the mean difference ± 1.96 SD.

intra- and interobserver reliability. Scatterplots and Bland-Altman plots of the interobserver reliability are given in supplemental Figure 2 and 3.

Time required for each measurement for both techniques is shown in supplemental Table 1. For both CRL and EV the longest time required is reported during the first series of measurements on the 3D VR desktop system by the first observer. On average, when using the 3D VR desktop system more time was required for CRL and EV measurements, although the median differences (I-Space – 3D VR desktop) expressed in seconds were not statistically significant for CRL (-29.50 , 95% CI -42.50 , 1.50 , $p=0.059$) and for EV (-86.50 , 95% CI -166.50 , 0.50 , $p=0.051$). The second series of measurements on the 3D VR desktop are, in comparison to the first series, significantly faster. This is graphically shown in supplemental Figure 4. The second observer required significantly less time to measure CRL and EV compared to both the first observer's first and second series of measurements (see supplemental Table 2).

Discussion

A user-friendly desktop VR system was developed using COTS hardware, at an acceptable price. When a new measuring tool is introduced, it has to be demonstrated that the measurements performed using the new method are valid and reproducible. In this study agreement and repeatability of length and volume measurements obtained with the 3D VR desktop have been compared to the gold standard, the I-Space. In an *in vitro* setting volume measurements using the I-Space exactly match the true (known) volume.¹⁰ It was shown that the 3D VR desktop is a valid and reliable system to measure CRL and EV as the mean relative difference were all below $\pm 2.5\%$ and limits of agreement were all smaller than $\pm 10\%$, and ICCs are all >0.99 .

In contrast to the high ICCs for both interobserver CRL and EV measurements, a significant difference of -1.52% was found between the EV measurements of both observers. One outlier, as can be seen in supplemental Figure 3b, causes this difference. The large difference between the measurements of both observers is most likely due to a gestational age of only seven weeks. In these early pregnancies a small measurement error accounts for a large percentage difference between measurements as the absolute difference was only 0.04 cm³.

When comparing the time that is required to measure the two parameters using both systems, the 3D VR desktop measurements are found to take longer compared to measurements performed using the I-Space, although not statistically significant. As the second series of measurements on the desktop were significantly faster than the first series ($p=0.015$) and the more experienced, observer (L.B.) needed significantly less time for the measurements compared to the other observer ($p<0.001$) it is suggested that more experience will shorten measurement time.

The lower costs and smaller work space of the 3D VR desktop come with a price. It requires the simultaneous use of a 3D mouse, a normal mouse, and a pointer device, instead of a single joystick and is therefore somewhat more complex to use. In addition, the current 3D VR desktop system, in contrast to the I-Space, does not offer motion parallax (i.e. head tracking) so the user cannot move his head in order to get a better view of the subject. However, it is relatively simple to extend the system to include this, should an application call for it.

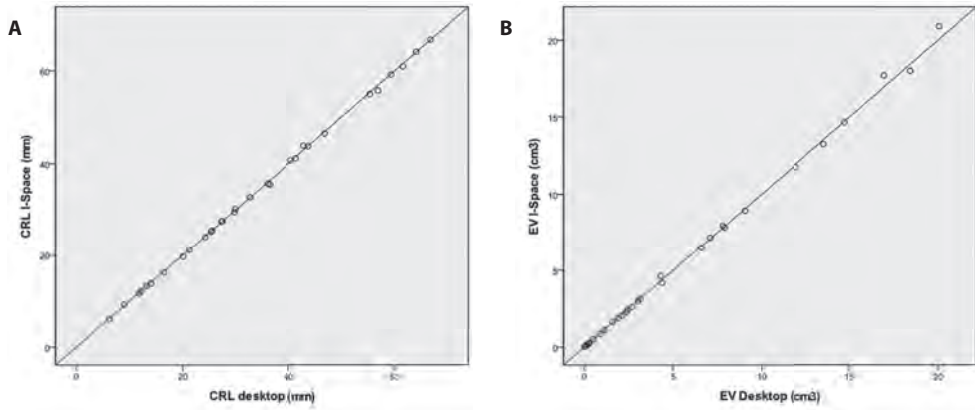
With the 3D VR desktop system semi-automatical volume measurements are now available to clinical practice. It can be expected that volume measurements, compared to length measurements, will prove to be more precise in estimating size and detecting growth deviations. Although volume measurements at this point aren't routinely used in the field of obstetrics, several studies point out the usefulness of these measurements. The relationship between abnormal first-trimester volume measurements and (adverse) pregnancy outcome is well established; embryonic volume measurements could predict early pregnancy failure²⁰, chromosomal abnormalities^{21,22}, growth disturbance in twins²³, and birth weight^{24,25}. If future studies can further establish these relationships this might lead to implementation of volume measurements in routine clinical practice in the near future.

In conclusion, the results of this study involving of first-trimester biometric measurements indicate that the 3D VR desktop system presented here can be reliably used for length and volume measurements. The 3D VR desktop system can be integrated in the normal clinical workflow due to its small size and low cost. Future studies should investigate the implementation of VR in clinical practice, although in several cases it already proved to be of help during the diagnostic process.^{4,5,12,26} In addition, research involving 3D datasets can now take place on the 3D VR desktop system, both in our own medical center, as well as in other hospitals.

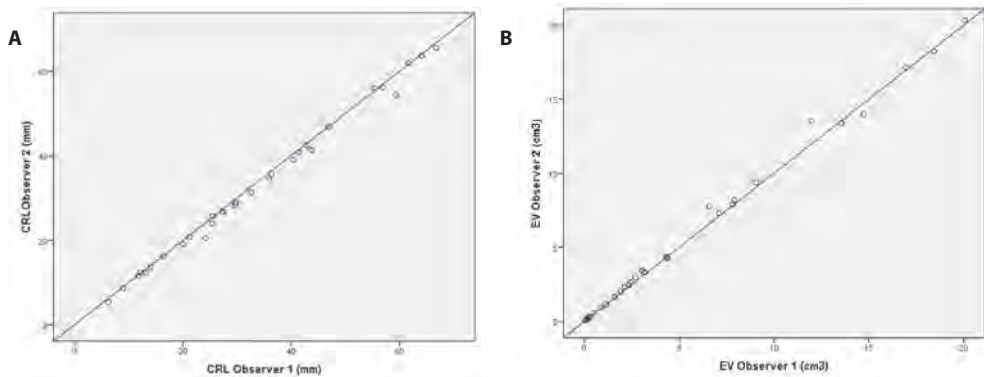
References

1. Cruz-Neira C, Sandin DJ, DeFanti TA. Surround-screen projection-based virtual reality: the design and implementation of the CAVE (tm). *Proceedings of the 20th Annual Conference on Computer Graphics and Interactive Techniques* 1993;135.
2. Koning AH, Rousian M, Verwoerd-Dikkeboom CM, et al. V-scope: design and implementation of an immersive and desktop virtual reality volume visualization system. *Stud Health Technol Inform* 2009;142:136.
3. van Adrichem LN, van Vlimmeren LA, Cadanova D, et al. Validation of a simple method for measuring cranial deformities (plagiocephalometry). *J Craniofac Surg* 2008;19(1):15.
4. Meuffels DE, Potters JW, Koning AH, et al. Visualization of postoperative anterior cruciate ligament reconstruction bone tunnels: reliability of standard radiographs, CT scans, and 3D virtual reality images. *Acta Orthop* 2011;82(6):699.
5. Bol Raap G, Koning AH, Scohy TV, et al. Virtual reality 3D echocardiography in the assessment of tricuspid valve function after surgical closure of ventricular septal defect. *Cardiovasc Ultrasound* 2007;5:8.
6. van den Bosch AE, Koning AH, Meijboom FJ, et al. Dynamic 3D echocardiography in virtual reality. *Cardiovasc Ultrasound* 2005;3:37.
7. van Oppenraaij RH, Koning AH, Lisman BA, et al. Vasculogenesis and angiogenesis in the first-trimester human placenta: an innovative 3D study using an immersive Virtual Reality system. *Placenta* 2009;30(3):220.
8. Verwoerd-Dikkeboom CM, Koning AH, Hop WC, et al. Innovative virtual reality measurements for embryonic growth and development. *Hum Reprod* 2010;25(6):1404.
9. Verwoerd-Dikkeboom CM, Koning AH, Hop WC, et al. Reliability of three-dimensional sonographic measurements in early pregnancy using virtual reality. *Ultrasound Obstet Gynecol* 2008;32(7):910.
10. Rousian M, Verwoerd-Dikkeboom CM, Koning AH, et al. Early pregnancy volume measurements: validation of ultrasound techniques and new perspectives. *BJOG* 2009;116(2):278.
11. Groenenberg IA, Koning AH, Galjaard RJ, et al. A virtual reality rendition of a fetal meningomyelocele at 32 weeks of gestation. *Ultrasound Obstet Gynecol* 2005;26(7):799.
12. Verwoerd-Dikkeboom CM, Koning AH, Groenenberg IA, et al. Using virtual reality for evaluation of fetal ambiguous genitalia. *Ultrasound Obstet Gynecol* 2008;32(4):510.
13. Rousian M, Verwoerd-Dikkeboom CM, Koning AH, et al. First-trimester umbilical cord and vitelline duct measurements using virtual reality. *Early Hum Dev* 2011;87(2):77.
14. Rousian M, Koning AH, Hop WC, et al. Gestational sac fluid volume measurements in virtual reality. *Ultrasound Obstet Gynecol* 2011;38(5):524.
15. Rousian M, Koning AH, van Oppenraaij RH, et al. An innovative virtual reality technique for automated human embryonic volume measurements. *Hum Reprod* 2010;25(9):2210.
16. Myers LM, Brinkley JF. Visualization of Brain Surface Features Using Registered Partially Segmented MRI Scans. *Image Display; SPIE Medical Imaging* 1995;2431:43.
17. Bland JM, Altman DG. A note on the use of the intraclass correlation coefficient in the evaluation of agreement between two methods of measurement. *Comput Biol Med* 1990;20(5):337.
18. Bland JM, Altman DG. Statistical methods for assessing agreement between two methods of clinical measurement. *Lancet* 1986;1(8476):307.

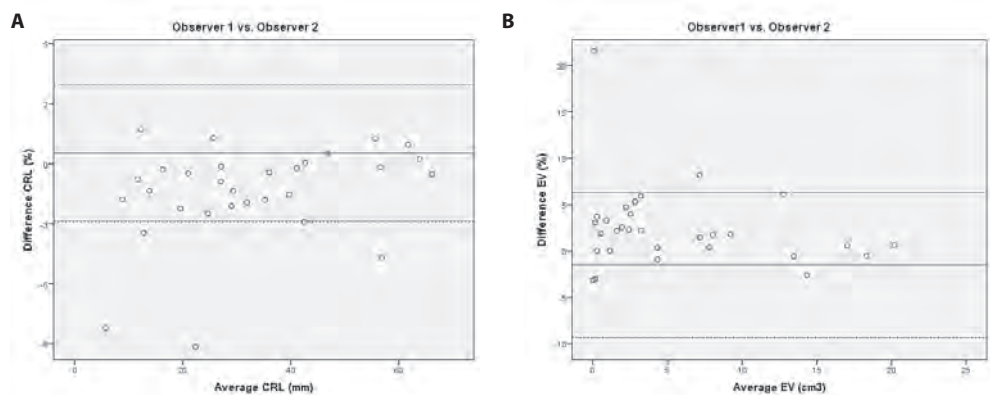
19. Kockro RA, Serra L, Tseng-Tsai Y, et al. Planning and simulation of neurosurgery in a virtual reality environment. *Neurosurgery* 2000;46(1):118.
20. Aviram R, Shpan DK, Markovitch O, et al. Three-dimensional first-trimester fetal volumetry: comparison with crown rump length. *Early Hum Dev* 2004;80(1):1.
21. Falcon O, Peralta CF, Cavoretto P, et al. Fetal trunk and head volume in chromosomally abnormal fetuses at 11+0 to 13+6 weeks of gestation. *Ultrasound Obstet Gynecol* 2005;26(5):517.
22. Baken L, van Heesch PN, Wildschut HJ, et al. First-trimester crown-rump length and embryonic volume of aneuploid fetuses measured in virtual reality. *Ultrasound Obstet Gynecol* 2013;41(5):521.
23. Fajardo-Exposito MA, Hervias B, Gonzalez FB, et al. First-trimester fetal head and trunk volume predict growth disturbance in twin pregnancy. *Prenat Diagn* 2011;31(6):543.
24. Antsaklis A, Anastasakis E, Komita O, et al. First-trimester 3D volumetry. Association of the gestational volumes with the birth weight. *J Matern Fetal Neonatal Med* 2011;24(8):1055.
25. Collins SL, Stevenson GN, Noble JA, et al. Rapid calculation of standardized placental volume at 11 to 13 weeks and the prediction of small for gestational age babies. *Ultrasound Med Biol* 2013;39(2):253.
26. Verwoerd-Dikkeboom CM, van Heesch PN, Koning AH, et al. Embryonic delay in growth and development related to confined placental trisomy 16 mosaicism, diagnosed by I-Space Virtual Reality. *Fertil Steril* 2008;90(5):2017 e19.

Supplemental material

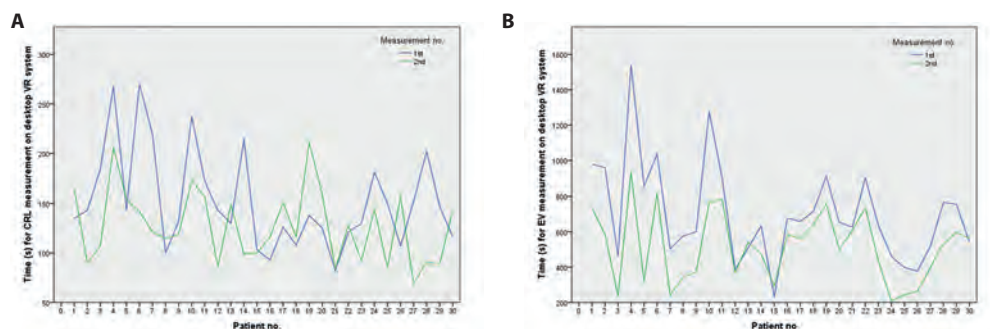
Supplemental Figure 1: Scatter plots comparing the I-Space en 3D VR Desktop system measurements: (A) crown-rump length (CRL); (B) embryonic volume (EV). The line of equality is indicated.



Supplemental Figure 2: Scatter plots comparing the measurements of the two observers: (A) crown-rump length (CRL); (B) embryonic volume (EV). The line of equality is indicated.



Supplemental Figure 3: Bland-Altman plots comparing the measurements of observer 1 (I.v.G.; initial measurement) and observer 2 (L.B.): (A) crown-rump length (CRL) and (B) embryonic volume (EV). The solid line represents the mean percentage difference and the broken lines represent the limits of agreement, calculated as the mean difference ± 1.96 SD.



Supplemental Figure 4: Line diagram showing the time (in seconds) per patient required for crown-rump length (CRL) measurements (A) and embryonic volume (EV) measurements (B) on the desktop 3D virtual reality system. The initial set of measurements is shown in blue and the second set of measurements are shown in green.

Supplemental Table 1: Mean time of the I-Space and 3D VR Desktop-system measurements of two biometric parameters.

Parameter	Technique	Mean time (sec) \pm SD	Mean time (min)
CRL	DT 1 st measurement	152 \pm 49	2:32
	DT 2 nd measurement	127 \pm 37	2:07
	DT 2 nd observer	76 \pm 28	1:16
	I-Space	131 \pm 38	2:11
EV	DT 1 st measurement	701 \pm 279	11:41
	DT 2 nd measurement	514 \pm 201	8:34
	DT 2 nd observer	218 \pm 81	3:38
	I-Space	619 \pm 294	10:19

CRL= crown-rump length, EV= embryonic volume, DT = 3D VR Desktop system, SD = Standard deviation

Supplemental Table 2: Time differences between all measurements.

	Parameters	Median (sec.)	95% CI	p*
I-Space – DT 1st	CRL	-29.50	-42.50 , 1.50	0.054
	EV	-86.50	-166.50 , 0.50	0.052
DT 2nd – DT 1st	CRL	-14.00	-46.00 , -2.50	0.035
	EV	-161.00	-228.00 , -124	<0.001
DT 2nd obs - DT 1st	CRL	-78.00	-107.50 , -69.50	<0.001
	EV	-402.50	-490.00 , -362.50	<0.001
DT 2nd obs – DT 2nd	CRL	-48.00	-63.50 , -36.00	<0.001
	EV	-241.50	-311.50 , -200.00	<0.001

* Wilcoxon signed-rank test

DT 1st = First measurement on 3D VR Desktop system by observer 1

DT 2nd = Second measurement on 3D VR Desktop system by observer 1

DT 2nd obs = Measurement on 3D VR Desktop system by second observer

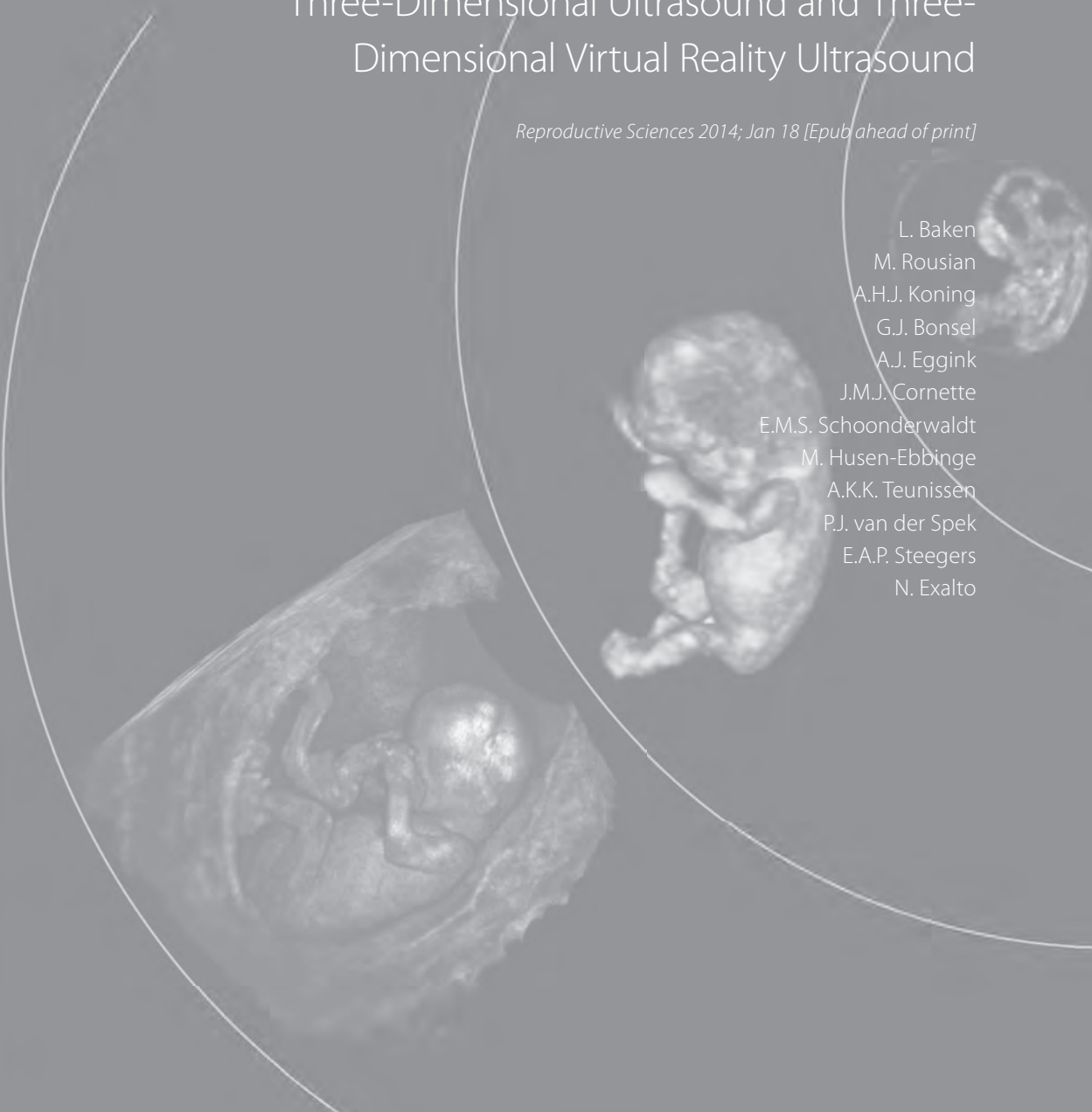
CRL= crown-rump length, EV= embryonic volume, DT = 3D VR Desktop system, 95% CI = 95% confidence interval

2.2

First-Trimester Detection of Surface Abnormalities: a Comparison of Two- and Three-Dimensional Ultrasound and Three-Dimensional Virtual Reality Ultrasound

Reproductive Sciences 2014; Jan 18 [Epub ahead of print]

L. Baken
M. Rousian
A.H.J. Koning
G.J. Bonsel
A.J. Eggink
J.M.J. Cornette
E.M.S. Schoonderwaldt
M. Husen-Ebbinge
A.K.K. Teunissen
P.J. van der Spek
E.A.P. Steegers
N. Exalto



Abstract

The aim was to determine the diagnostic performance of three-dimensional virtual reality ultrasound (3D VR US) and conventional two- and three-dimensional ultrasound (2D/3D US) for first-trimester detection of structural abnormalities. Forty-eight first-trimester cases (gold standard available, 22 normal, 26 abnormal) were evaluated off-line using both techniques by five experienced, blinded, sonographers. We analysed whether the case was correctly classified as (ab)normal, and whether the specific diagnosis was correctly made. Sensitivity in terms of (ab)normal was comparable for both techniques ($p=0.24$). The general sensitivity for specific diagnoses was 62.6% using 3D VR US and 52.2% using 2D/3D US ($p=0.075$). 3D VR US more often correctly diagnosed skeleton/limbs malformations (36.7% vs 10%; $p=0.013$). Mean evaluation time in 3D VR US was 4:24 minutes and in 2D/3D US 2:53 minutes ($p<0.001$). General diagnostic performance of 3D VR US and 2D/3D US apparently is comparable. Malformations of skeleton and limbs are more often detected using 3D VR US. Evaluation time is longer in 3D VR US.

Introduction

There is an increasing interest in detection of structural abnormalities in the first-trimester of pregnancy, in particular in high risk patients. Several factors have contributed to this shift of interest from the third and second trimesters of pregnancy to the first-trimester. First, nuchal translucency (NT) measurements have become available as an effective screening tool for Down syndrome. As a result more structural abnormalities have been detected during the late first-trimester. Second, ongoing technical development of ultrasound (US) equipment continues to improve visualization of first-trimester fetal anatomic structures.

The majority of structural abnormalities can now be detected during a first-trimester ultrasound scan.¹⁻⁶ The reliability of first-trimester screening for structural abnormalities is still at debate. However, if structural abnormalities can be reliably diagnosed in the first-trimester of pregnancy this will allow for earlier informed decision making.

Three-dimensional (3D) US is mainly used complementary to two-dimensional (2D) US in specific cases, where it may provide additional information.⁷ However, 3D US is still presented by means of a 2D medium, which is unable to provide all information offered by the 3D dataset.

In this study we report on a new display technology called virtual reality (VR). This technology aims to further improve visualization by presenting 3D US data as a hologram (3D VR US) in a four-walled CAVE like⁸ VR system in which investigators are surrounded by stereoscopic images (Figure 1C). A hologram is created by the V-Scope rendering application and polarized glasses enable the viewer to perceive depth and to interact with the 3D volume in an intuitive manner.⁹ In a research setting 3D VR US has already successfully been applied for determining various first-trimester reference values, and in individual cases of complex congenital malformations 3D VR US supported the diagnosis by adding clinically relevant details.¹⁰⁻¹⁶

While clinicians rapidly adopted conventional 3D US upon its introduction at the end of the 1990's without formal evaluation⁷, this study aims to provide diagnostic evidence to support a similar decision on 3D VR US. The application is investigated for the use of first-trimester screening for structural abnormalities. Study outcomes are feasibility (in particular evaluation time) and diagnostic accuracy (sensitivity or detection rate) for both 2D/3D US and 3D VR US compared to an independent gold standard.

Methods

In this comparative study 48 pregnancies with known outcomes were assessed by five reviewers unknown to the cases. The two imaging techniques were compared in this study are conventional 2D/3D US (Figure 1A-B) and experimental 3D VR US (Figure 1C). The known outcome (gold standard) is based on all available information at the time of inclusion (mid-gestation US scan, outcome of the pregnancy, pathology report etc.). Twenty-four pregnancies were classified as abnormal due to structural congenital and/or other abnormalities and 24 pregnancies were classified as normal. Study

outcome is limited to feasibility (in particular evaluation time) and diagnostic accuracy, both general and per organ system if a structural abnormality is present. The study was conducted between April and September 2011.

Data collection

Pregnancies were collected from an ongoing study, started in 2009, in which women are recruited for weekly US examinations between 6 and 12 weeks of gestational age (GA) and 2D/3D and 3D VR data are collected.^{14, 15, 17-19} This cohort aims to include uncomplicated pregnancies. Ultrasound examinations are performed transvaginal using a GE Voluson E8 system (GE, Zipf, Austria) with a 9-12 MHz probe. This study is approved by the institutional medical ethical committee.

Selection of used cases and controls

From the pregnancies of this cohort with available 2D/3D and 3D VR data we selected 24 abnormal pregnancies and, randomly, 24 normal pregnancies. Abnormality of pregnancy was determined at the time of inclusion by the clinical obstetrician in charge. Abnormal pregnancies were defined as cases with structural congenital abnormalities and/or maternal uterine abnormalities. All cases were selected on the availability of a postpartum diagnosis or a pathological investigation after termination of pregnancy. Only cases with reasonable image quality were included in the study. For this reason images with poor image quality due to incompleteness of the 3D dataset, an intermediate position of the uterus or movement artifacts were excluded. This diagnosis (normal or abnormal with the specific abnormality) we regard as the gold standard. The selected 24 abnormal cases were matched one to one to normal cases (birth of a child without congenital abnormalities, established in a similar way) with the same GA. The GA, based on the last menstrual period (LMP) or conception date, ranged from 8+2 to 13+5 weeks.

Due to a database error the assumed gold standard changed after reassessment: a twin pregnancy (classified as a normal singleton) and a pregnancy with a uterine myoma (classified as normal) were reclassified into the abnormal group. This led to a distribution of 22 normal and 26 abnormal pregnancies used for analysis. One or more abnormalities were present per case with a total of 54 structural abnormalities in our study population.

In Table 1 the number of included abnormalities per organ system is presented.

Reviewing process

Five sonographers (AE, JC, EMS, MH, KT), experienced in advanced US screening, the so called 'reviewers', evaluated all 48 US volumes once with 2D/3D US and once with 3D VR US. The clinical cases and images were unknown to the reviewers. The reviewers were also unaware of the distribution of normal and abnormal cases. Apart from GA, no other clinical information was provided.

All US volumes were evaluated offline with 2D/3D US using the 4D View software (version 9.1, GE Healthcare, Zipf, Austria) and with 3D VR US using V-Scope software in the BARCO I-Space.⁹ The

reviewers reviewed the 48 cases once using 3D VR US and once using 2D/3D US. To avoid recognition a four week interval was used between the evaluations using the two techniques and as well the order of the cases differed for the two techniques. Findings of the reviewer using the two techniques are therefore treated as independent observations. US volumes were anonymized and assigned an identification number and the reviewers randomly started with either 2D/3D US or 3D VR US. As both the I-Space (3D VR US) and the 4D-View software (2D/3D US) were new to the reviewers, a brief training session preceded the study. In this training session the reviewers were trained to translate, rotate and magnify the volumes, to use the clipping plane and to change the region of interest. No measurements were performed by the reviewers in this study.

During the study, the reviewer had a checklist available for every case containing all traceable structural abnormalities ($n=91$) in the first-trimester of pregnancy grouped by organ system. The reviewer scored for every category if an abnormality was present (or not), and if so which specific abnormality within the category was diagnosed. The time required for completion of the evaluation by the reviewer was recorded by the investigator (LB).

Finally we offered a small survey to each reviewer to record subjective experience with 2D/3D US and 3D VR US.

Analysis of data

Correctness of classification (accuracy) was established in two ways. More permissive accuracy assumed the classification to be accurate if the right organ category was indicated as abnormal, whereas the specific diagnosis did not necessarily had to be correct. Strict accuracy assumed a specific diagnosis to be correct if the diagnosis corresponded with the gold standard. Standard diagnostic performance measures could be calculated for both types of accuracy: sensitivity, specificity, positive likelihood ratio (LR+) and negative likelihood ratio (LR-).

The statistical analysis was complex as there were five reviewers, two techniques, two levels of diagnosis (more permissive and strict accuracy), and 48 cases. The latter number limited the application of multilevel techniques or complex ANOVA-techniques. Instead, we applied exploratory analyses where the five reviewer judgements on one case or one abnormality were treated as five separate observations. Statistical testing and interpretation was conservative in this explorative context.

First we calculated the sensitivity for the detection of structural abnormalities comparing both techniques. A total of 54 individual abnormalities with five reviewers accounts for 270 detected abnormalities as a maximum. At this stage we did not make a difference between cases and reviewers in order to get a rough comparison of sensitivity of 2D/3D US and 3D VR US. Secondly, we computed the average sensitivity, specificity, and other diagnostic measures across cases at the reviewer level. These average performance measures were calculated using the more permissive accuracy and the strict accuracy, respectively. The more permissive approach has a total of 240 (48 cases * 5 reviewers) observations. The strict approach accounts for a total of 21840 (48 cases * 5 reviewers* 91 possible abnormalities) observations.

Furthermore, the agreement among the reviewers in their final judgement and evaluation time of both techniques were analysed.

We used the dependent t-test and the McNemar test for diagnostic performance comparisons and between technique comparisons, and the independent t-test for within technique comparisons (i.e. evaluation time). We evaluated time differences over all cases and when omitting the first five or ten cases, to evaluate the possible effect of a learning curve in terms of time expenditure.

The survey results were used as additional qualitative information to support formal data analysis.

Results

The overall sensitivity of 3D VR US for detecting structural abnormalities was 62.6% (169/270) and was 52.2% (141/270) using 2D/3D US, $p=0.075$ (see Table 1 for a detailed comparison). Sensitivity of 3D VR US compared to 2D/3D US was higher for small details like polydactyly (4/5 vs 1/5) and facial clefts (5/5 vs 2/5) and lower for holoprosencephaly (2/5 vs 5/5). Malformations of skeleton and limbs were significantly more often correctly diagnosed using 3D VR US ($p=0.013$).

Table 1: The number of included abnormalities per organ system and their detection rates (sensitivity) among the five reviewers with both techniques are presented. In total 54 abnormalities were presented in 26 cases.

Structural abnormality	n	3D VR US Detection rate (n (%))	2D/3D US Detection rate (n (%))	p
Uterus	3	3/15 (20)	2/15 (13.3)	1.000
Myoma	1	1/5	1/5	
Subseptus	1	2/5	1/5	
Asherman	1	0/5	0/5	
Twins	6	25/30 (83.3)	22/30 (73.3)	0.248
Bichorionic	2	8/10	7/10	
Mono-chorionic bi-amniotic	2	7/10	7/10	
Acardiac twin	1	5/5	3/5	
Conjoined twins	1	5/5	5/5	
Central nervous system	8	17/40 (42.5)	18/40 (45)	1.000
Exencephaly	5	13/25	13/25	
Holoprosencephaly	1	2/5	5/5	
Spina bifida	2	2/10	0/10	
Face and neck	5	15/25 (60)	12/25 (48)	0.571
Facial cleft	1	5/5	2/5	
Micro/retrognathia	1	0/5	1/5	
(Cystic) hygroma	2	6/10	6/10	
Increased nuchal tranlucency	1	4/5	3/5	

Hydrops	9	34/45 (75.6)	34/45 (75.6)	0.250
Hydrops foetalis	8	29/40	29/40	
Hydrothorax	1	5/5	5/5	
Thoracic	1	2/5 (40)	2/5 (40)	1.000
Ectopia cordis	1	2/5	2/5	
Digestive	10	40/50 (80)	32/50 (64)	0.061
Omphalocele	2	10/10	8/10	
Gastroschisis	2	10/10	7/10	
Large bodywall defects	1	3/5	4/5	
External liver	2	7/10	4/10	
External stomach	2	5/10	5/10	
Intra-abdominal cyste	1	5/5	5/5	
Nephrouinary	2	7/10 (70)	6/10 (60)	1.000
Megacystis	1	4/5	4/5	
Ectopic bladder	1	3/5	2/5	
Skeletal / limbs	6	11/30 (36.7)	3/30 (10)	0.013
Skeletal dysplasia	1	1/5	0/5	
Radial aplasia	1	2/5	1/5	
Split hands/feet	1	2/5	1/5	
Polydactyly	1	4/5	1/5	
Scoliosis	1	1/5	0/5	
Kyphosis	1	1/5	0/5	
Other	4	8/20 (40)	6/20 (30)	1.000
Double yolk sac	1	4/5	3/5	
Umbilical cord cyste	1	4/5	3/5	
Short umbilical cord	2	0/10	0/10	
Total	54	169/270 (62.6)	141/270 (52.2)	

Table 2.1 displays data on the reliability of the two techniques to distinguish normal pregnancies from pregnancies with structural abnormalities. The average sensitivity, specificity, LR+ and LR- were not statistically different.

Table 2.2 shows the same comparison, but now analysing the correctness of the specific diagnoses of structural abnormalities that were made. The average sensitivity, specificity, LR+ and LR- were not statistically different comparing the two techniques.

Furthermore, the agreement between the five reviewers was analysed. The agreement in the distinction between normal and abnormal cases and the agreement on the specific diagnoses were studied separately. The agreement on classifying a case as 'abnormal' was higher for 3D VR US, whereas 2D/3D US had higher agreement in distinguishing the normal pregnancies (supplemental Table 1). A better agreement between the reviewers was observed with 3D VR US as compared to 2D/3D US in

Table 2.1: Test characteristics of 3D VR US versus 2D/3D US in the discernment of abnormal (1 or more structural abnormalities) from normal cases. A and B: two-by-two tables combining all 5 reviewers of respectively 3D VR US and 2D/3D US. C: Average sensitivity, specificity, LR+ and LR- of both techniques. (n=48*5; 26 abnormal cases, 22 normal cases; all judged by 5 different reviewers using both techniques.)

A

3D VR US	Reference		
	Abnormal	Normal	Total
Abnormal	112	29	141
Normal	18	81	99
Total	130	110	240

B

2D/3D US	Reference		
	Abnormal	Normal	Total
Abnormal	106	18	124
Normal	24	92	116
Total	130	110	240

C

	3D VR US	2D/3D US	p
Sens. (SD)	86.2% (2.1)	81.5% (6.3)	0.235
Spec. (SD)	73.6% (14.5)	83.6% (16.6)	0.051
LR+	3.27	4.98	0.339
LR-	0.19	0.22	0.370

3D VR US = three-dimensional virtual reality ultrasound, 2D/3D US = two- and three-dimensional ultrasound, SD = standard deviation, Sens. = sensitivity, Spec. = specificity, LR+ = positive likelihood ratio, LR- = negative likelihood ratio.

diagnosing malformations of the central nervous system (CNS) and malformations of the skeleton and extremities (data available from the authors).

The reported mean time to evaluate a case using 3D VR US was 4:24 minutes and 2:53 minutes using 2D/3D US ($p<0.001$). More time was required with 3D VR US in the evaluation of normal pregnancies (+2:00 minutes $p<0.001$) as well as in pregnancies with structural abnormalities (+1:51 minutes $p<0.001$). If structural abnormalities were present, using 3D VR US time expenditure was less as compared to time expenditure in normal cases (-1:05 min $p<0.001$). This difference was not seen with 2D/3D US (-0:13 min $p=0.152$) (supplemental Table 2). When excluding the first five or ten cases per reviewer the average evaluation time did not change, thereby excluding the possible effect of a learning curve in terms of time expenditure.

The subjective reviewers experience, as reported by the survey, showed that the required information intuitively was provided faster and depth perception was better appreciated in 3D VR US. Operating 3D VR US was reported by the reviewers to be easy.

Table 2.2: Test characteristics of 3D VR US versus 2D/3D US in making the correct diagnosis per case. A and B: two-by-two tables combining all 5 reviewers of respectively 3D VR US and 2D/3D US. C: Average sensitivity, specificity, LR+, and LR- of both techniques. (n=48*5*91; 48 cases (26 abnormal cases, 22 normal cases); 91 possible first-trimester structural abnormalities on score sheet; all cases judged by 5 different reviewers with both techniques). Fifty-four different structural abnormalities were present in the 26 abnormal cases.

A

3D VR US	Reference		
	Structural abnormality	Normal	Total
Structural abnormality	169	76	245
Normal	101	21494	21595
Total	270	21570	21840

B

2D/3D US	Reference		
	Abnormal	Normal	Total
Abnormal	141	64	205
Normal	129	21506	21635
Total	270	21570	21840

C

	3D VR US	2D/3D US	p
Sens. (SD)	62.6% (8.4)	52.2% (9.0)	0.075
Spec. (SD)	99.6% (0.22)	99.7% (0.16)	0.445
LR+	177.6	176.0	0.851
LR-	0.375	0.479	0.074

3D VR US = three-dimensional virtual reality ultrasound, 2D/3D US = two- and three-dimensional ultrasound, SD = standard deviation, Sens. = sensitivity, Spec. = specificity, LR+ = positive likelihood ratio, LR- = negative likelihood ratio

Discussion

The overall sensitivity for the detection of first-trimester structural abnormalities is high for both 3D VR US (62.6%) and 2D/3D US (52.2%; $p_{\text{diff}}=0.075$). Thus, 3D VR US detected 10% more abnormalities, but this difference was not statistically significant. As available studies reported first-trimester detection rates (sensitivity) of structural abnormalities ranging from 18% to 84%^{4, 20-25}, our study results are within the same range.

Whereas overall detection was quite similar, the sensitivity of malformations of the skeleton and extremities was significantly higher using 3D VR US. These malformations included for example polydactyly and radial aplasia. Holoprosencephaly was more often diagnosed using 2D/3D US. It can be envisaged that the more spatial presentation of 3D VR US represents in particular a benefit in abnormalities at the exterior of the embryo, while the regular planes for brain evaluation using 2D/3D US perform better for early detection of holoprosencephaly. This is also emphasized in the survey, where the reviewers stated that better depth perception was perceived using 3D VR US. The reviewers

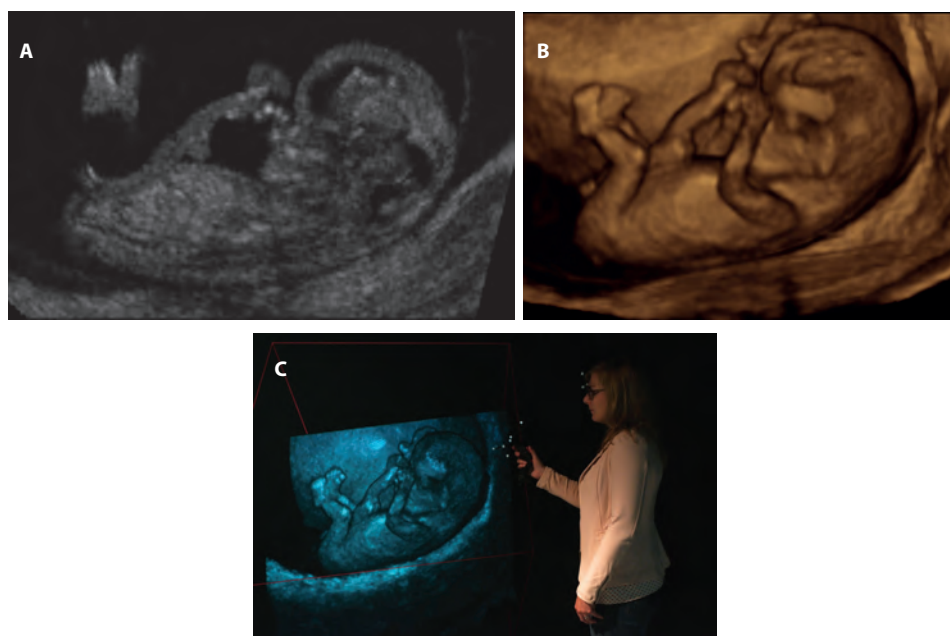


Figure 1: A fetus of 10+3 weeks' gestational age is visualized in (A) two-dimensional ultrasound, (B) three-dimensional ultrasound (3D) and (C) the Barco I-Space 3D virtual reality system. The viewer is wearing polarized glasses and is holding the wireless joystick, both equipped with a tracking system. Please note that this two-dimensional picture cannot express the three-dimensionality of the original 'hologram'.

experience of faster information retrieval and easy to learn technique of 3D VR US further confirmed professional appreciation.

The higher yield and perhaps higher professional appreciation of 3D VR US has a price. The complete evaluation of a case requires on average more time for 3D VR US compared to 2D/3D US, in particular in normal cases. In view of the larger amount of volume data in a hologram compared to 2D/3D US, it requires more time to exclude abnormalities. We believe that more experience will turn this balance more to the advantage of 3D VR US. Remarkably, the reviewers stated in the questionnaire that the information they needed was provided faster using 3D VR US.

Some features of early pregnancy, like the position of the feet and the omphalocele, were scored as pathological while at this stage they are physiological. Before first-trimester screening of structural abnormalities will be effective these misunderstandings have to be elucidated. Other groups of assumed abnormalities showed considerable inter-reviewer differences with both techniques. These included malformations of the abdominal wall, the uterus and the umbilical cord. Foremost this can be explained by lack of experience in evaluation of early pregnancy. This study stresses the need for more basic information on the normal appearance of the early pregnancy. Other studies have shown that with increasing experience at first-trimester ultrasound screening the detection rates (sensitivity) of structural abnormalities increase.^{26, 27}

A lower detection rate than expected on beforehand was seen for some abnormalities. For example, the detection rate of ectopia cordis in this study was 40% for both techniques. This might be explained by the fact that heart action is not visualized in the offline, static images that were used for the evaluation of cases. During real-time ultrasound a detection rate of near 100% is most likely achieved. At this point four-dimensional (4D, the 4th dimension being time) ultrasound is not routinely obtained. These 4D datasets can however also be evaluated using virtual reality thereby overcoming the limitations of static images. Moreover, the detection rate of an increased nuchal fold was detected in 60% of cases using 2D/3D US. Detection rate would likely have been near 100% if the reviewers would have measured the nuchal fold in all cases. However, this would significantly prolong evaluation time and was therefore not performed in this study. Finally, it must be pointed out that 100% of twin pregnancies were detected in this study. The data in Table 1 reflect the percentage of twins that were correctly type regarding chorionicity and amnionity.

A limitation of the study is the retrospective design. We performed thorough blinding to account for this aspect. Furthermore, the retrospective design allows for comparison to a gold standard and therefore investigation of the validity of 3D VR US and 2D/3D US, whereas a prospective study measures the agreement between two techniques. Secondly, due to the wide range and rarity of structural abnormalities we choose to select our cases, instead of following a cohort, for efficiency reasons. This can be seen as another limitation of the study. A third limitation is the small number of studied cases. We deliberately aimed for a proof of concept study. Now we know that 3D VR US has the promise of improving the detection of first-trimester structural abnormalities, larger size studies are warranted to study the effect of 3D VR US in routine conditions. Agreeable, the BARCO I-Space does not lend itself for wide spread dissemination as it is too large (requiring a separate room of at least 40m²/400 sq. ft.) and too expensive (approximately 500,000 USD). However, a desktop version of this 3D VR US system is developed, making this new and innovative technique broadly accessible to hospitals in the near future. A prototype is being evaluated at our department for use in daily clinical practice, and if successful, performance data like the ones shown in this paper can be established over time.

We conclude that in this proof of concept study the diagnostic performance of 3D VR US and 2D/3D US are statistically equal. A higher sensitivity was observed for abnormalities of skeleton and limbs in 3D VR US. Results suggest an additive value of 3D VR US in specific cases. As the time required for completion of the procedure was about two minutes longer for 3D VR US and reviewers subjectively reported better representation, the technique for now might be implemented under research conditions.

References

1. Persico N, Moratalla J, Lombardi CM, Zidere V, Allan L, Nicolaides KH. Fetal echocardiography at 11-13 weeks by transabdominal high-frequency ultrasound. *Ultrasound Obstet Gynecol.* 2011;37(3):296-301.
2. Chaoui R, Nicolaides KH. Detecting open spina bifida at the 11-13-week scan by assessing intracranial translucency and the posterior brain region: mid-sagittal or axial plane? *Ultrasound Obstet Gynecol.* 2011;38(6):609-12.
3. Syngelaki A, Chelemen T, Dagklis T, Allan L, Nicolaides KH. Challenges in the diagnosis of fetal non-chromosomal abnormalities at 11-13 weeks. *Prenat Diagn.* 2011;31(1):90-102.
4. Whitlow BJ, Chatzipapas IK, Lazanakis ML, Kadir RA, Economides DL. The value of sonography in early pregnancy for the detection of fetal abnormalities in an unselected population. *Br J Obstet Gynaecol.* 1999;106(9):929-36.
5. Saltvedt S, Almstrom H, Kublickas M, Valentin L, Grunewald C. Detection of malformations in chromosomally normal fetuses by routine ultrasound at 12 or 18 weeks of gestation-a randomised controlled trial in 39,572 pregnancies. *BJOG.* 2006;113(6):664-74.
6. Nicolaides KH. A model for a new pyramid of prenatal care based on the 11 to 13 weeks' assessment. *Prenat Diagn.* 2011;31(1):3-6.
7. Duckelmann AM, Kalache KD. Three-dimensional ultrasound in evaluating the fetus. *Prenat Diagn.* 2010;30(7):631-8.
8. Cruz-Neira C, Sandin D, DeFanti T. Surround-screen projection-based virtual reality: the design and implementation of the CAVE (tm). *Proceedings of the 20th annual conference on computer graphics and interactive techniques*; New York: ACM Press; 1993.
9. Koning AH, Rousian M, Verwoerd-Dikkeboom CM, Goedknecht L, Steegers EA, van der Spek PJ. V-scope: design and implementation of an immersive and desktop virtual reality volume visualization system. *Stud Health Technol Inform.* 2009;142:136-8.
10. Verwoerd-Dikkeboom CM, Koning AH, Groenenberg IA, Smit BJ, Brezinka C, Van Der Spek PJ, et al. Using virtual reality for evaluation of fetal ambiguous genitalia. *Ultrasound Obstet Gynecol.* 2008;32(4):510-4.
11. Verwoerd-Dikkeboom CM, van Heesch PN, Koning AH, Galjaard RJ, Exalto N, Steegers EA. Embryonic delay in growth and development related to confined placental trisomy 16 mosaicism, diagnosed by I-Space Virtual Reality. *Fertil Steril.* 2008;90(5):2017 e19-22.
12. Groenenberg IA, Koning AH, Galjaard RJ, Steegers EA, Brezinka C, van der Spek PJ. A virtual reality rendition of a fetal meningomyelocele at 32 weeks of gestation. *Ultrasound Obstet Gynecol.* 2005;26(7):799-801.
13. Rousian M, Koning AH, Hop WC, van der Spek PJ, Exalto N, Steegers EA. Gestational sac fluid volume measurements in virtual reality. *Ultrasound Obstet Gynecol.* 2011.
14. Rousian M, Koning AH, van Oppenraaij RH, Hop WC, Verwoerd-Dikkeboom CM, van der Spek PJ, et al. An innovative virtual reality technique for automated human embryonic volume measurements. *Hum Reprod.* 2010;25(9):2210-6.
15. Rousian M, Verwoerd-Dikkeboom CM, Koning AH, Hop WC, van der Spek PJ, Exalto N, et al. Early pregnancy volume measurements: validation of ultrasound techniques and new perspectives. *BJOG.* 2009;116(2):278-85.

16. Verwoerd-Dikkeboom CM, Koning AH, Hop WC, Rousian M, Van Der Spek PJ, Exalto N, et al. Reliability of three-dimensional sonographic measurements in early pregnancy using virtual reality. *Ultrasound Obstet Gynecol.* 2008;32(7):910-6.
17. Rousian M, Koning AH, Hop WC, van der Spek PJ, Exalto N, Steegers EA. Gestational sac fluid volume measurements in virtual reality. *Ultrasound Obstet Gynecol.* 2011;38(5):524-9.
18. Verwoerd-Dikkeboom CM, Koning AH, Hop WC, van der Spek PJ, Exalto N, Steegers EA. Innovative virtual reality measurements for embryonic growth and development. *Hum Reprod.* 2010;25(6):1404-10.
19. Verwoerd-Dikkeboom CM, Koning AH, van der Spek PJ, Exalto N, Steegers EA. Embryonic staging using a 3D virtual reality system. *Hum Reprod.* 2008;23(7):1479-84.
20. Hernadi L, Torocsik M. Screening for fetal anomalies in the 12th week of pregnancy by transvaginal sonography in an unselected population. *Prenat Diagn.* 1997;17(8):753-9.
21. D'Ottavio G, Mandruzzato G, Meir YJ, Rustico MA, Fischer-Tamaro L, Conoscenti G, et al. Comparisons of first and second trimester screening for fetal anomalies. *Ann N Y Acad Sci.* 1998;847:200-9.
22. Carvalho MH, Brizot ML, Lopes LM, Chiba CH, Miyadahira S, Zugaib M. Detection of fetal structural abnormalities at the 11-14 week ultrasound scan. *Prenat Diagn.* 2002;22(1):1-4.
23. Taipale P, Ammala M, Salonen R, Hiilesmaa V. Two-stage ultrasonography in screening for fetal anomalies at 13-14 and 18-22 weeks of gestation. *Acta Obstet Gynecol Scand.* 2004;83(12):1141-6.
24. Souka AP, Pilalis A, Kavalakis I, Antsaklis P, Papantoniou N, Mesogitis S, et al. Screening for major structural abnormalities at the 11- to 14-week ultrasound scan. *Am J Obstet Gynecol.* 2006;194(2):393-6.
25. Becker R, Wegner RD. Detailed screening for fetal anomalies and cardiac defects at the 11-13-week scan. *Ultrasound Obstet Gynecol.* 2006;27(6):613-8.
26. Levi S, Schaaps JP, De Havay P, Coulon R, Defoort P. End-result of routine ultrasound screening for congenital anomalies: the Belgian Multicentric Study 1984-92. *Ultrasound Obstet Gynecol.* 1995;5(6):366-71.
27. Taipale P, Ammala M, Salonen R, Hiilesmaa V. Learning curve in ultrasonographic screening for selected fetal structural anomalies in early pregnancy. *Obstet Gynecol.* 2003;101(2):273-8.

Supplemental Material

Supplemental table 1: Agreement between reviewers in the discernment of abnormal (1 or more structural abnormalities) from normal pregnancies where misclassification of the specific diagnosis was allowed for in the same organ category (permissive accuracy). The upper table shows the results for 3D virtual reality ultrasound (3D VR US), the lower table shows the results for 2D/3D ultrasound (2D/3D US). 5-0 = Five reviewers agreed on the case to be normal/with abnormalities. 4-1 = Four reviewers agreed, 1 disagreed etc.

Reference	3D VR US						
	5-0	4-1	3-2	2-3	1-4	0-5	Total
Abnormal	19	2	2	1	1	1	26
Normal	5	8	6	3	0	0	22
Total	24	10	8	4	1	1	48

Reference	2D/3D US						
	5-0	4-1	3-2	2-3	1-4	0-5	Total
Abnormal	15	4	4	1	1	1	26
Normal	9	8	4	1	0	0	22
Total	24	12	8	2	1	1	48

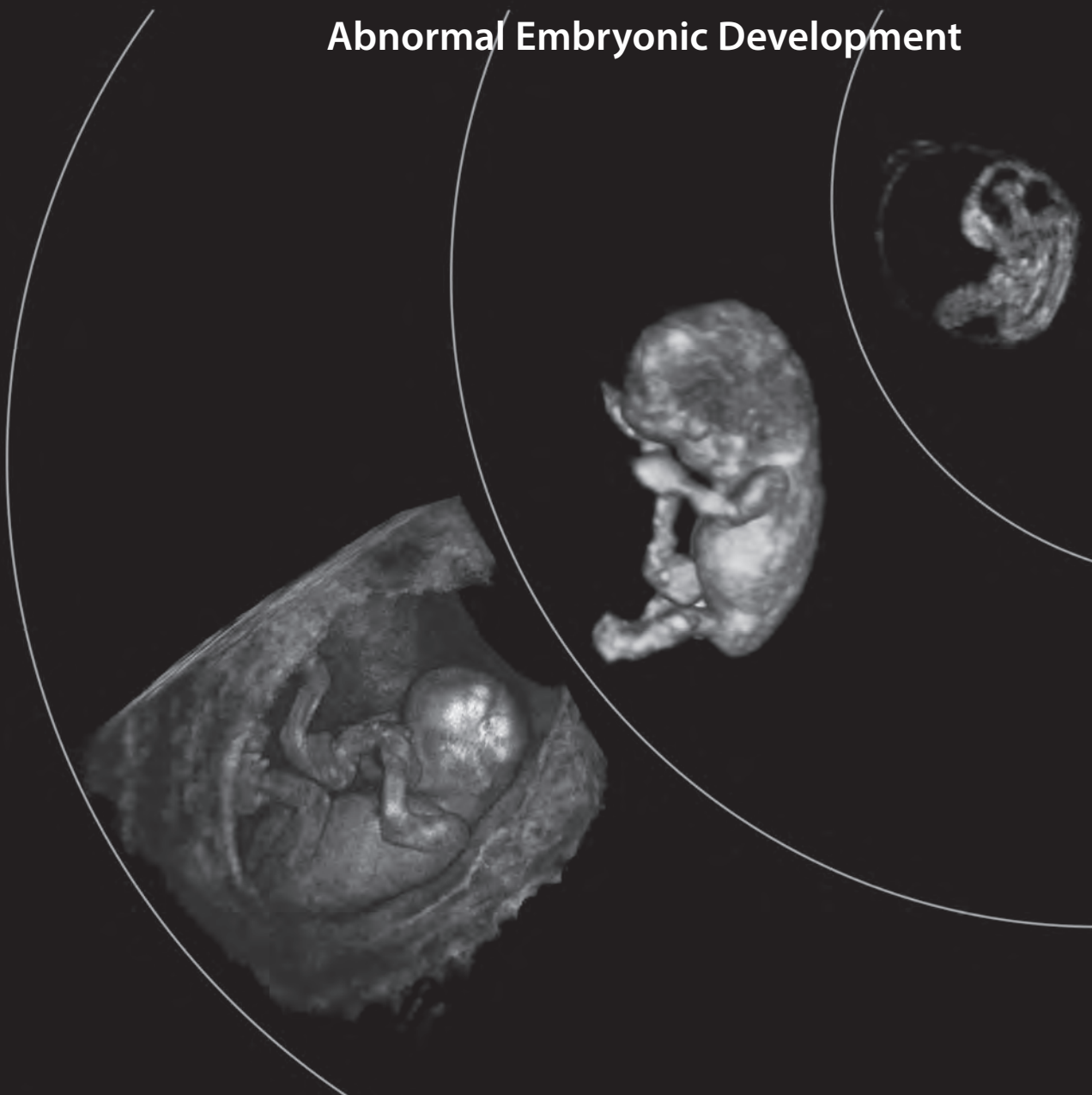
Supplemental Table 2: Mean time required for evaluation of an ultrasound volume, expressed in minutes.

	Mean (SD)	Mean difference	p
All cases			
3D VR US	4:24 (2:00)	1:31	<0.001
2D/3D US	2:53 (1:11)		
Abnormal			
3D VR US	3:56 (1:43)	1:51	<0.001
2D/3D US	2:47 (1:12)		
Normal			
3D VR US	5:01 (2:09)	2:00	<0.001
2D/3D US	3:00 (1:09)		
3D VR US			
Abnormal	3:56 (1:43)	-1:05	<0.001
Normal	5:01 (2:09)		
2D/3D US			
Abnormal	2:47 (1:12)	-0:13	0.152
Normal	3:00 (1:09)		

3D VR US = three-dimensional virtual reality ultrasound, 2D/3D US = two- and three-dimensional ultrasound

CHAPTER 3

Automated Embryonic Volume Measurements in the Detection of Abnormal Embryonic Development

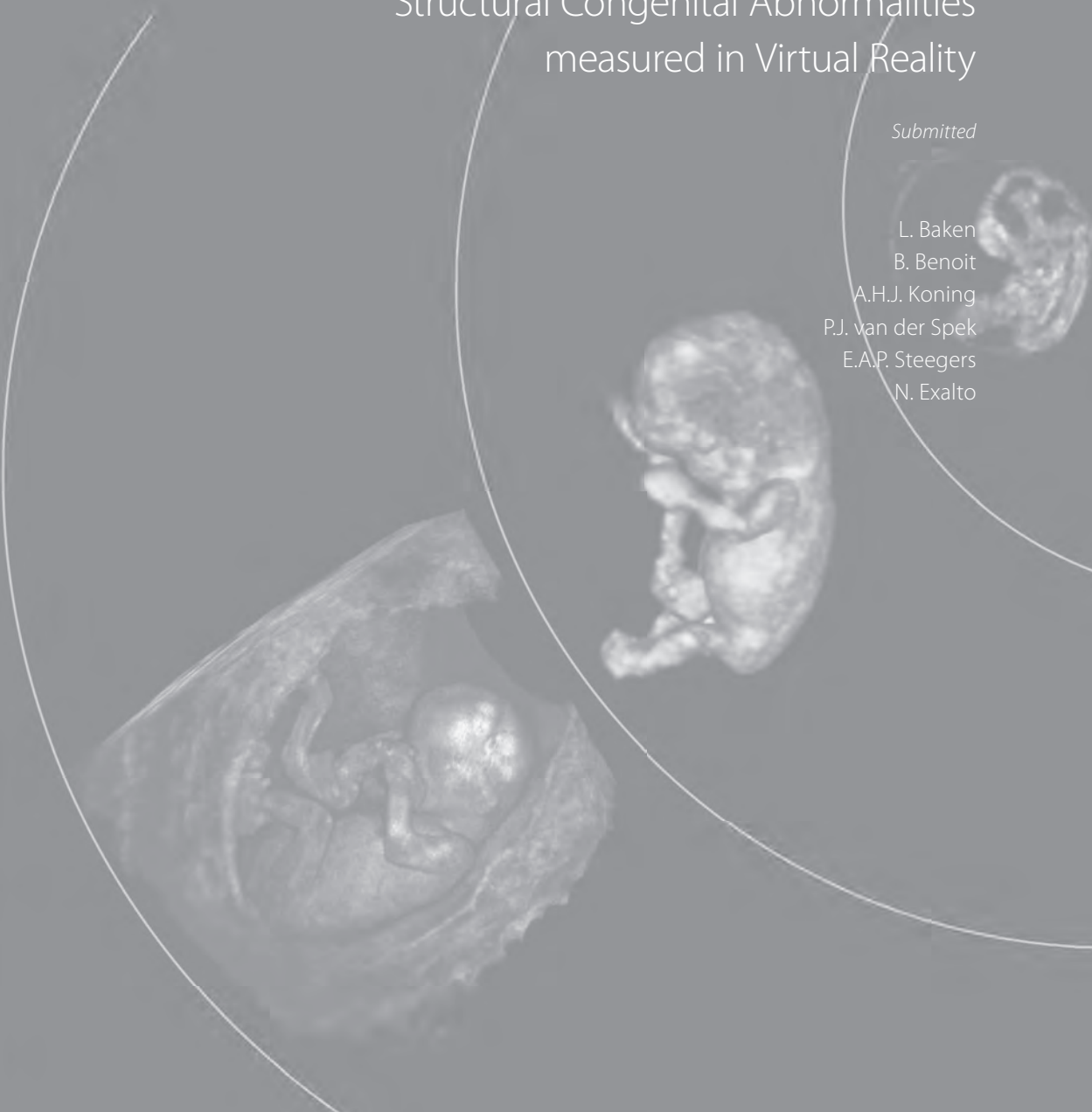


3.1

First-Trimester Crown-rump Length and Embryonic Volume of Fetuses with Structural Congenital Abnormalities measured in Virtual Reality

Submitted

L. Baken
B. Benoit
A.H.J. Koning
P.J. van der Spek
E.A.P. Steegers
N. Exalto



Abstract

Objectives. A significant proportion of structural congenital abnormalities can be detected during the first-trimester of pregnancy. With the introduction of three-dimensional (3D) ultrasound it has become possible to measure volumes. As the relative increase in embryonic volume (EV) is much larger than that of the crown-rump length (CRL) over the same time period, we examined whether EV is a better measure of growth restriction in fetuses with structural congenital abnormalities.

Methods. CRL and EV were measured using a Barco I-Space virtual reality (VR) system in prospectively collected 3D ultrasound volumes of 56 fetuses supposed to be euploid and diagnosed with structural congenital abnormalities in the first-trimester of pregnancy (gestational age 7⁺⁵ to 14⁺⁵ weeks). Measured CRL and EV were converted to *z*-scores and to percentages of the expected mean using previously published reference curves of euploid fetuses. The one-sample *t*-test was used to test significance.

Results. The EV was smaller than expected for gestational age in fetuses with structural congenital abnormalities (-35% *p*<0.001, *z*-score -1.44 *p*<0.001), whereas CRL was not smaller than expected (-6.43% *p*=0.118, *z*-score -0.43 *p*=0.605). After correction of EV for the observed CRL the statistical differences were no longer present, suggesting proportional growth restriction.

Conclusions. CRL is a less reliable indicator for growth restriction in fetuses with structural congenital abnormalities as compared to EV. By measuring EV, growth restriction in first-trimester fetuses with structural congenital abnormalities becomes more evident and might enable an earlier detection of these cases. The underlying pathophysiology of structural congenital abnormalities seems to impair first-trimester growth.

Introduction

In the past decade prenatal screening has shifted from the second-trimester to the first-trimester of pregnancy. Because of vast improvements in imaging technology the embryo and fetus in early pregnancy can be evaluated in much more detail allowing screening for structural abnormalities between 11 and 14 weeks GA.¹⁻⁵ A significant proportion of major structural abnormalities can be detected already in this period. In some cases, non-specific findings, like increased nuchal translucency, may be the first sign for existing structural abnormalities, leading to additional ultrasound examinations.⁶

It is well known that first-trimester growth is associated with pregnancy outcome⁷⁻¹⁰ and that several factors influence first-trimester growth.¹¹⁻¹⁵ Traditionally, first-trimester fetal growth has been documented by two-dimensional (2D) crown-rump length (CRL) measurements. With the introduction of three-dimensional (3D) ultrasound it has become possible to measure embryonic volumes (EV). Earlier studies show that the relative increment of the EV is much larger than the increment of the CRL during the same period.¹⁶ Using an innovative 3D virtual reality (VR) technique, Rousian *et al.* demonstrated that when the CRL doubles the EV increases 6.5-fold.¹⁶ Volume measurement might therefore enable earlier detection of fetal growth restriction in pregnancy. It is well known that a too small CRL is a clinical predictor for miscarriage, chromosomal abnormalities (especially trisomy 18) and fetal growth restriction in the second and third trimester of pregnancy.^{10, 17-20} It has been suggested that EV is smaller in aneuploid pregnancies and by using VR it was proven that, compared to CRL, EV was not only smaller in trisomy 18 pregnancies but also in trisomy 21 and trisomy 13 pregnancies.^{21, 22} EV therefore turns out to be a better measure for growth restriction caused by aneuploidy than CRL.

From these observations it is suspected that underlying pathophysiological changes in these cases might influence embryonic and early fetal growth. First-trimester growth might also be impaired in pregnancies diagnosed with a congenital abnormality. An association between the presence of structural congenital abnormalities and second- and third-trimester growth restriction has been previously found.²³⁻²⁵

The aim of this study is to examine the first-trimester growth pattern in embryos and fetuses with structural congenital abnormalities. CRL and EV are compared between pregnancies with and without first-trimester structural congenital abnormalities.

Methods

Between December 2008 and November 2013 three-dimensional (3D) ultrasound volumes were collected of first-trimester pregnancies in which a structural congenital abnormality was diagnosed ($n=71$). Cases were collected at the department of Obstetrics and Prenatal Medicine at Erasmus MC University Medical Center Rotterdam ($n=47$) and at Princess Grace Hospital in Monaco ($n=15$). An additional nine cases were included from the Rotterdam Predict study^{11, 12, 26-29}, a periconception cohort aimed at early pregnancy. Ultrasound scans were performed using the Voluson E8 Expert system (GE Medical Systems, Zipf, Austria).

In spontaneously conceived pregnancies dating was based on the first day of the last menstrual period (LMP). When the menstrual cycle was regular but >3 days different from 28 days the gestational

age (GA) was adjusted for the cycle length. In pregnancies conceived by *in vitro* fertilization (IVF) with or without intra-cytoplasmic sperm injection (ICSI) GA was calculated from the day of oocyte retrieval plus 14 days. If the first day of the LMP was missing or if the menstrual cycle was irregular, these pregnancies were excluded from this analysis. The GA ranged from 7⁺⁵ to 14⁺⁵ weeks.

The 3D volumes were converted to Cartesian volumes, using 3D software (4D View, GE Medical Systems, Zipf, Austria), and transferred to the BARCO (Kortrijk, Belgium) I-Space VR system at the department of Bioinformatics of Erasmus MC University Medical Center Rotterdam. This is a four-walled CAVE™ like³⁰ VR system in which investigators are surrounded by stereoscopic images. A 'hologram' of the ultrasound data is created by the V-Scope³¹ volume rendering application (Erasmus MC, Rotterdam, the Netherlands) and polarized glasses enable the viewer to perceive depth and to interact with 3D volumes in an intuitive manner. In the I-Space all 3D ultrasound volumes were evaluated and the best volume for each case was selected based on image quality and completeness of the volume. A fetus with structural congenital abnormalities visualised in VR is shown in Figure 1.

CRL and EV were measured in the BARCO I-Space using the V-Scope software. The V-Scope³¹ application includes a region-growing segmentation algorithm for semi-automatical volume calculation in selected structures.^{30, 31} The innovative VR technique has already successfully been applied in various prenatal studies.³²⁻³⁴

The procedure for measuring EV is described in detail by Rousian et. al.¹⁶ The omphalocele, physiological or pathological, is included in the EV calculation as well as hydrops, frequently present in fetuses with structural congenital abnormalities. All measurements were performed by the same investigator (LB). The accuracy and reproducibility of CRL and EV measurements has been proven in previous



Figure 1: Transvaginal ultrasound dataset of a fetus with ectrodactyly ectodermal dysplasia-cleft (EEC) syndrome in virtual reality. Bilateral split hands and splits feet are seen as well as a bilateral cheilo-gnathoschisis. An overriding aorta with a ventricle septum defect was diagnosed additionally.

studies and CRL and EV reference curves have been established.^{16, 35-37} The data of the present study are compared to these reference curves.

Statistical analysis

The observed CRL and EV were subtracted from the expected mean CRL and EV of reference fetuses of the same GA. This expected value was obtained from reference curves published in earlier studies.^{16, 36, 37} This difference was expressed as the *z*-score and as a percentage of the mean CRL and EV of reference fetuses. The same analysis was performed when the EV was corrected for the measured CRL.

The one-sample *t*-test was used to test for statistically significant differences between observed values of CRL and EV in pregnancies with a structural congenital abnormality and expected values of CRL and EV in reference pregnancies. This analysis was performed in the overall group of cases with structural congenital abnormalities and in the different subgroups of various structural congenital abnormalities.

Data analysis was performed using SPSS v.21 (SPSS Inc., Chicago, IL, USA). A *p*-value <0.05 was considered statistically significant.

Results

Three cases were excluded from the analysis because of uncertain GA and one because of a twin pregnancy. We excluded 11 cases for the measurements of both CRL and EV due to poor image quality (*n*=9), due to incompleteness of the volume (*n*=1) and because of negative heart action at the time of the ultrasound scan (*n*=1). A total of 56 cases remained for analysis of CRL. As in five of these cases the image quality was too poor for performing EV measurement 51 cases remained for analysis of EV.

In the overall group of fetuses with structural congenital abnormalities the EV was smaller than expected for GA (-35% *p*<0.001, *z*-score -1.44 *p*<0.001), whereas CRL was not smaller than expected

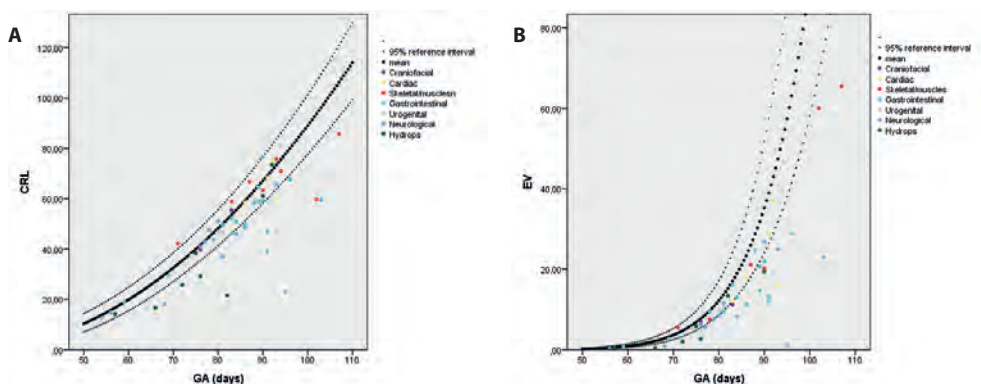


Figure 2: CRL and EV of all cases with structural congenital abnormalities plotted relative to the reference curves for healthy pregnancies.

Table 1: Mean percentage difference and z-scores for CRL and EV in both the overall group of structural congenital abnormalities and in the various subgroups.

Variable / congenital abnormality	Mean difference in:				
	n	% (95% CI)	p*	z-score (95% CI)	p*
<i>CRL</i>					
Overall	56	-6.43 (-14.55,1.69)	0.118	-0.46 (-2.21,1.30)	0.605
Craniofacial	2	-0.60 (-50.36,49.15)	0.903	-0.05 (-6.25,6.15)	0.931
Cardiac	5	-5.03 (-16.46,6.39)	0.288	-1.34 (-2.27,0.90)	0.296
Skeletal/muscles	8	-3.02 (-18.58,12.54)	0.660	-0.55 (-2.62,1.51)	0.547
Gastro-intestinal	15	-7.02 (-18.05,4.02)	0.194	-1.08 (-2.44,0.28)	0.111
Urogenital	5	-4.98 (-7.87,-2.09)	0.009	-0.64 (-1.04,-0.25)	0.010
Neurological	14	0.12 (-30.53,30.77)	0.993	1.59 (-5.74,8.94)	0.646
Hydrops	7	-26.89 (-43.26,-8.51)	0.011	-2.94 (-5.18,-0.71)	0.018
<i>EV</i>					
Overall	51	-34.91 (-41.97,-27.85)	<0.001	-1.44 (-1.71,-1.16)	<0.001
Craniofacial	2	-21.22 (-187.3,144.85)	0.351	-1.00 (-8.73,6.73)	0.349
Cardiac	5	-31.86 (-56.43,-7.28)	0.023	-1.34 (-2.30,-0.39)	0.017
Skeletal/muscles	6	-26.18 (-60.67,8.30)	0.108	-0.92 (-2.21,0.37)	0.127
Gastro-intestinal	13	-35.78 (-49.45,-22.11)	<0.001	-1.53 (-2.09,-0.96)	<0.001
Urogenital	4	-16.26 (-25.21,-7.31)	0.010	-0.75 (-1.22,-0.27)	0.016
Neurological	14	-43.24 (-59.20,-27.28)	<0.001	-1.70 (-2.27,-1.13)	<0.001
Hydrops	7	-40.85 (-66.34,-15.36)	0.008	-1.76 (-2.88,-0.64)	0.008

*For observed mean difference vs 0.

Table 2: The mean percentage differences and z-scores for EV after correction for the observed CRL both in the overall group of structural congenital abnormalities and the subgroups of structural congenital abnormalities.

Variable / congenital abnormality	Mean difference in:				
	n	% (95% CI)	p*	z-score (95% CI)	p*
<i>EV</i>					
Overall	51	27.86 (-14.34,70.05)	0.191	0.92 (-0.66,2.49)	0.247
Craniofacial	2	-6.18 (-266.27,253.92)	0.813	-0.40 (-11.64,10.84)	0.730
Cardiac	5	2.90 (-11.97,17.76)	0.617	-0.10 (-0.71,0.51)	0.673
Skeletal/muscles	6	29.69 (-71.29,130.66)	0.484	0.88 (-3.07,4.82)	0.591
Gastro-intestinal	13	14.94 (-4.72,34.60)	0.124	0.47 (-0.38,1.31)	0.254
Urogenital	4	4.95 (-2.93,12.82)	0.139	0.008 (-27.34,28.98)	0.932
Neurological	14	-1.82 (-25.66,22.03)	0.872	-0.12 (-1.11,0.87)	0.798
Hydrops	7	150.26 (-211.03,511.54)	0.348	5.50 (-7.89,18.89)	0.354

*For observed mean difference vs 0.

(-6.43% $p=0.118$, z -score -0.43 $p=0.605$). The CRL was significantly smaller in the subgroups with urogenital abnormalities and in the subgroup with hydropic abnormalities. The EV was significantly smaller in the subgroup with cardiac abnormalities, gastro-intestinal abnormalities, urogenital abnormalities, neurological abnormalities, and in the group with hydropic abnormalities (Table 1).

In Figure 2 CRL and EV of all cases with structural congenital abnormalities are plotted in the reference curves for pregnancies without structural congenital abnormalities.

In Table 2 the percentage difference and z -score for observed versus expected EV after correction for the observed CRL is presented. No statistical differences were found.

Discussion

To the best of our knowledge this is the first study that investigates the relationship between EV and first-trimester structural congenital abnormalities. Whereas overall the CRL was not significantly smaller in fetuses with structural congenital abnormalities, a smaller than expected CRL was observed in hydropic fetuses and fetuses with urogenital abnormalities. In contrast to CRL, EV was statistically significant smaller than expected in the overall group of structural congenital abnormalities. In all subgroups, except for those with craniofacial and skeletal/muscle abnormalities, we found a significantly smaller EV than expected.

The mean difference in EV was more evident than the mean difference in CRL and went up to -43% (z -score -1.70) in fetuses with neurological abnormalities. This can be explained by the fact that a volume is a three-dimensional measurement in contrast to CRL which is a flat, two-dimensional distance measurement. It was already demonstrated by Rousian *et al.* that when the CRL doubles EV increases 6.5 times.¹⁶ However, after correcting the EV for the measured CRL significant differences were no longer present suggesting proportional growth restriction. EV turned out to be a better indicator for first-trimester growth restriction as compared to CRL.

From the literature it has recently become evident that a detailed anatomical scan can be successfully performed at the end of the first-trimester. The majority of major structural congenital abnormalities can therefore be diagnosed between 11 and 14 weeks GA. EV measurements can be performed from 6 weeks GA onwards¹⁶ and may therefore possibly be used as a marker of an underlying abnormality long before an early anomaly scan can be performed. The effectiveness of EV as a marker for structural congenital abnormalities should be subject of further study.

The combination of early growth restriction and the presence of structural congenital abnormalities might be due to underlying pathological mechanisms. Growth restriction might either occur as a result of a structural congenital abnormality or growth restriction and structural congenital abnormalities might have a common etiological factor.

Limitations of the study are the low numbers in some of the subgroups of structural congenital abnormalities. Still finding significant differences for EV suggest a strong relationship of first-trimester structural congenital abnormalities and a decreased EV. Therefore, increasing the numbers in future studies will most likely only strengthen this relationship. Pregnancies with known chromosomal

abnormalities were not included in the study. However, as fetal karyotyping was not performed in all cases it may be possible that a single case with a chromosomal abnormality in our study group remained unnoticed. Furthermore, the BARCO I-Space is too large and too expensive to become a routine method for the measurement of EV. However, a much smaller and more affordable 3D VR desktop system is currently being evaluated and will provide a good alternative, making this technique broadly available to hospitals.

In conclusion, CRL, the current golden standard for the detection of first-trimester growth restriction, seems a less reliable indicator for growth restriction in fetuses with structural congenital abnormalities as compared to EV, which is significantly decreased in these pregnancies. By measuring EV, first-trimester growth restriction becomes more evident and might enable an earlier detection of cases at risk for a congenital abnormality.

References

1. Sonek J. First-trimester ultrasonography in screening and detection of fetal anomalies. *Am J Med Genet C Semin Med Genet.* 2007;145C(1):45-61.
2. Katorza E, Achiron R. Early pregnancy scanning for fetal anomalies—the new standard? *Clin Obstet Gynecol.* 2012;55(1):199-216.
3. Iliescu D, Tudorache S, Comanescu A, Antsaklis P, Cotarcea S, Novac L, et al. Improved detection rate of structural abnormalities in the first-trimester using an extended examination protocol. *Ultrasound Obstet Gynecol.* 2013.
4. Donnelly JC, Malone FD. Early fetal anatomical sonography. *Best Pract Res Clin Obstet Gynaecol.* 2012;26(5):561-73.
5. Becker R, Wegner RD. Detailed screening for fetal anomalies and cardiac defects at the 11-13-week scan. *Ultrasound Obstet Gynecol.* 2006;27(6):613-8.
6. Salman Guraya S. The associations of nuchal translucency and fetal abnormalities; significance and implications. *J Clin Diagn Res.* 2013;7(5):936-41.
7. Abuelghar WM, Fathi HM, Ellaithy MI, Anwar MA. Can a smaller than expected crown-rump length reliably predict the occurrence of subsequent miscarriage in a viable first-trimester pregnancy? *J Obstet Gynaecol Res.* 2013;39(10):1449-55.
8. Choong S, Rombauts L, Ugoni A, Meagher S. Ultrasound prediction of risk of spontaneous miscarriage in live embryos from assisted conceptions. *Ultrasound Obstet Gynecol.* 2003;22(6):571-7.
9. Papaioannou GI, Syngelaki A, Maiz N, Ross JA, Nicolaides KH. Ultrasonographic prediction of early miscarriage. *Hum Reprod.* 2011;26(7):1685-92.
10. D'Antonio F, Khalil A, Mantovani E, Thilaganathan B, Southwest Thames Obstetric Research C. Embryonic growth discordance and early fetal loss: the STORK multiple pregnancy cohort and systematic review. *Hum Reprod.* 2013;28(10):2621-7.
11. van Uiter E, van Ginkel S, Willemsen S, Lindemans J, Koning A, Eilers P, et al. An optimal periconception maternal folate status for embryonic size: the Rotterdam Predict study. *BJOG.* 2014.
12. van Uiter EM, van der Elst-Otte N, Wilbers JJ, Exalto N, Willemsen SP, Eilers PH, et al. Periconception maternal characteristics and embryonic growth trajectories: the Rotterdam Predict study. *Hum Reprod.* 2013;28(12):3188-96.
13. Mook-Kanamori DO, Steegers EA, Eilers PH, Raat H, Hofman A, Jaddoe VW. Risk factors and outcomes associated with first-trimester fetal growth restriction. *JAMA.* 2010;303(6):527-34.
14. Bottomley C, Daemen A, Mukri F, Papageorgiou AT, Kirk E, Pexsters A, et al. Assessing first-trimester growth: the influence of ethnic background and maternal age. *Hum Reprod.* 2009;24(2):284-90.
15. Bouwland-Both MI, Steegers-Theunissen RP, Vujkovic M, Lesaffre EM, Mook-Kanamori DO, Hofman A, et al. A periconceptional energy-rich dietary pattern is associated with early fetal growth: the Generation R study. *BJOG.* 2013;120(4):435-45.
16. Rousian M, Koning AH, van Oppenraaij RH, Hop WC, Verwoerd-Dikkeboom CM, van der Spek PJ, et al. An innovative virtual reality technique for automated human embryonic volume measurements. *Hum Reprod.* 2010;25(9):2210-6.

17. Dickey RP, Gasser RF, Olar TT, Curole DN, Taylor SN, Matulich EM, et al. The relationship of initial embryo crown—rump length to pregnancy outcome and abortion karyotype based on new growth curves for the 2-31 mm embryo. *Hum Reprod.* 1994;9(2):366-73.
18. Bukowski R, Gahn D, Denning J, Saade G. Impairment of growth in fetuses destined to deliver preterm. *Am J Obstet Gynecol.* 2001;185(2):463-7.
19. Vafaei H, Samsami A, Zolghadri J, Hosseini-Nohadani A. Correlation of first-trimester fetal crown-rump length with outcome of pregnancy and birth weight. *Int J Gynaecol Obstet.* 2012;119(2):141-4.
20. Smith GC, Stenhouse EJ, Crossley JA, Aitken DA, Cameron AD, Connor JM. Early-pregnancy origins of low birth weight. *Nature.* 2002;417(6892):916.
21. Baken L, van Heesch PN, Wildschut HI, Koning AH, van der Spek PJ, Steegers EA, et al. First-trimester crown-rump length and embryonic volume of aneuploid fetuses measured in virtual reality. *Ultrasound Obstet Gynecol.* 2013;41(5):521-5.
22. Falcon O, Peralta CF, Cavoretto P, Auer M, Nicolaides KH. Fetal trunk and head volume in chromosomally abnormal fetuses at 11+0 to 13+6 weeks of gestation. *Ultrasound Obstet Gynecol.* 2005;26(5):517-20.
23. Khoury MJ, Erickson JD, Cordero JF, McCarthy BJ. Congenital malformations and intrauterine growth retardation: a population study. *Pediatrics.* 1988;82(1):83-90.
24. Lituania M, Passamonti U, Esposito V. Genetic factors and fetal anomalies in intrauterine growth retardation. *J Perinat Med.* 1994;22 Suppl 1:79-83.
25. Dashe JS, McIntire DD, Lucas MJ, Leveno KJ. Effects of symmetric and asymmetric fetal growth on pregnancy outcomes. *Obstet Gynecol.* 2000;96(3):321-7.
26. Reus AD, El-Harbachi H, Rousian M, Willemsen SP, Steegers-Theunissen RP, Steegers EA, et al. Early first-trimester trophoblast volume in pregnancies that result in live birth or miscarriage. *Ultrasound Obstet Gynecol.* 2013;42(5):577-84.
27. Rousian M, Groenenberg IA, Hop WC, Koning AH, van der Spek PJ, Exalto N, et al. Human embryonic growth and development of the cerebellum using 3-dimensional ultrasound and virtual reality. *Reprod Sci.* 2013;20(8):899-908.
28. Rousian M, Hop WC, Koning AH, van der Spek PJ, Exalto N, Steegers EA. First-trimester brain ventricle fluid and embryonic volumes measured by three-dimensional ultrasound with the use of I-Space virtual reality. *Hum Reprod.* 2013;28(5):1181-9.
29. van Uiter EM, van der Elst-Otte N, Wilbers JJ, Exalto N, Willemsen SP, Eilers PH, et al. Periconception maternal characteristics and embryonic growth trajectories: the Rotterdam Predict study. *Hum Reprod.* 2013.
30. Cruz-Neira C, Sandin D, DeFanti T. Surround-screen projection-based virtual reality: the design and implementation of the CAVE (tm). *Proceedings of the 20th annual conference on computer graphics and interactive techniques*; New York: ACM Press; 1993.
31. Koning AH, Rousian M, Verwoerd-Dikkeboom CM, Goedknecht L, Steegers EA, van der Spek PJ. V-scope: design and implementation of an immersive and desktop virtual reality volume visualization system. *Stud Health Technol Inform.* 2009;142:136-8.
32. Verwoerd-Dikkeboom CM, Koning AH, Groenenberg IA, Smit BJ, Brezinka C, Van Der Spek PJ, et al. Using virtual reality for evaluation of fetal ambiguous genitalia. *Ultrasound Obstet Gynecol.* 2008;32(4):510-4.

33. Groenenberg IA, Koning AH, Galjaard RJ, Steegers EA, Brezinka C, van der Spek PJ. A virtual reality rendition of a fetal meningomyelocele at 32 weeks of gestation. *Ultrasound Obstet Gynecol.* 2005;26(7):799-801.
34. Verwoerd-Dikkeboom CM, van Heesch PN, Koning AH, Galjaard RJ, Exalto N, Steegers EA. Embryonic delay in growth and development related to confined placental trisomy 16 mosaicism, diagnosed by I-Space Virtual Reality. *Fertil Steril.* 2008;90(5):2017 e19-22.
35. Rousian M, Verwoerd-Dikkeboom CM, Koning AH, Hop WC, van der Spek PJ, Exalto N, et al. Early pregnancy volume measurements: validation of ultrasound techniques and new perspectives. *BJOG.* 2009;116(2):278-85.
36. Verwoerd-Dikkeboom CM, Koning AH, Hop WC, Rousian M, Van Der Spek PJ, Exalto N, et al. Reliability of three-dimensional sonographic measurements in early pregnancy using virtual reality. *Ultrasound Obstet Gynecol.* 2008;32(7):910-6.
37. Verwoerd-Dikkeboom CM, Koning AH, Hop WC, van der Spek PJ, Exalto N, Steegers EA. Innovative virtual reality measurements for embryonic growth and development. *Hum Reprod.* 2010;25(6):1404-10.

3.2

Crown-Rump Length and Embryonic Volume in Miscarriages measured in Virtual Reality

Submitted

L. Baken

A.H.J. Koning

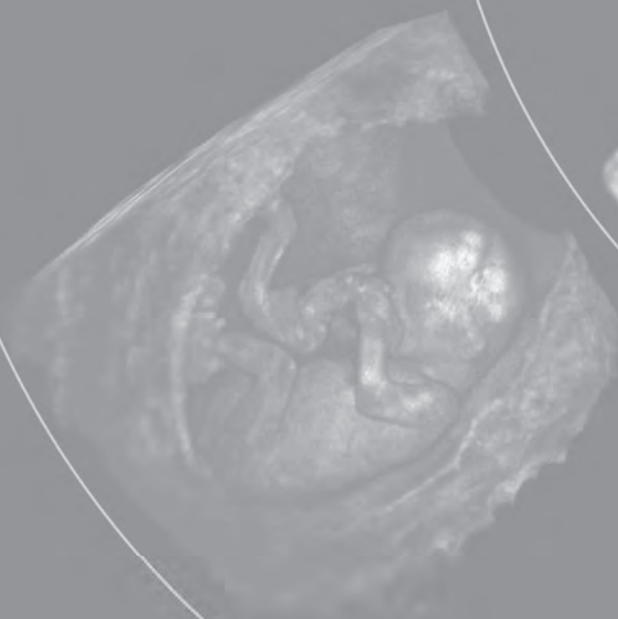
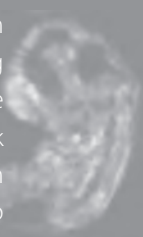
E. Birnie

P.J. van der Spek

R.P.M. Steegers-Theunissen

N. Exalto

E.A.P. Steegers



Abstract

Objective. To investigate whether there is an additional value of the embryonic volume (EV) measurement compared to the crown-rump length (CRL) measurement in the analysis of singleton pregnancies that will subsequently end in a miscarriage.

Methods. Forty-eight miscarriages from a prospective periconception study in a tertiary center were included before eight weeks gestational age (GA). We performed weekly three-dimensional (3D) ultrasound scans from enrolment up to subsequent diagnosis of miscarriages. Only the last ultrasound examination with positive heart action was used for analysis. CRL and EV measurements ($n=48$ and $n=33$, respectively) were performed using 3D virtual reality (3D VR) in the BARCO I-Space. Z-scores for CRL and EV were calculated for each pregnancy by using previously published 3D VR references values of normal uncomplicated singleton pregnancies.

Results. The mean z-score for CRL is -1.64 ($p<0.001$) and for EV -1.27 ($p<0.001$) as compared to the reference values. The mean z-scores for CRL and EV are not significantly different from each other ($p=0.109$). When EV is adjusted for the measured CRL the mean z-score is no longer smaller than expected (mean z-score -0.08 , $p=0.489$).

Conclusion. CRL and EV are smaller in subsequent miscarriages compared to reference values of normal uncomplicated singleton pregnancies. No significant difference is observed between the mean z-scores of EV and CRL. EV measurements are not expected to provide additional information in the diagnosis of miscarriages as compared to CRL measurements.

Introduction

It is well known that ultrasound findings are predictors of first-trimester outcome of pregnancy.¹⁻⁴ The detection of positive heart action by ultrasound however does not guarantee ongoing pregnancy as the miscarriage risk still remains 5-20%.⁵⁻⁸

Embryonic size, most commonly determined by crown-rump length (CRL) measurements, is an important and well-studied predictor of adverse pregnancy outcome.⁹⁻¹¹ Some studies suggest that a difference in embryonic size might be more accurately assessed using volume rather than length measurements. The increment of embryonic volume (EV) is much larger than the respective increment in CRL due to the cubic physical quantity of a volume.^{12,13} This was also confirmed by Rousian *et al.* showing that a doubling of the CRL results in a 6.5 times larger EV.¹⁴

In aneuploid pregnancies EV seems to be a better indicator of growth delay when compared to the CRL.^{15,16} These observations suggest that EV measurements might enable earlier and more accurate detection of abnormal embryonic growth preceding a miscarriage. This may be clinically relevant for detailed early pregnancy evaluation in a new pregnancy after recurrent miscarriage.

The aim of this study is to assess the potential additional value of the EV measurement, as compared to the CRL measurement, in singleton pregnancies that will subsequently end in a miscarriage.

Material and methods

Study design

This study is embedded in the Rotterdam Predict Study, a prospective periconceptional birth cohort study in a tertiary center.¹⁷⁻²⁰ Pregnant women who participated in this study were enrolled through the outpatient clinic of the department of Obstetrics and Gynaecology, Erasmus MC, Rotterdam, the Netherlands, and local midwifery practices. An additional cohort of miscarriages was included in the study through the early pregnancy unit of the same outpatient clinic. All women received weekly three-dimensional (3D) ultrasound scans between 6+0 and 12+6 weeks gestational age (GA). At enrolment, participants signed an informed consent form.

Ultrasound data

The transvaginal ultrasonographic volumes were obtained using a Voluson E8 (GE Medical Systems, Zipf, Austria) with a 4.5–11.9 MHz GE-probe (RIC-6-12-D). The 3D volumes were converted to Cartesian volumes using 3D software (4D View, GE Medical Systems) and transferred to the BARCO I-Space (Barco N.V., Kortrijk, Belgium) at the Department of Bioinformatics at the Erasmus MC, Rotterdam, The Netherlands. The I-Space is a four-walled CAVETM-like virtual reality system that creates 'holograms' of 3D data sets that allows for true depth perception and interaction with the dataset.²¹ The V-Scope²² software allows fully three-dimensional interaction with the dataset and enables precise length

and volume measurements. These measurements obtained in the I-Space are described in detail before.^{14,23,24}

Pregnancy dating

In spontaneously conceived pregnancies dating was based on the first day of the last menstrual period (LMP) recorded by the researcher during the first visit. When the menstrual cycle was regular but >3 days different from 28 days the GA was adjusted for the cycle length. In pregnancies conceived by *in vitro* fertilization (IVF) with or without intra-cytoplasmic sperm injection (ICSI) GA was calculated from the day of oocyte retrieval plus 14 days. In case of cryopreserved embryos GA was calculated from the day of embryo transfer plus 17 or 18 days depending on the number of days between oocyte retrieval and cryopreservation of the embryo. In pregnancies originating from intrauterine insemination GA was calculated based on the LMP or insemination date plus 14 days. Pregnancies were excluded from the study if the LMP was missing or if the menstrual cycle was irregular. Pregnancies in which GA was adjusted for CRL, in case of a difference ≥ 7 days from the expected CRL according to the Robinson curve²⁵, were excluded from the analysis.

Study population

Women of ≥ 18 years old with a singleton pregnancy of 6-8 weeks GA were eligible to participate in our study. Informed written consent was obtained from all participants. Eighty-three subsequent miscarriages were recruited from the Rotterdam Predict study from January 2009 - January 2013. Another seven miscarriages were collected at our early pregnancy unit. Part of this study population has been used in a previous study.²⁰ Of the total of 90 subsequent miscarriages 11 had unknown

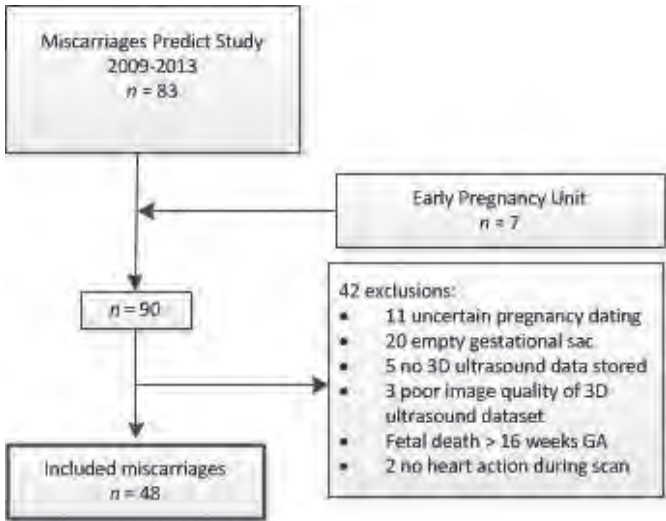


Figure 1: Flowchart of the study population.

LMP or an irregular cycle and were excluded. Twenty were diagnosed as an empty gestational sac and therefore excluded. An additional 11 cases were excluded because of missing data or missing 3D ultrasounds datasets ($n=5$), poor image quality of the 3D datasets ($n=3$), intrauterine fetal death > 16 weeks GA ($n=1$) and no available 3D datasets with positive heart action ($n=2$). Forty-eight miscarriages remained for analysis (Figure 1). If multiple measurements were available per miscarriage only the last measurement with positive heart action was used for comparing the additional value of EV measurements with CRL measurements. CRL was available in all 48 cases and EV only in 33 of these 48 cases (68.8%).

Statistical analysis

In each pregnancy complicated by miscarriage the observed value for CRL or EV was subtracted from the expected mean for GA, obtained from the reference values of normal uncomplicated pregnancies.^{14,24} This difference was divided by the standard deviation (SD) for GA of the reference values in order to obtain the *z*-score. Only the last measurement with positive heart action was used in the analysis, resulting in one *z*-score per pregnancy.

The one-sample t-test was used to test for a statistically significant difference in *z*-score as compared to the reference value. The paired t-test was used to test for a significant difference between CRL *z*-scores and EV *z*-scores in miscarriages. In a subgroup analysis recurrent miscarriages, defined as three or more consecutive miscarriages, were compared to non-recurrent miscarriages. To compare proportions of dichotomous variables, i.e. the proportion of miscarriages with a CRL $\leq 2SD$ versus the proportion of miscarriages with an EV $\leq 2SD$, the McNemar test for paired samples was used. Statistical analysis was performed using IBM SPSS statistical software version 21 (SPSS Inc., Chicago, IL, USA). A *p*-value of <0.05 was considered statistically significant.

Ethical approval

This study has been approved by the Central Committee on Research in The Hague and the local Medical Ethical and Institutional Review Board of the Erasmus MC.

Results

The patient characteristics of the miscarriage group are presented in Table 1. In Figure 2 the individual growth trajectories (each line represents a case) of all CRL and EV measurements are displayed in relation to previously published reference curves of CRL²⁴ and EV¹⁴.

The mean *z*-score for the overall group of miscarriages is -1.64 (SD 2.08, $p<0.001$) for the CRL and -1.27 (SD 1.58, $p<0.001$) for the EV. The mean *z*-scores for CRL and EV are not significantly different from each other ($p=0.109$) (Table 2). When the EV measurement is adjusted for the CRL the association lost significance (mean *z*-score -0.08, $p=0.489$).

A smaller CRL for GA is observed in 39/48 (81.2%) of cases, being comparable to a smaller EV for GA in 27/33 (81.8%). A too small CRL (below 2SD) is observed in 18/48 (37.5%) of the miscarriages and a

Table 1: The mean and ranges or percentages of the patient characteristics of the miscarriages (n=48).

Characteristic	Median (range) or percentage
Maternal age (years)	32 (24-45)
Parity	
0	56.3%
1	35.4%
≥2	8.3%
Gravidity	3 (1-11)
Miscarriages ≥ 2	58.4%
Conception mode	
Spontaneous	64.6%
IVF/ICSI	31.2%
IUI	4.2%

IVF=in vitro fertilization, ICSI=intracytoplasmic sperm injection, IUI=intrauterine insemination

Table 2: Z-score of crown-rump length and embryonic volume in pregnancies subsequently ending in a miscarriage.

	CRL n=48	EV n=33	p
Mean z-score (SD)	-1.6375 (2,08)	-1.2681 (1.56)	0.109*
smaller than expected (n, %)	37 (77.1)	27 (81.8)	0.999#
≤ -1SD (n, %)	28 (58.3)	23 (69.7)	0.375#
≤ -2SD (n, %)	18 (37.5)	11 (33.3)	0.999#
≤ -3SD (n, %)	12 (25.0)	3 (9.1)	0.063#

CRL=crown-rump length

EV=embryonic volume

SD=standard deviation

* paired t-test

McNemar test for paired samples

too small EV (below 2SD) in 9/33 (27.3%). In two cases of a too small CRL the EV is normal (within ± 2SD) and there are no cases in which the CRL is in the normal range in combination with a too small EV (Supplemental Table 1).

In supplemental Table 2 women with and without recurrent miscarriages (n=16 and n=32, respectively), defined as three or more consecutive miscarriages, are compared. No significant differences are found for mean z-score for CRL and EV between the two groups.

Discussion

To the best of our knowledge this is the first study that evaluates the potential role of EV measurements in the prediction of miscarriage. In this study we found that both CRL and EV are significantly

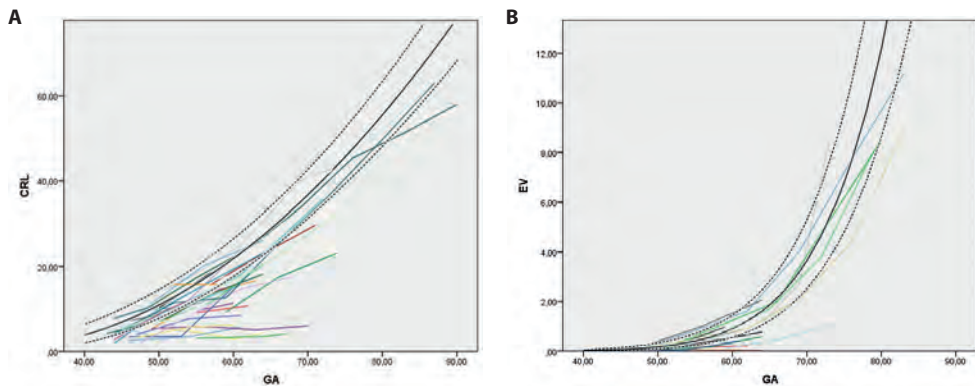


Figure 2: CRL (A) and EV (B) growth trajectories for the miscarriages plotted on the references curves (solid line p50, dashed lines p5 and p95). Each line represents the course of a different case.

smaller than expected in pregnancies subsequently ending in a miscarriage. However, mean CRL and EV *z*-scores in miscarriages were not significantly different from each other and moreover, significance was lost when EV was adjusted for measured CRL. Therefore, EV measurements are not expected to provide additional information in the diagnosis of miscarriages as compared to CRL measurements. No differences were observed between the mean *z*-scores for CRL and EV between the groups with and without recurrent miscarriage.

Whereas the mean *z*-score for CRL is lower than the mean *z*-score for EV, both mean *z*-scores are not below 2SD. Inspection of Figures 2A and 2B suggest that this might be explained by the fact that pregnancies that will subsequently end in a miscarriage can broadly be divided into two groups; one with an early and marked growth delay and one without an evident growth delay.

Many growth parameters have been studied in the light of pregnancy outcome prediction. Several studies have demonstrated the relationship between a smaller than expected CRL and subsequent miscarriage in early, viable singleton pregnancies.^{1,9,26} In the present study this was confirmed.

Logically, it was presumed that volume measurements, due to their cubical quantity, might enable earlier and more accurate detection of growth disturbances. This was previously demonstrated in aneuploid pregnancies where EV is a better indicator of growth disturbances compared to CRL.^{15,16} Although nearly 70% of miscarriages are related to chromosomal abnormalities²⁷, a different growth pattern seems to be present between aneuploid pregnancies and miscarriages. EV is a better indicator of growth restriction than CRL in aneuploid pregnancies diagnosed at the end of the first-trimester whereas it is not in miscarriages not surviving until the end of the first-trimester. However, it should be noted that the percentage of chromosomal abnormalities in our cohort is not known. Abnormal placental development has been suggested as a possible explanation for a different growth pattern in miscarriages.^{20,28,29} Another possible explanation might be that in pregnancies that will subsequently end in a miscarriage hydropic changes are present prior to embryonic death masking a difference

in EV. In future studies this could be analysed by studying CRL and EV measurements even earlier in pregnancy when possible hydropic changes might not be present yet.

As this study compares the course of miscarriages to previously published references curves cut-off values cannot be calculated from these data and should be obtained from large cohort studies. Furthermore, cut-off values should be based on more than just CRL or EV, as cut-off values and the risk of miscarriage might also be influenced by maternal characteristics, like age and race.^{3,19,30-32} Discordant growth of other, non-embryonic, structures have also been related to poor first-trimester outcome. However, different studies report conflicting results for gestational sac diameter^{2,3,33,34} and yolk sac diameter³⁵⁻³⁸ and their use in the prediction of miscarriage is still at debate.

A limitation of our study is that it depends on accurate pregnancy dating. We only included cases with regular menstrual cycles or a known conception date in the study and as a consequence our results can only be applied to these women. Secondly, our population was mainly recruited through a tertiary hospital and is therefore more likely to be at risk for pregnancy complications. A high percentage of pregnancies analysed in our study was conceived by artificial reproductive technique. Furthermore, a significant part of our cohort were recurrent miscarriages. These points might limit the external validity of our study. Furthermore, at this time the BARCO I-Space is too large (requiring a separate 40m²/400 sq ft) and too expensive (500,000 USD) for 3D VR becoming a routine diagnostic procedure. However, a desktop version of this 3D VR is recently being developed and evaluated, making this new and innovative technique broadly accessible to hospitals in the near future.³⁹

In conclusion, a discrepancy in first-trimester embryonic size in pregnancies that will subsequently end in a miscarriage can be quantified by CRL or EV measurements. As the mean *z*-score for EV is not smaller than that of CRL, EV measurements are not expected to provide additional information in the diagnosis of miscarriages as compared to CRL measurements.

References

1. Choong S, Rombauts L, Ugoni A, Meagher S. Ultrasound prediction of risk of spontaneous miscarriage in live embryos from assisted conceptions. *Ultrasound Obstet Gynecol.* 2003;22(6):571-7.
2. Abdallah Y, Daemen A, Kirk E, Pexsters A, Naji O, Stalder C, et al. Limitations of current definitions of miscarriage using mean gestational sac diameter and crown-rump length measurements: a multicenter observational study. *Ultrasound Obstet Gynecol.* 2011;38(5):497-502.
3. Papaioannou GI, Syngelaki A, Maiz N, Ross JA, Nicolaides KH. Ultrasonographic prediction of early miscarriage. *Hum Reprod.* 2011;26(7):1685-92.
4. Abuelghar WM, Fathi HM, Ellaithy MI, Anwar MA. Can a smaller than expected crown-rump length reliably predict the occurrence of subsequent miscarriage in a viable first-trimester pregnancy? *J Obstet Gynaecol Res.* 2013;39(10):1449-55.
5. Hill LM, Guzick D, Fries J, Hixson J. Fetal loss rate after ultrasonically documented cardiac activity between 6 and 14 weeks, menstrual age. *J Clin Ultrasound.* 1991;19(4):221-3.
6. Cashner KA, Christopher CR, Dysert GA. Spontaneous fetal loss after demonstration of a live fetus in the first-trimester. *Obstet Gynecol.* 1987;70(6):827-30.
7. Frates MC, Benson CB, Doubilet PM. Pregnancy outcome after a first-trimester sonogram demonstrating fetal cardiac activity. *J Ultrasound Med.* 1993;12(7):383-6.
8. Wilson RD, Kendrick V, Wittmann BK, McGillivray B. Spontaneous abortion and pregnancy outcome after normal first-trimester ultrasound examination. *Obstet Gynecol.* 1986;67(3):352-5.
9. Reljic M. The significance of crown-rump length measurement for predicting adverse pregnancy outcome of threatened abortion. *Ultrasound Obstet Gynecol.* 2001;17(6):510-2.
10. Mukri F, Bourne T, Bottomley C, Schoeb C, Kirk E, Papageorgiou AT. Evidence of early first-trimester growth restriction in pregnancies that subsequently end in miscarriage. *BJOG.* 2008;115(10):1273-8.
11. Bottomley C, Daemen A, Mukri F, Papageorgiou AT, Kirk E, Pexsters A, et al. Functional linear discriminant analysis: a new longitudinal approach to the assessment of embryonic growth. *Hum Reprod.* 2009;24(2):278-83.
12. Aviram R, Shpan DK, Markovitch O, Fishman A, Tepper R. Three-dimensional first-trimester fetal volumetry: comparison with crown rump length. *Early Hum Dev.* 2004;80(1):1-5.
13. Falcon O, Peralta CF, Cavoretto P, Faiola S, Nicolaides KH. Fetal trunk and head volume measured by three-dimensional ultrasound at 11 + 0 to 13 + 6 weeks of gestation in chromosomally normal pregnancies. *Ultrasound Obstet Gynecol.* 2005;26(3):263-6.
14. Rousian M, Koning AH, van Oppenraaij RH, Hop WC, Verwoerd-Dikkeboom CM, van der Spek PJ, et al. An innovative virtual reality technique for automated human embryonic volume measurements. *Hum Reprod.* 2010;25(9):2210-6.
15. Baken L, van Heesch PN, Wildschut HI, Koning AH, van der Spek PJ, Steegers EA, et al. First-trimester crown-rump length and embryonic volume of aneuploid fetuses measured in virtual reality. *Ultrasound Obstet Gynecol.* 2013;41(5):521-5.
16. Falcon O, Peralta CF, Cavoretto P, Auer M, Nicolaides KH. Fetal trunk and head volume in chromosomally abnormal fetuses at 11+0 to 13+6 weeks of gestation. *Ultrasound Obstet Gynecol.* 2005;26(5):517-20.

17. Rousian M, Hop WC, Koning AH, van der Spek PJ, Exalto N, Steegers EA. First-trimester brain ventricle fluid and embryonic volumes measured by three-dimensional ultrasound with the use of I-Space virtual reality. *Hum Reprod.* 2013;28(5):1181-9.
18. van Uitert E, van Ginkel S, Willemsen S, Lindemans J, Koning A, Eilers P, et al. An optimal periconception maternal folate status for embryonic size: the Rotterdam Predict study. *BJOG.* 2014.
19. van Uitert EM, van der Elst-Otte N, Wilbers JJ, Exalto N, Willemsen SP, Eilers PH, et al. Periconception maternal characteristics and embryonic growth trajectories: the Rotterdam Predict study. *Hum Reprod.* 2013;28(12):3188-96.
20. Reus AD, El-Harbachi H, Rousian M, Willemsen SP, Steegers-Theunissen RP, Steegers EA, et al. Early first-trimester trophoblast volume in pregnancies that result in live birth or miscarriage. *Ultrasound Obstet Gynecol.* 2013;42(5):577-84.
21. Cruz-Neira C, Sandin DJ, DeFanti TA. Surround-screen projection-based virtual reality: the design and implementation of the CAVE (tm). *Proceedings of the 20th Annual Conference on Computer Graphics and Interactive Techniques.* 1993:135-42.
22. Koning AH, Rousian M, Verwoerd-Dikkeboom CM, Goedknegt L, Steegers EA, van der Spek PJ. V-scope: design and implementation of an immersive and desktop virtual reality volume visualization system. *Stud Health Technol Inform.* 2009;142:136-8.
23. Verwoerd-Dikkeboom CM, Koning AH, Hop WC, Rousian M, Van Der Spek PJ, Exalto N, et al. Reliability of three-dimensional sonographic measurements in early pregnancy using virtual reality. *Ultrasound Obstet Gynecol.* 2008;32(7):910-6.
24. Verwoerd-Dikkeboom CM, Koning AH, Hop WC, van der Spek PJ, Exalto N, Steegers EA. Innovative virtual reality measurements for embryonic growth and development. *Hum Reprod.* 2010;25(6):1404-10.
25. Robinson HP, Fleming JE. A critical evaluation of sonar "crown-rump length" measurements. *Br J Obstet Gynaecol.* 1975;82(9):702-10.
26. Mantoni M, Pedersen JF. Fetal growth delay in threatened abortion: an ultrasound study. *Br J Obstet Gynaecol.* 1982;89(7):525-7.
27. Fritz B, Hallermann C, Olert J, Fuchs B, Bruns M, Aslan M, et al. Cytogenetic analyses of culture failures by comparative genomic hybridisation (CGH)-Re-evaluation of chromosome aberration rates in early spontaneous abortions. *Eur J Hum Genet.* 2001;9(7):539-47.
28. Jauniaux E, Burton GJ. Pathophysiology of histological changes in early pregnancy loss. *Placenta.* 2005;26(2-3):114-23.
29. Reus AD, Stephenson MD, van Dunne FM, de Krijger RR, Joosten M, Steegers EA, et al. Chorionic villous vascularization related to phenotype and genotype in first-trimester miscarriages in a recurrent pregnancy loss cohort. *Hum Reprod.* 2013;28(4):916-23.
30. Bottomley C, Daemen A, Mukri F, Papageorgiou AT, Kirk E, Pexsters A, et al. Assessing first-trimester growth: the influence of ethnic background and maternal age. *Hum Reprod.* 2009;24(2):284-90.
31. Mook-Kanamori DO, Steegers EA, Eilers PH, Raat H, Hofman A, Jaddoe VW. Risk factors and outcomes associated with first-trimester fetal growth restriction. *JAMA.* 2010;303(6):527-34.
32. Nybo Andersen AM, Wohlfahrt J, Christens P, Olsen J, Melbye M. Maternal age and fetal loss: population based register linkage study. *BMJ.* 2000;320(7251):1708-12.

33. Makrydimas G, Sebire NJ, Lolis D, Vlassis N, Nicolaides KH. Fetal loss following ultrasound diagnosis of a live fetus at 6-10 weeks of gestation. *Ultrasound Obstet Gynecol.* 2003;22(4):368-72.
34. Abdallah Y, Daemen A, Guha S, Syed S, Naji O, Pexsters A, et al. Gestational sac and embryonic growth are not useful as criteria to define miscarriage: a multicenter observational study. *Ultrasound Obstet Gynecol.* 2011;38(5):503-9.
35. Tan S, Pektas MK, Arslan H. Sonographic evaluation of the yolk sac. *J Ultrasound Med.* 2012;31(1):87-95.
36. Berdahl DM, Blaine J, Van Voorhis B, Dokras A. Detection of enlarged yolk sac on early ultrasound is associated with adverse pregnancy outcomes. *Fertil Steril.* 2010;94(4):1535-7.
37. Cho FN, Chen SN, Tai MH, Yang TL. The quality and size of yolk sac in early pregnancy loss. *Aust N Z J Obstet Gynaecol.* 2006;46(5):413-8.
38. Reece EA, Scioscia AL, Pinter E, Hobbins JC, Green J, Mahoney MJ, et al. Prognostic significance of the human yolk sac assessed by ultrasonography. *Am J Obstet Gynecol.* 1988;159(5):1191-4.
39. Baken L, van Gruting IM, Steegers EA, van der Spek PJ, Exalto N, Koning AH. Design and validation of a 3D virtual reality desktop system for sonographic length and volume measurements in early pregnancy evaluation. *J Clin Ultrasound.* Jul 9 2014.

Supplemental material

Supplemental Table 1: Comparison of crown-rump length and embryonic volume in 33 cases for which CRL and EV z-scores are available.

CRL	EV		
	> -2SD	< -2SD	
> -2SD	22	0	22
< -2SD	2	9	11
Total	24	9	33

CRL = crown-rump length
 EV= embryonic volume
 SD = standard deviation

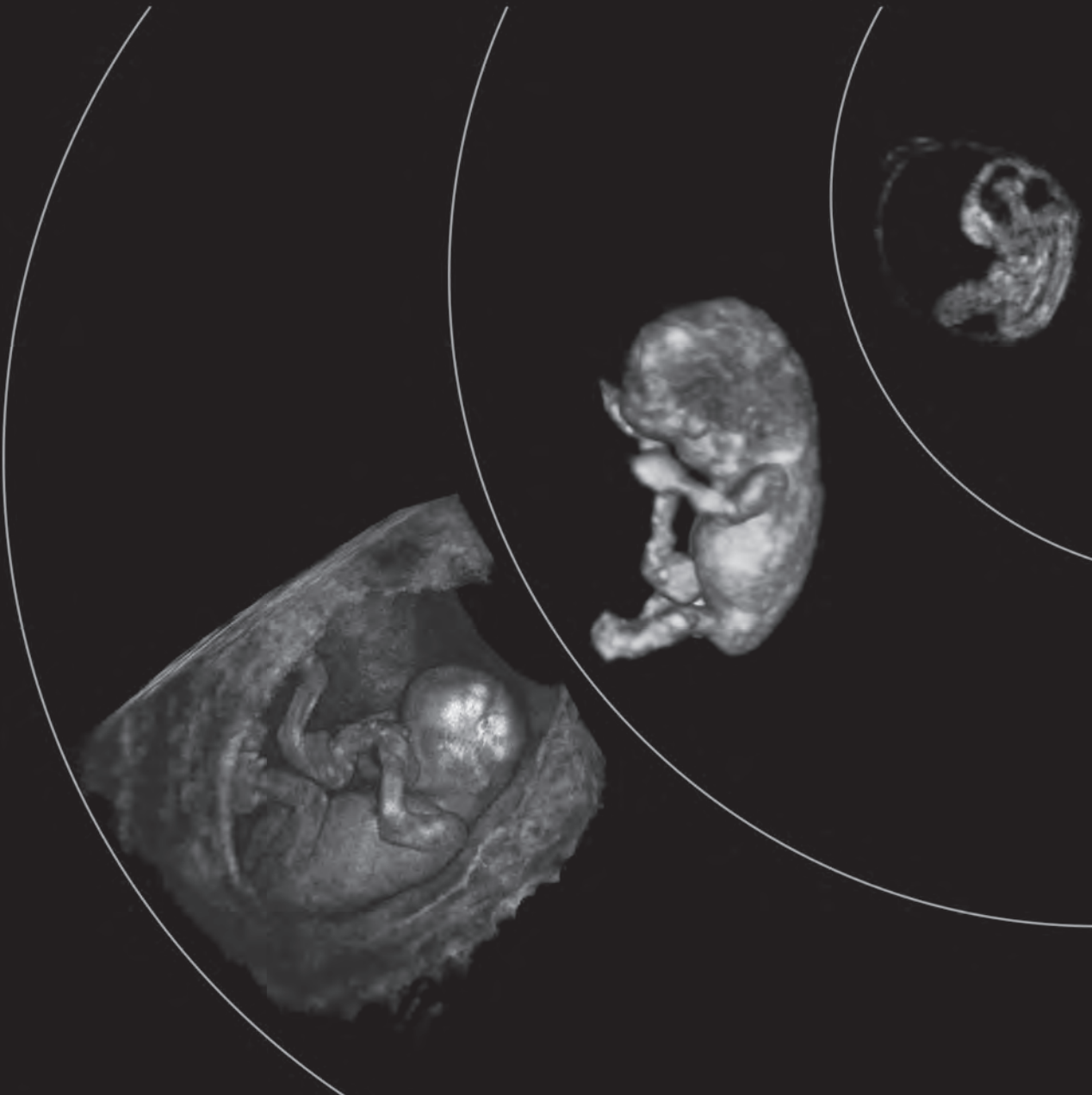
Supplemental Table 2: Z-score of crown-rump length and embryonic volume in pregnancies with and without previous recurrent miscarriages (three or more consecutive miscarriages).

	Recurrent miscarriage	No recurrent miscarriage	p
	n=16	n=32	
CRL z-score (SD)	-1.26 (1.98)	-1.83 (2.13)	0.375*
	n=12	n=21	
EV z-score (SD)	-1.06 (1.79)	-1.39 (1.47)	0.577*

CRL=crown-rump length
 EV=embryonic volume
 SD=standard deviation
 * paired t-test

CHAPTER 4

Biometry and Volumetry in Aneuploid Pregnancies

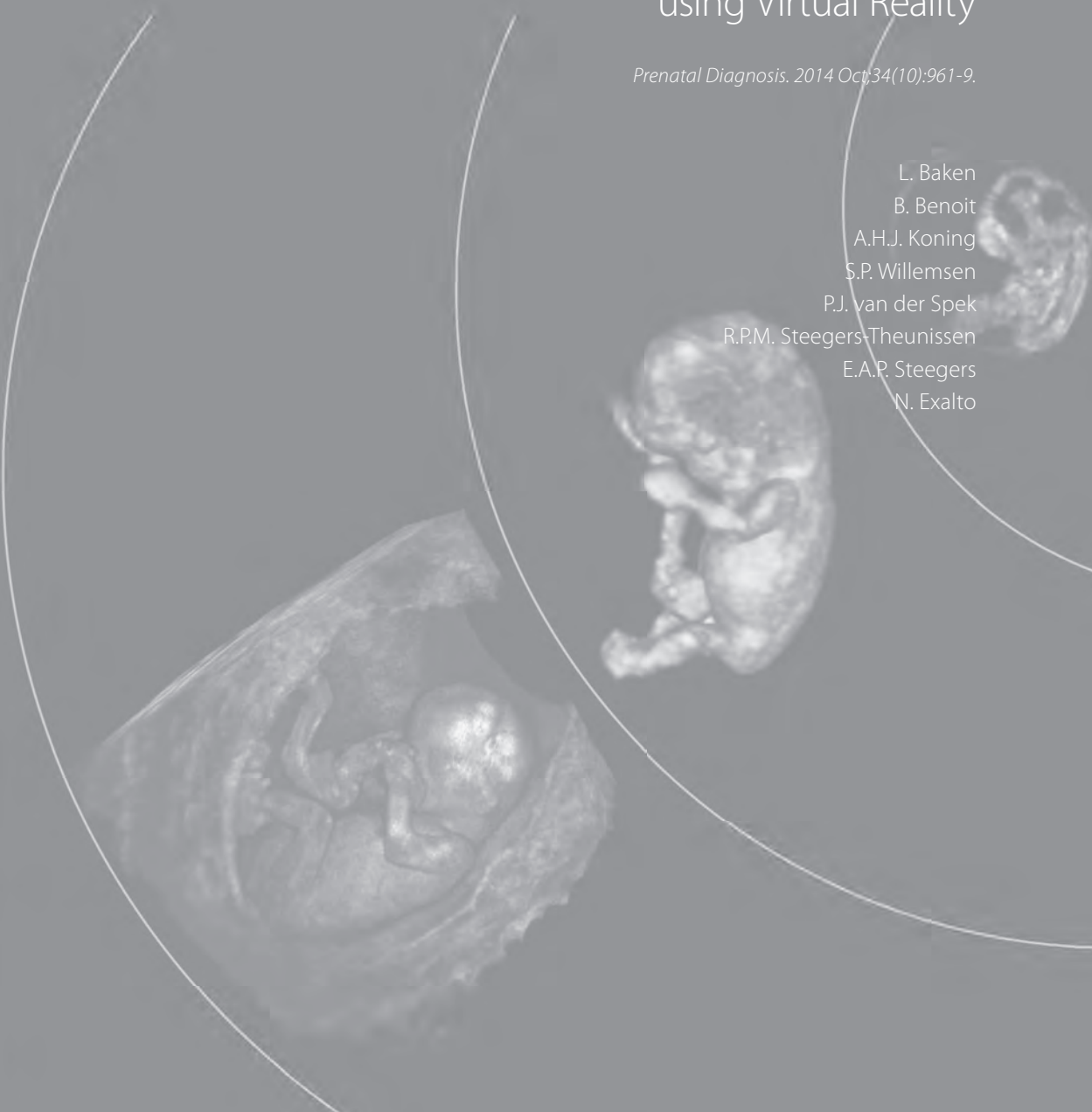


4.1

First-Trimester Hand Measurements in Euploid and Aneuploid Human Fetuses using Virtual Reality

Prenatal Diagnosis. 2014 Oct;34(10):961-9.

L. Baken
B. Benoit
A.H.J. Koning
S.P. Willemsen
P.J. van der Spek
R.P.M. Steegers-Theunissen
E.A.P. Steegers
N. Exalto



Abstract

Objective. Although second-trimester and third-trimester reference curves for human foetal hand growth allow for identification several genetic syndromes, little is known about first-trimester hand growth. We investigated first-trimester hand growth in euploid and aneuploid fetuses.

Methods. Between 9 and 12 weeks' gestational age (GA), wrist width, hand width, hand length, and hand index were measured in three-dimensional (3D) ultrasound datasets of 112 euploid and 65 aneuploid pregnancies. We constructed reference curves for these measurements in euploid pregnancies and calculated *z*-scores for measurements in aneuploid pregnancies. Reproducibility was established in a subset of 20 datasets.

Results. While wrist width, hand width, and hand length increased with GA, hand index decreased. Intraobserver and interobserver intraclass correlation coefficient values were >0.97 .

In trisomy 21 cases, wider wrists and hands were observed compared with euploid pregnancies (mean *z*-scores 1.06, SD 2.04, $p<0.001$ and 1.16, SD 1.30, $p<0.001$, respectively). Trisomy 18 cases showed narrower and shorter hands (mean *z*-scores -0.74, SD 1.20, $p=0.009$ and -0.97, SD 0.86, $p=0.005$, respectively). In trisomy 13 cases, no differences were observed.

Conclusion. Reference values are available for first-trimester studies on human hand development. First-trimester hand measurements in trisomy 21 and 18 differ significantly from those in euploid pregnancies and may be useful for early identification of abnormal development.

Introduction

The upper limb buds of the human embryo appear and start to enlarge at day 26 after conception; at day 32, the paddle-shaped hand becomes manifest. From day 41 onwards, the digits of the upper limb can be distinguished.^{1,2}

Numerous ultrasound (US) studies have been performed during the second and third gestational trimesters on the development of foetal limbs. Reference curves for prenatal finger length have been reported from 14 weeks' gestational age (GA) onwards using two-dimensional (2D) US.^{3,4} These reference curves made it possible to identify several genetic syndromes. Apart from genetic syndromes, abnormalities of the hands may be associated with limb-reduction defects, genetic syndromes, and skeletal dysplasia. Aneuploid pregnancies are characterized by hand abnormalities. In trisomy 21, short fingers and a dysplastic middle phalanx of the fifth finger are seen. A clenched fist with an overlapping index finger is typically for trisomy 18 and polydactyly is often observed in trisomy 13.^{5,6}

Very limited data are available on the first-trimester growth of the hand.⁷ As first-trimester US is becoming more popular for first-trimester screening and diagnosis of foetal congenital anomalies, there is a need for first-trimester reference charts on hand growth parameters.

The primary aim of this study was therefore to investigate growth patterns of the human hand during the first-trimester of pregnancy. We also hypothesized that hand abnormalities in aneuploid pregnancies, observed in the second- and third-trimesters, are most likely already present in the first-trimester.

Methods

In this retrospective study stored three-dimensional (3D) US datasets of first-trimester pregnancies were used. Data were collected within the periconception Rotterdam Predict study⁸⁻¹⁴ at the Department of Obstetrics and Gynaecology at Erasmus MC, University Medical Center Rotterdam, the Netherlands. Women of ≥ 18 years with a singleton pregnancy of 6 to 8 weeks' GA were eligible to participate.

As part of the Rotterdam Predict study, women received weekly transvaginal 3D US scans in the first-trimester (up to 12+6 weeks' GA) of their pregnancy. In spontaneously conceived pregnancies, GA was based on the first day of the last menstrual period by the researcher during the first visit. If the menstrual cycle was regular but >3 days different from 28 days, the GA was adjusted for the cycle length. In pregnancies conceived by *in vitro* fertilization with or without intra-cytoplasmic sperm injection, GA was calculated from the day of oocyte retrieval plus 14 days. In case of an unknown LMP or when the observed crown-rump length (CRL) differed more than six days from the expected CRL according to the Robinson curve, GA was determined by the CRL.

The transvaginal ultrasonographic volumes were obtained using a Voluson E8 (GE Medical Systems, Zipf, Austria; with GE-probe RIC-6-12-D (4.5–11.9 MHz)). The 3D volumes were converted to Cartesian volumes using 3D software (4D View, GE Medical Systems) and transferred to the BARCO I-Space

(Barco N.V., Kortrijk, Belgium) at the Department of Bioinformatics at Erasmus MC. The I-Space is a four-walled CAVETM-like¹⁵ virtual reality system that creates holograms of 3D datasets that allow for true depth perception and interaction with the dataset. The V-Scope¹⁶ software allows for precise length and volume measurements.^{17,18}

The study population consisted of 112 pregnancies resulting in the birth of phenotypically normal neonates (considered to be euploid) recruited from the 2009 cohort of the Rotterdam Predict Study, which constituted the controls, and 65 aneuploid pregnancies (30 cases of trisomy 21, 29 cases of trisomy 18, and 6 cases of trisomy 13). The aneuploid pregnancies were recruited through the outpatient clinic of the department of Obstetrics and Gynaecology at Erasmus MC University Medical Center and the Hôpital Princesse Grace Monaco between 2008 and March 2013. Of these aneuploidy cases 26 with trisomy 21, 19 with trisomy 18 and five with trisomy 13 were used in an earlier study.¹⁹

Measurements

Ultrasound scans were performed using a 9 to 12 MHz transvaginal transducer of the GE Voluson E8 system (GE Medical systems, Zipf, Austria). The 3D datasets were acquired, stored as Cartesian volumes and visualized using the I-Space virtual reality system.

From nine weeks' GA onwards, wrist width, hand width, and hand length were measured in the hand that had been best visualized (closest to the transducer). Measurements were defined as follows (Figure 1):

- Wrist width: transverse distance of the narrowest point of the wrist distal to the radius/ulna complex.
- Hand width: transverse distance between the outermost points of the second and fifth digit (above the bifurcation of the thumb).
- Hand length: distance perpendicular to and starting at the transverse axis of the wrist width to the tip of the third finger.
- Hand index: hand width divided by hand length.

Wrist width and hand width were measured by placing callipers in a straight line at the above points indicated. Hand length was measured using the tracing function of the V-Scope software. Measurements take approximately one minute per hand.

Reproducibility

The intraobserver and interobserver reliability and agreement were calculated in 20 datasets of randomly chosen patients. A total of five datasets per gestational week (9 to 12 weeks' GA) were selected. To study the intraobserver agreement of the 3D measurements, all hand growth measurements were performed three times by one observer (LB) using the I-Space virtual reality system and repeated three times after two weeks. The mean of the three measurements was used for comparison. To study the interobserver agreement, the measurements were repeated independently by another observer

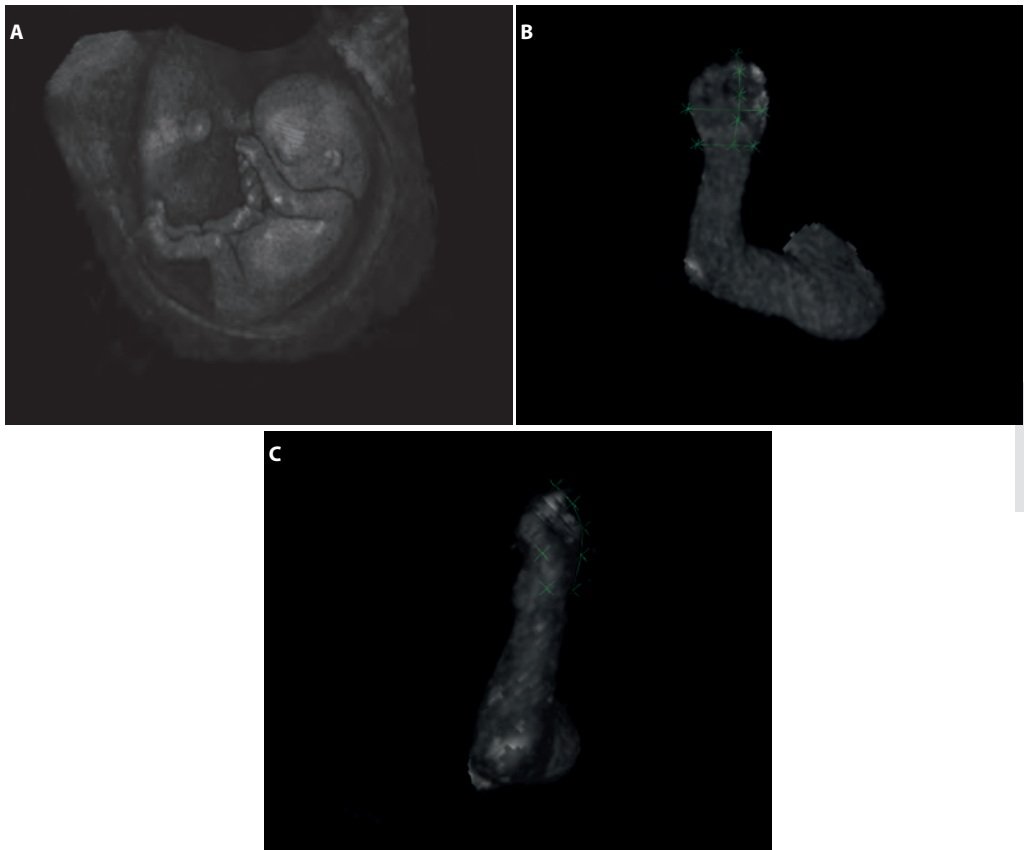


Figure 1: A fetus of 11+6 weeks' gestational age as rendered by the V-Scope software in the I-Space (A). The left hand and arm of the same foetus are magnified in order to measure the hand parameters (B,C). Wrist width and hand width are measured by placing callipers in a straight line. Hand length is measured using the trace function.

(NE). The observers were blinded to each other's results. Both observers were experienced in using virtual reality at the beginning of the study.

Statistical analysis

Intraobserver and interobserver reliability was determined using 95% limits of agreement, Bland-Altman plots, and intraclass correlation coefficients.

We used the lambda-mu-sigma method by Cole²⁰ as implemented in the R package GAMLSS (Rigby2005, R2012) to estimate centile curves for the euploid pregnancies. In this method, we assume that after performing a Box-Cox transformation to remove skewness, the measurements follow a normal distribution. We modelled the median of the distribution with a spline in GA, and we assumed

that the coefficient of variation depends linearly on the GA. The number of degrees of freedom for the spline, that is, its smoothness, is chosen based on the information criterion.

The measurements in the aneuploid pregnancies were transformed into **z**-scores and compared with the estimated distribution of the euploid pregnancies using Kolmogorov-Smirnov tests. Note that because there are no established statistical techniques to compare distributions when the measurements are not independent, this fact had to be ignored, and the test has to be considered approximate.

Analyses were performed using R 3.0.1 (R Core Team, Vienna, Austria) and IBM SPSS20 (IBM Inc., Armonk, NY, USA). A **p**-value of <0.05 was considered statistically significant.

Results

One hundred and twelve women carrying healthy euploid pregnancies were studied to evaluate normal first-trimester growth of the hand. The median maternal age was 33 years (19-43 years) in the euploid group versus 35 years (23-44 years) in the aneuploid group. In this article, 62.5% versus 35.5% of women was nulliparous, and 70.5% versus 91.9% conceived spontaneous in the euploid and

Table 1: Mean of wrist width, hand width, hand length, hand index, and crown-rump length measurements in euploid pregnancies with corresponding standard deviation (SD), number of cases (N), and range grouped per completed week gestational age.

GA (weeks)	N	Mean CRL (mm)	SD (mm)		Mean (mm)	SD (mm)	Range (mm)
9	41	25.97	4.27	Wrist width	2.02	0.26	1.53-2.62
				Hand width	2.92	0.43	2.09-3.79
				Hand length	4.36	0.80	2.55-6.17
				Hand index	0.68	0.11	0.51-0.93
10	60	36.15	5.90	Wrist width	2.29	0.37	1.51-3.06
				Hand width	3.47	0.55	2.31-4.80
				Hand length	5.56	1.06	3.77-8.88
				Hand index	0.63	0.09	0.45-0.87
11	63	48.48	7.02	Wrist width	2.80	0.47	1.92-3.78
				Hand width	4.55	0.80	3.00-6.98
				Hand length	7.47	1.33	4.93-11.59
				Hand index	0.61	0.08	0.47-0.86
12	44	61.68	7.26	Wrist width	3.33	0.41	2.32-4.24
				Hand width	5.43	0.80	3.85-8.13
				Hand length	9.04	1.56	5.64-12.29
				Hand index	0.61	0.07	0.43-0.81

aneuploidy group, respectively. In the euploid group, 52.7% of the newborns was female versus 35.4% of the fetuses in the aneuploid group.

A total of 434 scans were performed from 63 to 93 days' GA. Hand measurements could be performed in 209 of the 422 scans (49.5%). The median number of datasets per patient in which measurements were obtained was 2 (range 1-4). The GA ranged from 63 to 93 days (median 77 days, SD 7.38 days) and the CRL ranged from 20 to 76 mm (median 42 mm, SD 13 mm). Measurements of wrist width, hand width, hand length, and hand index are presented per completed gestational

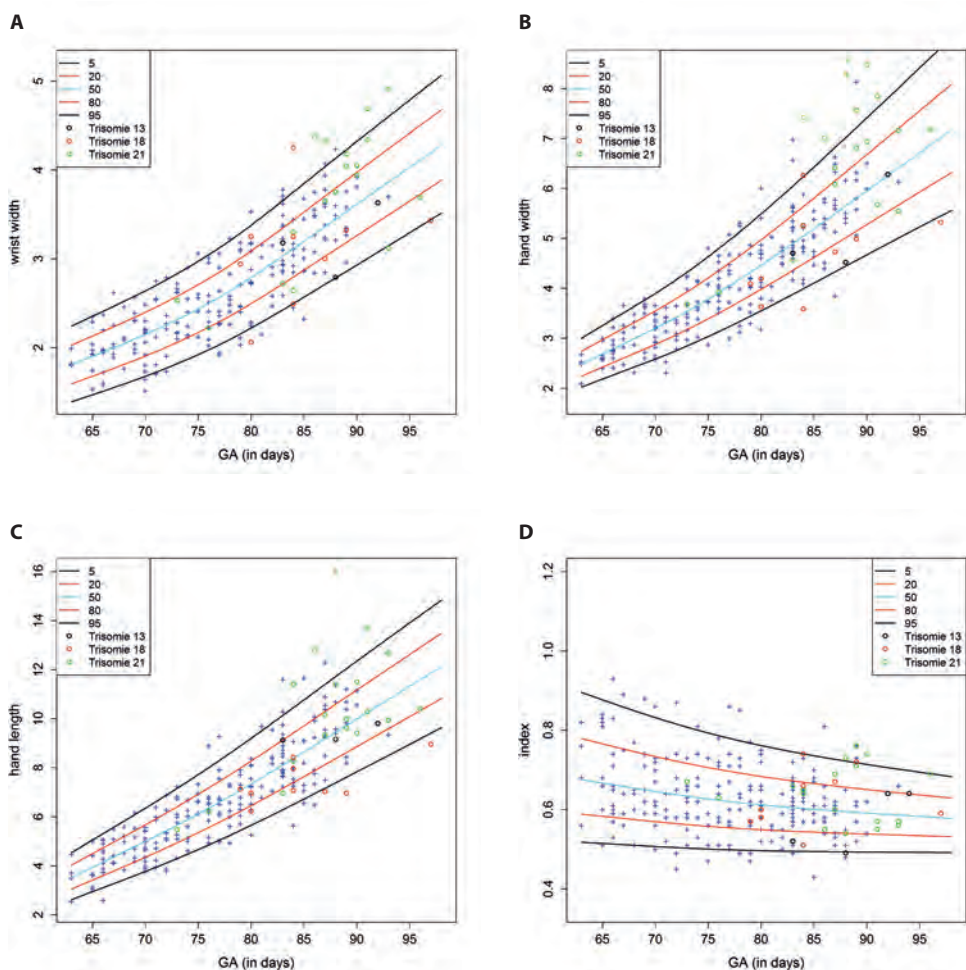


Figure 2: Graphical presentation of first-trimester wrist width (A), hand width (B), hand length (C), and hand index (D) in relation to gestational age (GA). Blue crosses indicated the individual measurements in euploid pregnancies (+). The mean (p50, cyan line) and the 5% and 95% reference interval (black line) and 20% and 80% reference interval (red line) are plotted. Each circle indicates a case of trisomy 21 (green), trisomy 18 (red) and trisomy 13 (black).

Table 2: Expected mean (p50) and p5, p20, p80 and p95 of wrist width, hand width, hand length, and hand index from 60 to 90 days gestational age.

GA	Wrist width					Hand width					Hand length					Hand index				
	p5	p20	p50	p80	p95	p5	p20	p50	p80	p95	p5	p20	p50	p80	p95	p5	p20	p50	p80	p95
60	1.27	1.46	1.66	1.87	2.07	1.78	1.96	2.17	2.39	2.62	2.14	2.50	2.90	3.32	3.75	0.52	0.60	0.69	0.80	0.92
62	1.35	1.55	1.76	1.97	2.18	1.94	2.15	2.38	2.62	2.87	2.46	2.87	3.32	3.79	4.27	0.52	0.59	0.68	0.79	0.91
64	1.43	1.63	1.85	2.08	2.30	2.10	2.33	2.59	2.86	3.13	2.78	3.24	3.74	4.26	4.79	0.52	0.59	0.67	0.77	0.89
66	1.51	1.72	1.95	2.18	2.41	2.26	2.51	2.79	3.09	3.38	3.11	3.60	4.15	4.73	5.31	0.51	0.58	0.66	0.76	0.87
68	1.59	1.81	2.05	2.29	2.52	2.42	2.70	3.00	3.32	3.64	3.44	3.97	4.57	5.20	5.83	0.51	0.57	0.65	0.75	0.85
70	1.68	1.90	2.15	2.40	2.64	2.58	2.88	3.20	3.55	3.90	3.77	4.35	4.99	5.67	6.35	0.51	0.57	0.65	0.73	0.83
72	1.77	2.00	2.26	2.51	2.76	2.76	3.07	3.42	3.80	4.17	4.12	4.74	5.43	6.16	6.88	0.50	0.56	0.64	0.72	0.82
74	1.87	2.11	2.37	2.64	2.90	2.94	3.28	3.66	4.07	4.48	4.48	5.15	5.88	6.66	7.44	0.50	0.56	0.63	0.71	0.80
76	1.97	2.23	2.50	2.78	3.05	3.13	3.50	3.92	4.35	4.80	4.85	5.57	6.35	7.18	8.01	0.50	0.56	0.62	0.70	0.79
78	2.09	2.36	2.64	2.93	3.20	3.34	3.74	4.18	4.66	5.13	5.24	6.00	6.84	7.72	8.59	0.50	0.55	0.62	0.69	0.77
80	2.22	2.49	2.79	3.09	3.38	3.55	3.98	4.46	4.97	5.49	5.65	6.45	7.34	8.27	9.20	0.50	0.55	0.61	0.68	0.76
82	2.35	2.64	2.95	3.26	3.56	3.77	4.23	4.75	5.30	5.86	6.07	6.92	7.86	8.84	9.82	0.50	0.55	0.61	0.68	0.75
84	2.50	2.79	3.11	3.44	3.75	3.99	4.49	5.04	5.64	6.24	6.50	7.40	8.38	9.42	10.45	0.49	0.54	0.60	0.67	0.74
86	2.64	2.95	3.28	3.62	3.94	4.22	4.75	5.34	5.98	6.62	6.94	7.88	8.92	10.00	11.08	0.49	0.54	0.60	0.66	0.73
88	2.78	3.11	3.45	3.80	4.13	4.45	5.01	5.65	6.33	7.02	7.39	8.37	9.45	10.59	11.72	0.49	0.54	0.59	0.66	0.72
90	2.93	3.26	3.61	3.97	4.32	4.67	5.28	5.95	6.68	7.41	7.83	8.86	9.99	11.17	12.35	0.49	0.54	0.59	0.65	0.71

GA = gestational age

week in Table 1. The graphical presentation of the relationship between the measurements and GA is illustrated in Figure 2. In Table 2 the expected mean (p50) and the p5, p20, p80 and p95 of the different hand measurements from 63 to 90 days GA are presented. Wrist width, hand width, and hand length increase with GA. Hand index decreases with GA, showing that with increasing GA fingers become longer and hands become smaller relatively. The relationship between the measurements and CRL is presented on a comparable way in Supplemental figure 1 and Supplemental table 1.

A total of 65 aneuploidy pregnancies were evaluated. Hand measurements could be performed in 31 of the 74 scans (41.9%, trisomy 21 $n=19$, trisomy 18 $n=9$, trisomy 13 $n=3$). Of the 19 trisomy 21 cases three presented with an hypoplastic nasal bone and one with hygroma colli. Of the nine trisomy 18 cases three presented with an omphalocele, three with a hygroma colli, one with a mega bladder, one with spina bifida, and one with holoprosencephaly. In the group of trisomy 13 cases ($n=3$) one case with holoprosencephaly and one case with a hygroma colli was seen. The median number of datasets per patient in which measurements were performed was one (range 1-2). GA ranges from 73 to 97 (median 87 days, SD 5.46 days) and de CRL ranged from 35 to 74 (median 60 mm, SD 11.12). Aneuploid pregnancies are plotted on the GA based reference ranges in Figure 2. In trisomy 13 no significant differences were found in hand measurements compared to euploid pregnancies. In trisomy 18 hand width and hand length were significantly smaller compared to euploid pregnancies ($p=0.009$ and $p=0.005$, respectively). In trisomy 21 a significantly larger wrist width and hand width were observed compared to euploid pregnancies ($p<0.001$ and $p<0.001$, respectively) (Table 3).

All intraclass correlation coefficient values were > 0.97 , indicating excellent reliability. Bland-Altman statistics (Table 4) and Bland-Altman plots (Figure 3) showed good agreement between the measurements. There were no systematic differences between the measurements of two different observers and between the repeated measurements of one observer.

Table 3: Z-scores of wrist width, hand width, hand length and hand index of aneuploid pregnancies with corresponding standard deviation (SD). $p<0.05$ shows a significant difference from euploid pregnancies.

	Trisomy 13		Trisomy 18		Trisomy 21	
	z-score (SD)	p	z-score (SD)	p	z-score (SD)	p
Wrist width	-0.52 (1.03)	0.841	-0.18 (1.64)	0.292	1.06 (2.04)	<0.001
Hand width	-0.60 (0.82)	0.344	-0.74 (1.20)	0.009	1.16 (1.30)	<0.001
Hand length	0.03 (0.71)	0.740	-0.97 (0.86)	0.005	0.70 (1.43)	0.230
Index	-0.33 (1.33)	0.436	0.30 (1.04)	0.912	0.59 (1.01)	0.136

Discussion

The present study is the first to provide an *in vivo* description of normal first-trimester hand growth in the human embryo. New charts for wrist width, hand width, hand length, and hand index are established between 9 and 13 weeks' GA, facilitated by a virtual reality system. Both intraobserver and interobserver reliability and agreement proved to be excellent.

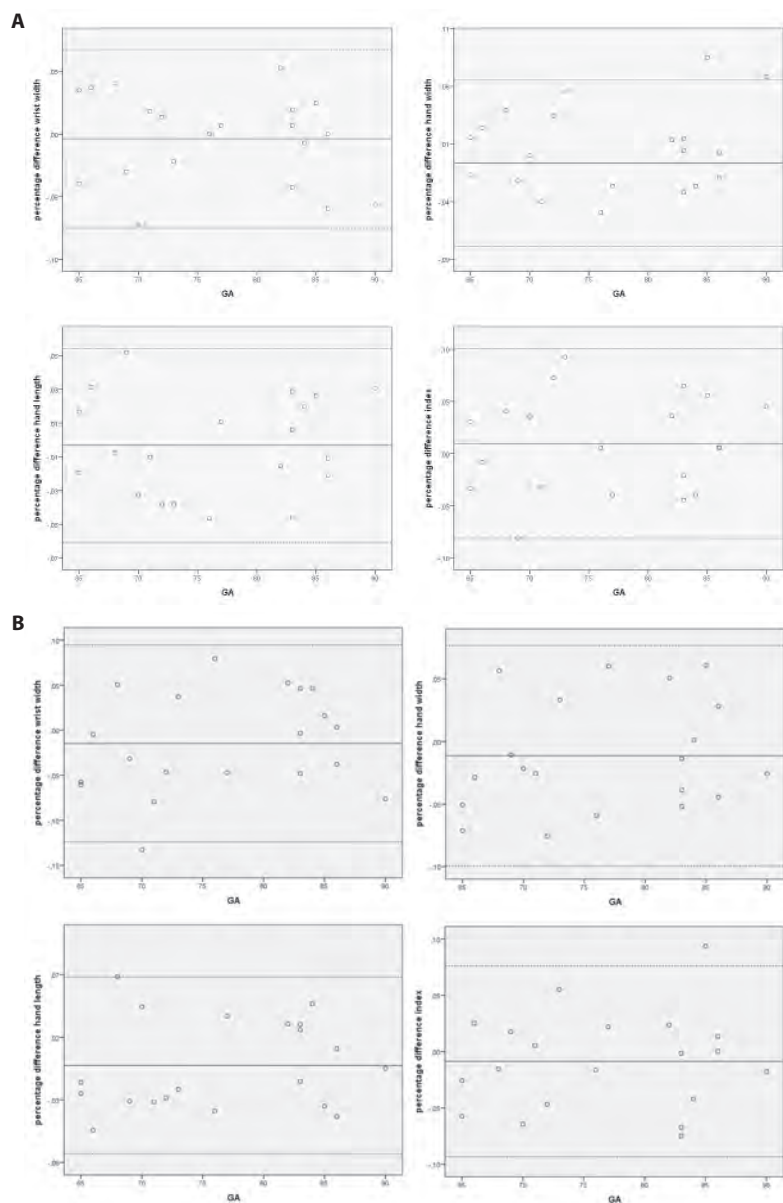


Figure 3: Bland-Altman plots of the four measured hand parameters (wrist width, hand width, hand length, and hand index) of intraobserver (A) and interobserver variability (B). The solid line represents the mean percentage difference and the broken lines the limits of agreement, calculated as the mean difference ± 1.96 SD. Index = hand width / hand length.

Table 4: Mean differences between measurements with corresponding 95% confidence interval, the limits of agreement and the ICCs with their 95% confidence interval are displayed. Measurements between two different observers (interobserver) and repeated measurements of the same observer (intraobserver) are compared.

	N	Mean difference (%)	95% CI mean difference (%)	p	limits of agreement (%)	ICC	95% CI ICC
Interobserver							
Wrist width	20	-1.468	-4.08-11.4	0.254	-12.40-9.46	0.984	0.960-0.994
Hand width	20	-1.139	-3.024-0.96	0.271	-9.95-7.67	0.992	0.981-0.997
Hand length	20	-0.253	-1.94-1.43	0.757	-7.31-6.81	0.997	0.994-0.999
Hand index	20	-0.860	-2.88-1.16	0.385	-9.34-7.62	0.984	0.959-0.993
Intraobserver							
Wrist width	20	-0.364	-2.06-1.34	0.659	-7.48-6.76	0.993	0.983-0.997
Hand width	20	0.622	-1.10-2.35	0.460	-6.60-7.84	0.993	0.982-0.997
Hand length	20	-0.319	-1.69-1.05	0.632	-6.06-5.43	0.998	0.995-0.999
Hand index	20	0.954	-1.22-3.12	0.369	-8.13-10.04	0.978	0.945-0.991

In euploid pregnancies, wrist width, hand width, and hand length increased with GA. Hand index decreased with GA, showing that the increase in embryonic hand length exceeds that of hand width. In cases with trisomy 21 and trisomy 18, first-trimester hand parameters are significantly different from those in euploid pregnancies. Trisomy 18 cases have both smaller and shorter hands, whereas trisomy 21 cases have wider wrists and wider hands. Hand growth in trisomy 13 pregnancies did not appear to be different.

As in the evaluation of both normal and abnormal hands, three-dimensional imaging was found to be helpful in evaluating spatial relationships.^{21,22} 3D US allows for complete evaluation of all fingers in a substantially higher percentage of cases than does 2D US.²³ The innovative VR tool used in this study both uses and enhances the information from the data that are obtained during 3D US. The VR technique is unique in its ability to truly visualize the third dimension and provides an intuitive understanding of the spatial relationships. Due to its tracing function, VR enables measurements of the hands and fingers, in any position, which is not possible using 3D US alone.

We are aware that the BARCO I-Space is not currently widely available. However, a desktop version of this 3D VR system is currently being developed, making this new and innovative technique broadly accessible to hospitals in the near future.

In this study, hand measurements were performed off-line on stored 3D US datasets. During the weekly US scans, a 3D sweep of the entire embryo or fetus was made. No targeted sweeps of the hand were made, which might explain the low success rate of 49.5%. In a clinical setting, higher success rates can be achieved by increasing scanning time and obtaining targeted sweeps of the hand.

To the best of our knowledge, only one other study, by Malas *et al.*,⁷ has described normal hand development in the first-trimester. The results of their measurements of hand growth parameters were considerably larger compared to ours. However, because of differences in study design, it is

hard to compare their findings with ours. Whereas Malas *et al.* performed hand measurements on abortion material, we performed our measurements *in vivo* using ultrasound. Their reference curves may therefore not be applicable for prenatal diagnosis. Moreover, they studied only 21 apparently normal cases from 9 to 12 weeks' GA.

Several other studies showed that hand growth is correlated to GA and CRL,^{3,4,7,24} emphasizing that hand parameters are good indicators of foetal development and possibly also for congenital malformations such as skeletal dysplasia.²⁵ In cases of increased risk for limb or skeletal abnormalities, it might be of clinical value to incorporate foetal hand length and hand width measurements within the foetal assessment in early pregnancy.

The aetiology of different hand growth patterns in trisomy 21 and trisomy 18 pregnancies is unclear. Several studies have been performed on finger length in trisomy 21. Kjaer *et al.* found normal finger length in trisomy 21 cases in the first half of the foetal period, but with shorter bones of the hand.⁵ Maymon *et al.* reported that all five digits of fetuses with trisomy 21 are short around mid-gestation.²⁶ Hypoplasia of the middle phalanx of the fifth digit has also been reported to be a characteristic of trisomy 21.^{4,27} In our study, we could not confirm that hand length was shorter in trisomy 21 in the first-trimester of pregnancy. It can be envisaged that any delayed maturation of the bones in trisomy 21 becomes evident after the first-trimester. In our first-trimester study population, it was not possible to evaluate the middle phalanx of the fifth digit.

Conclusion

Our study provides detailed information on human first-trimester hand development. *In vivo* first-trimester measurements of the hand appears feasible using a VR technique. Reference values are now available for studies on hand development in the first-trimester and for diagnosing abnormal hand growth. First-trimester hand measurement in cases affected by trisomy 21 and trisomy 18 differ significantly from that in euploid pregnancies.

Other than aneuploidy cases, we did not have cases available that were diagnosed with abnormalities of the hand. For this reason, no clear cut-off value below or above which the hand growth parameters are called abnormal can be given until more data is available on these cases. For now, we suggest that the presented p5/p95 intervals can be used as cut-off values. More research is needed on both aneuploid pregnancies and pregnancies at risk for abnormalities of the hand, to study the implications for first-trimester screening. These insights into hand size during normal and abnormal foetal development might be useful in future shift of prenatal diagnosis towards early pregnancy.

References

1. Cole P, Kaufman Y, Hatef DA, Hollier LH, Jr. Embryology of the hand and upper extremity. *J Craniofac Surg*. 2009;20(4):992-5.
2. Zguricas J, Bakker WF, Heus H, Lindhout D, Heutink P, Hovius SE. Genetics of limb development and congenital hand malformations. *Plast Reconstr Surg*. 1998;101(4):1126-35.
3. Tovbin J, Maymon R, Tovbin L, Dreazen E, Bukovsky I, Herman A. Prenatal age-specific reference intervals for measuring all five digits of the fetal hand. *Ultrasound Obstet Gynecol*. 2002;19(6):583-7.
4. Goldstein I, Gomez K, Copel JA. Fifth digit measurement in normal pregnancies: a potential sonographic sign of Down's syndrome. *Ultrasound Obstet Gynecol*. 1995;5(1):34-7.
5. Kjaer MS, Keeling JW, Andersen E, Fischer Hansen B, Kjaer I. Hand development in trisomy 21. *Am J Med Genet*. 1998;79(5):337-42.
6. Benacerraf BR. Prenatal sonography of autosomal trisomies. *Ultrasound Obstet Gynecol*. 1991;1(1):66-75.
7. Malas MA, Dogan S, Evcil EH, Desdicioglu K. Fetal development of the hand, digits and digit ratio (2D:4D). *Early Hum Dev*. 2006;82(7):469-75.
8. Rousian M, Groenenberg IA, Hop WC, Koning AH, van der Spek PJ, Exalto N, et al. Human embryonic growth and development of the cerebellum using 3-dimensional ultrasound and virtual reality. *Reprod Sci*. 2013;20(8):899-908.
9. Rousian M, Hop WC, Koning AH, van der Spek PJ, Exalto N, Steegers EA. First-trimester brain ventricle fluid and embryonic volumes measured by three-dimensional ultrasound with the use of I-Space virtual reality. *Hum Reprod*. 2013;28(5):1181-9.
10. van Uitert EM, van der Elst-Otte N, Wilbers JJ, Exalto N, Willemsen SP, Eilers PH, et al. Periconception maternal characteristics and embryonic growth trajectories: the Rotterdam Predict study. *Hum Reprod*. 2013;28(12):3188-96.
11. Reus AD, El-Harbachy H, Rousian M, Willemsen SP, Steegers-Theunissen RP, Steegers EA, et al. Early first-trimester trophoblast volume in pregnancies that result in live birth or miscarriage. *Ultrasound Obstet Gynecol*. 2013;42(5):577-84.
12. van Uitert E, van Ginkel S, Willemsen S, Lindemans J, Koning A, Eilers P, et al. An optimal periconception maternal folate status for embryonic size: the Rotterdam Predict study. *BJOG*. 2014;121(7):821-9.
13. van Uitert EM, Exalto N, Burton GJ, Willemsen SP, Koning AH, Eilers PH, et al. Human embryonic growth trajectories and associations with fetal growth and birthweight. *Hum Reprod*. 2013;28(7):1753-61.
14. van Uitert EM, van der Elst-Otte N, Wilbers JJ, Exalto N, Willemsen SP, Eilers PH, et al. Periconception maternal characteristics and embryonic growth trajectories: the Rotterdam Predict study. *Hum Reprod*. 2013;28(12):3188-96.
15. Cruz-Neira C, Sandin DJ, DeFanti TA. Surround-screen projection-based virtual reality: the design and implementation of the CAVE (tm). *Proceedings of the 20th Annual Conference on Computer Graphics and Interactive Techniques*. 1993:135-42.
16. Koning AH, Rousian M, Verwoerd-Dikkeboom CM, Goedknegt L, Steegers EA, van der Spek PJ. V-scope: design and implementation of an immersive and desktop virtual reality volume visualization system. *Stud Health Technol Inform*. 2009;142:136-8.

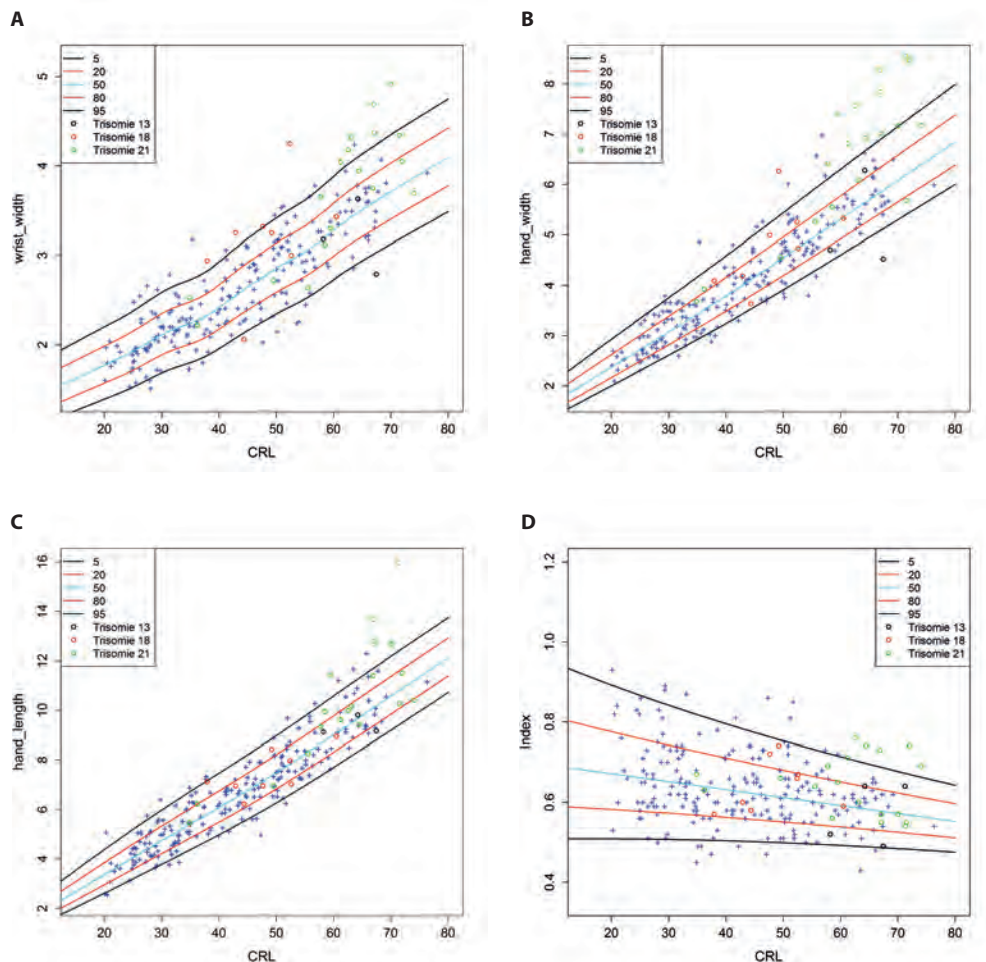
17. Verwoerd-Dikkeboom CM, Koning AH, Hop WC, Rousian M, Van Der Spek PJ, Exalto N, et al. Reliability of three-dimensional sonographic measurements in early pregnancy using virtual reality. *Ultrasound Obstet Gynecol.* 2008;32(7):910-6.
18. Rousian M, Koning AH, van Oppenraaij RH, Hop WC, Verwoerd-Dikkeboom CM, van der Spek PJ, et al. An innovative virtual reality technique for automated human embryonic volume measurements. *Hum Reprod.* 2010;25(9):2210-6.
19. Baken L, van Heesch PN, Wildschut HI, Koning AH, van der Spek PJ, Steegers EA, et al. First-trimester crown-rump length and embryonic volume of aneuploid fetuses measured in virtual reality. *Ultrasound Obstet Gynecol.* 2013;41(5):521-5.
20. Cole TJ. The LMS method for constructing normalized growth standards. *Eur J Clin Nutr.* 1990;44(1):45-60.
21. Budorick NE, Pretorius DH, Johnson DD, Tartar MK, Lou KV, Nelson TR. Three-dimensional ultrasound examination of the fetal hands: normal and abnormal. *Ultrasound Obstet Gynecol.* 1998;12(4):227-34.
22. Kos M, Hafner T, Funduk-Kurjak B, Bozek T, Kurjak A. Limb deformities and three-dimensional ultrasound. *J Perinat Med.* 2002;30(1):40-7.
23. Ploekinger-Ulm B, Ulm MR, Lee A, Kratochwil A, Bernaschek G. Antenatal depiction of fetal digits with three-dimensional ultrasonography. *Am J Obstet Gynecol.* 1996;175(3 Pt 1):571-4.
24. Kjaer MS, Kjaer I. Human fetal hand size and hand maturity in the first half of the prenatal period. *Early Hum Dev.* 1998;50(2):193-207.
25. Goncalves L, Jeanty P. Fetal biometry of skeletal dysplasias: a multicentric study. *J Ultrasound Med.* 1994;13(12):977-85.
26. Maymon R, Tovbin Y, Dreazen E, Weinraub Z, Herman A. All five digits of the hands of fetuses with Down syndrome are short. *Ultrasound Obstet Gynecol.* 2004;23(6):557-60.
27. Benacerraf BR, Harlow BL, Frigoletto FD, Jr. Hypoplasia of the middle phalanx of the fifth digit. A feature of the second trimester fetus with Down's syndrome. *J Ultrasound Med.* 1990;9(7):389-94.

Supplemental Material

Supplemental Table 1: Expected mean (p50) and p5, p20, p80 and p95 of wrist width, hand width, hand length, and hand index for crown-rump length (20–70 mm).

CRL	Wrist width					Hand width					Hand length					Hand index				
	p5	p20	p50	p80	p95	p5	p20	p50	p80	p95	p5	p20	p50	p80	p95	p5	p20	p50	p80	p95
20	1.39	1.57	1.77	1.99	2.20	2.00	2.16	2.37	2.62	2.93	2.61	2.96	3.37	3.85	4.38	0.51	0.58	0.67	0.78	0.89
25	1.53	1.72	1.93	2.15	2.38	2.30	2.49	2.72	3.00	3.34	3.19	3.59	4.06	4.60	5.20	0.51	0.58	0.66	0.76	0.87
30	1.68	1.89	2.11	2.35	2.59	2.61	2.82	3.07	3.38	3.75	3.78	4.22	4.74	5.33	5.98	0.51	0.57	0.65	0.74	0.84
35	1.80	2.01	2.24	2.48	2.73	2.92	3.15	3.43	3.77	4.16	4.38	4.85	5.41	6.05	6.73	0.51	0.57	0.64	0.73	0.82
40	1.96	2.17	2.42	2.67	2.93	3.24	3.49	3.79	4.16	4.58	4.98	5.49	6.08	6.75	7.47	0.50	0.56	0.63	0.71	0.80
45	2.16	2.39	2.65	2.92	3.19	3.57	3.84	4.16	4.55	5.01	5.61	6.14	6.77	7.47	8.21	0.50	0.56	0.62	0.70	0.77
50	2.35	2.59	2.86	3.14	3.42	3.91	4.19	4.54	4.96	5.44	6.27	6.83	7.49	8.21	8.97	0.50	0.55	0.61	0.68	0.75
55	2.51	2.76	3.04	3.33	3.62	4.25	4.55	4.92	5.36	5.87	6.97	7.56	8.24	8.98	9.76	0.50	0.54	0.60	0.67	0.73
60	2.73	2.99	3.28	3.58	3.88	4.60	4.92	5.31	5.77	6.30	7.70	8.31	9.01	9.77	10.57	0.49	0.54	0.59	0.65	0.71
65	2.94	3.21	3.51	3.82	4.13	4.95	5.28	5.69	6.18	6.73	8.44	9.07	9.79	10.57	11.38	0.49	0.53	0.58	0.64	0.70
70	3.13	3.41	3.71	4.03	4.35	5.30	5.65	6.08	6.58	7.15	9.20	9.84	10.57	11.36	12.18	0.48	0.53	0.57	0.62	0.68

CRL = crown-rump length



Supplemental Figure 1: Graphical presentation of first-trimester wrist width (A), hand width (B), hand length (C), and hand index (D) in relation to crown-rump length (CRL). Blue crosses indicated the individual measurements in euploid pregnancies (+). The mean (p50, cyan line) and the 5% and 95% reference interval (black line) and 20% and 80% reference interval (red line) are plotted. Each circle indicates a case of trisomy 21 (green), trisomy 18 (red) and trisomy 13 (black).

4.2

First-Trimester Crown-Rump Length and Embryonic Volume of Aneuploid Fetuses measured in Virtual Reality

Ultrasound in Obstetrics and Gynaecology. 2013;51(5):521-525

L. Baken

P.N.A.M. van Heesch

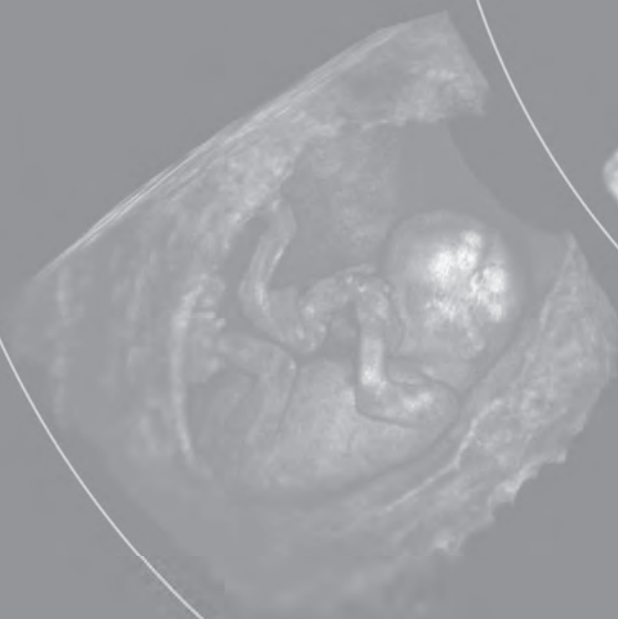
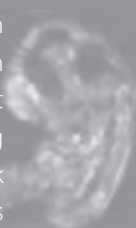
H.I.J. Wildschut

A.H.J. Koning

P.J. van der Spek

E.A.P. Steegers

N. Exalto



Abstract

Objective. To examine whether embryonic volume (EV), as measured using three-dimensional (3D) ultrasound and a virtual reality (VR) approach, is a better measure of growth restriction than crown-rump length (CRL) in aneuploid fetuses.

Methods. We retrospectively measured CRL and EV in prospectively collected 3D ultrasound volumes of 55 aneuploid fetuses using our Barco I-Space VR system. The gestational age ranged from 11+2 to 14+4 weeks. We compared our measured data with previously published reference curves for euploid fetuses. Delta-values were calculated by subtracting observed values from the expected mean for euploid fetuses of the same gestational age. The one-sample t-test was used to test the significance of differences observed.

Results. The CRL measurements of fetuses with trisomy 21 ($n=26$), trisomy 13 ($n=5$) and monosomy X ($n=5$) were comparable to those of euploid fetuses, but in fetuses with trisomy 18 ($n=19$) the CRL was 14.5% smaller ($p<0.001$). The EV in fetuses with trisomy 21, 18, 13 and monosomy X was smaller than in euploid fetuses (-27.8%, $p<0.001$; -39.4%, $p<0.001$; -40.9%, $p=0.004$; and -27.3%, $p=0.055$; respectively).

Conclusion. When relying on CRL measurements alone, first-trimester growth restriction is especially manifest in trisomy 18. Using EV, growth restriction is also evident in trisomy 21, 13 and monosomy X. EV seems to be a more effective measurement for the assessment of first-trimester growth restriction in aneuploid fetuses.

Introduction

It has been known for a long time that fetal growth restriction may be a marker for aneuploidy.¹⁻³ Typically, growth restriction in aneuploid pregnancies is of early onset, and is evident from the first-trimester onwards. In trisomy 21, however, crown-rump length (CRL) measurements are similar to chromosomally normal fetuses of the same gestational age (GA).^{1,3}

Traditionally, first-trimester fetal growth has been documented by two-dimensional (2D) CRL measurements. With the introduction of three-dimensional (3D) ultrasound it became possible to measure embryonic and fetal volumes. Earlier studies show that the relative increment of fetal volume is much larger than the increment of CRL during the same period.⁴ Rousian et. al. (2010) demonstrated that when the CRL doubles the embryonic volume (EV) increases 6.5-fold.⁴ Volume measurement might therefore enable earlier detection of fetal growth restriction in pregnancy.

Several other studies have been performed measuring fetal volumes using 3D ultrasound.⁵⁻⁸ To estimate the embryonic or fetal volume in these studies 2D contours were defined manually in several different planes. As various methods have been used and different normal values for EV have been reported there is a need for standardization.⁹⁻¹⁰

The introduction of the virtual reality (VR) visualization technique enables us to use all three dimensions of these 3D ultrasound scans. The Erasmus MC operates a BARCO I-Space VR system. This is a four-walled CAVETM-like¹¹ VR system in which investigators are surrounded by stereoscopic images. A hologram is created by the V-Scope¹² volume rendering application and polarized glasses enable the viewer to perceive depth and to interact with 3D volumes in an intuitive manner. Using V-Scope it is possible to perform precise EV calculations semi-automatically⁴ while benefitting from true 3D depth perception.

The aim of this study was to examine fetal growth pattern in aneuploid fetuses (trisomy 21, 18, 13, and monosomy X) during the late first-trimester and to compare EV and CRL between euploid and aneuploid pregnancies.

Methods

Between 2008 and 2012 3D ultrasound volumes were collected of singleton pregnancies in which an increased nuchal translucency (NT) was measured (>3.5 mm) during routine ultrasound examination. Ultrasound scans were performed using the Voluson 730 Expert (GE Medical Systems, Zipf, Austria) ultrasound machine. Later, following invasive prenatal diagnosis, aneuploid pregnancies were identified ($n=63$). The GA was calculated based on the first day of the last menstrual period or, when assisted reproductive technology was performed, on the day of conception. The GA ranged from 11+2 to 14+4 weeks.

The 3D volumes were converted to Cartesian volumes using 3D software (4D View, GE Medical Systems) and transferred to the BARCO I-Space. In the I-Space all volumes were evaluated and the best volume for each case was selected based on image quality and completeness of the volume.

We excluded eight cases for the measurements of both CRL and EV due to poor image quality ($n=5$), due to incompleteness of the volume ($n=1$), and because of absence of fetal heart activity at the time of the ultrasound scan ($n=2$). Of these eight cases three were diagnosed with trisomy 21, three with trisomy 18, and two with monosomy X (45, XO). Four 3D volumes, two cases with trisomy 21 and two cases with trisomy 18, were excluded for analysis of EV alone. Due to poor image quality it was not possible to measure EV; however in these cases it was possible to measure CRL. Following exclusions, 26 pregnancies diagnosed with trisomy 21, 19 with trisomy 18, five with trisomy 13 and five with monosomy X were available for analysis. A fetus affected by trisomy 18 in the I-Space VR-system is shown in Figure 1.

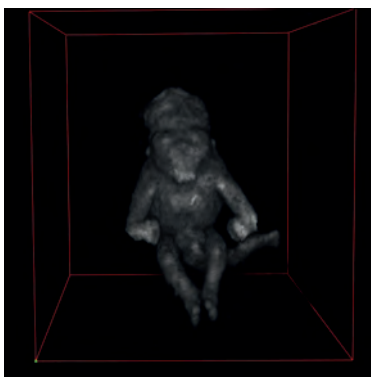


Figure 1: Fetus with trisomy 18 in the I-Space virtual reality system. Multiple congenital abnormalities can be seen: exencephaly, radial aplasia, and omphalocele. Spina bifida and polydactyly were also present.

CRL and EV were measured using the V-Scope software. The V-Scope¹² application includes a region-growing segmentation algorithm for semi-automatic volume calculation in selected structures.¹¹⁻¹² The innovative VR technique has already successfully been applied in prenatal medicine.¹³⁻¹⁵

The procedure for measuring EV has been described in detail by Rousian et. al.⁴ Both physiological and pathological omphalocele were included in the embryonic volume. Hydrops, frequently present in fetuses with chromosomal abnormalities, was also included in the embryonic volume calculation. This is relatively easy to achieve by performing a second segmentation of the anechoic fluid layer of the hydrops, aside from the segmentation of the body volume. If necessary this fluid layer can also be segmented manually. All measurements in the I-Space were performed by the same investigator (L.B.). The accuracy and reproducibility of length and volume measurements have been demonstrated in previous studies^{4,16-18}, in which the growth trajectories of euploid pregnancies for CRL and EV have also been determined and reference curves established. The collected data in the present study were compared to the results of these previous studies on euploid fetuses.

Statistical analysis

The expected mean EV of euploid fetuses at the same GA was subtracted from the observed EV of the aneuploid fetuses. This expected value was obtained from equations published in earlier studies^{4,17-18}, and the difference was expressed as a proportion of the mean embryonic volume of euploid fetuses. The same analysis was performed to investigate the possible association of EV and CRL, and for CRL and GA. We furthermore determined the difference in days' GA, comparing observed days of GA and expected days of GA according to the observed EV and CRL.

The one-sample t-test was used to test for statistically significant differences between observed values of aneuploid pregnancies and expected values of euploid pregnancies.

Data analysis was performed using SPSS v.17.0.2 (SPSS Inc., Chicago, IL, USA). A *p*-value <0.05 was considered statistically significant.

Results

Of the 26 trisomy 21 cases three presented with hydrops and/or hygroma colli. In the trisomy 18 group nine were diagnosed with a pathological omphalocele and four with hydrops fetalis. Three of the 19 trisomy 18 cases had multiple congenital malformations (i.e. exencephaly, holoprosencephaly, spina bifida, skeletal abnormalities, nephrourological abnormalities). Two cases of holoprosencephaly, three cases with hydrops and/or hygroma colli, one omphalocele and one hypoplastic left heart syndrome were diagnosed in the trisomy 13 group. Three of the five cases with monosomy X presented with a hydrops. Other congenital abnormalities diagnosed in this group were hydronephrosis and cardiac abnormalities.

Table 1: Mean percentage difference and mean difference in days' gestational age (GA) for crown-rump length (CRL) and embryonic volume (EV) for aneuploid fetuses in comparison to the normal mean according to GA for euploid fetuses.

		Mean difference in:			
Variable/karyotype	n	% (95% CI)	P*	Days' GA (95%CI)	P*
CRL					
Trisomy 21	26	-1.29 (-4.97 to 2.38)	0.475	-0.55 (-1.79 to 0.69)	0.369
Trisomy 18	19	-14.53 (-19.94 to -9.12)	<0.001	-4.78 (-6.77 to -2.78)	<0.001
Trisomy 13	5	-5.44 (-14.39 to 3.52)	0.167	-1.75 (-4.55 to 1.06)	0.159
Monosomy X	5	-3.65 (-18.72 to 11.43)	0.539	-1.43 (-6.18 to 3.32)	0.450
EV					
Trisomy 21	24	-27.76 (-35.80 to -19.72)	<0.001	-3.45 (-4.56 to -2.34)	<0.001
Trisomy 18	17	-39.37 (-48.23 to -30.50)	<0.001	-5.14 (-7.04 to -3.23)	<0.001
Trisomy 13	5	-40.87 (-59.75 to -22.00)	0.004	-5.25 (-8.63 to -1.88)	0.012
Monosomy X	5	-27.29 (-55.56 to 0.0097)	0.055	-3.63 (-8.33 to 1.07)	0.097

* For observed mean difference vs 0.

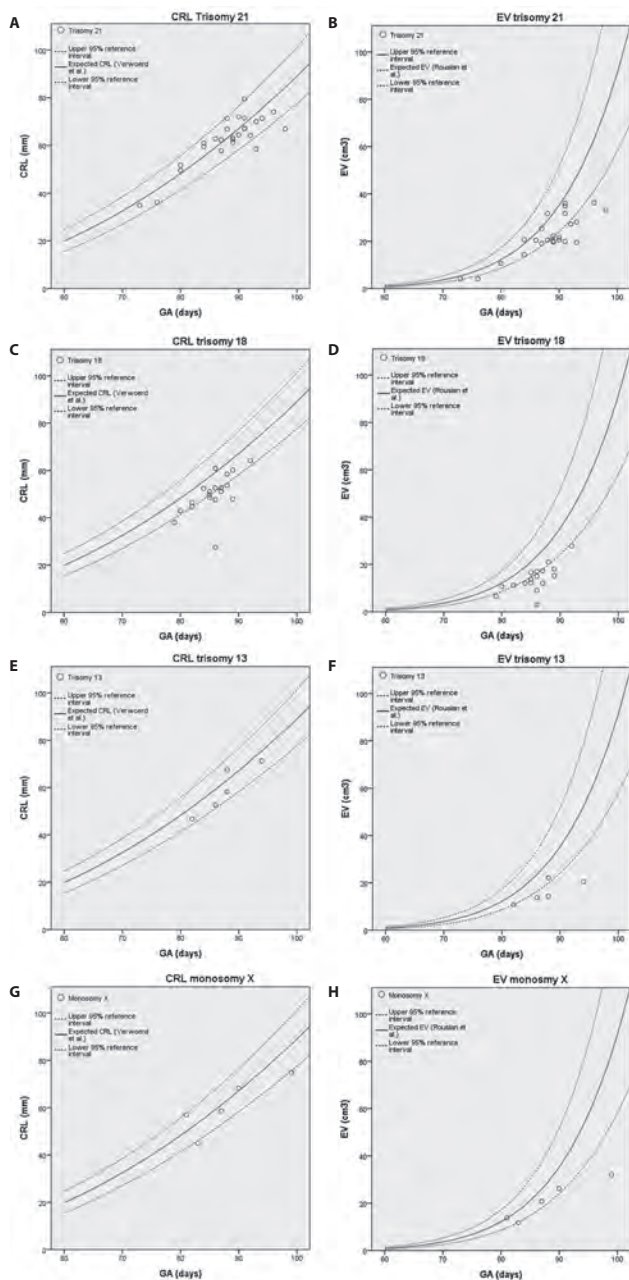


Figure 2: First-trimester measurements of crown-rump length (CRL) and embryonic volume (EV) according to gestational age in fetuses affected by (A,B) trisomy 21, (C,D) trisomy 18, (E,F) trisomy 13 and (G,H) monosomy X plotted on references curves (median (solid line) and 95% reference interval (dashed line) for CRL and EV of euploid fetuses by Verwoerd-Dikkeboom *et al.*¹⁸ and Rousian *et al.*⁴, respectively.

Fetuses diagnosed with trisomy 18 showed a 14.53% smaller CRL than expected ($p<0.001$), corresponding to a -4.78 differences in days GA. The other groups of aneuploid fetuses, trisomy 21, 13 and monosomy X, showed a non-significantly smaller CRL than did euploid fetuses (Table 1). In all groups of aneuploid fetuses the EV was smaller than expected for GA: -27.76% for trisomy 21 ($p<0.001$), -39.37% for trisomy 18 ($p<0.001$) and -40.87% for trisomy 13 ($p=0.004$), although the difference was not quite statistically significant for monosomy X (-27.29%; $p=0.055$). In terms of days' GA, these differences ranged from -3.45 to -5.14 (Table 1). In Figure 2, the CRL and EV of fetuses with trisomy 21, trisomy 18, trisomy 13 and monosomy X are plotted relative to the reference range with respect to gestational age of euploid fetuses.

The difference between observed EV for the aneuploid fetuses and that expected according to their CRL is presented in Table 2. Significant differences were found for fetuses affected by trisomy 18, which had on average a 17.37% smaller EV compared to the normal mean for CRL ($p=0.003$). Smaller measurements of EV than expected for CRL were also found for cases of trisomy 13, although this was not statistically significant. For trisomy 21 and monosomy X, no difference was observed.

Table 2: Mean percentage difference in embryonic volume (EV) in aneuploidy fetuses compared to normal mean EV in euploid fetuses for crown-rump length.

Karyotype	n	Mean % difference (95% CI)	p
Trisomy 21	24	-0.37 (-8.56 to 7.83)	0.927
Trisomy 18	17	-17.37 (-6.68 to -28.04)	0.003
Trisomy 13	5	-9.75 (-31.78 to 12.28)	0.287
Monosomy X	5	5.48 (-20.63 to 31.60)	0.591

Discussion

The results of this study are in line with previous research demonstrating that chromosomal abnormalities are often accompanied by growth restriction. The data show that based on CRL growth restriction can be observed in trisomy 18 at 11–14 weeks (-14.53%, $p<0.001$). Small, non-significant, differences in CRL were found for trisomy 13, monosomy X and trisomy 21.

In contrast to CRL, EV was significantly smaller than expected in trisomy 21, trisomy 18 and trisomy 13, with a large but marginally non-significant difference in the small sample of fetuses with monosomy X. The mean percentage difference in EV was also more evident than the mean percentage difference in CRL and was as high as -40.87% for trisomy 13. These findings show the same trend as the reported birth weights in these conditions; infants with trisomy 18 are the most likely and those with trisomy 21 the least likely to be small for GA.¹⁹ The EV in fetuses affected by trisomy 21, 13 and monosomy X was found to be in proportion to their CRL, as no significant difference from that expected was found when EV was corrected for the observed CRL. However, disproportionate growth restriction

was found in the fetuses with trisomy 18; when correcting for CRL, EV was significantly decreased by 17% on average. This disproportionality points at an asymmetric growth disturbance that affects the internal organs more than the skeleton, with this being associated with more severe growth restriction. To further examine the aspects of disproportionality, future research will be performed on the head-to-body volume ratio in both euploid and aneuploid fetuses in order to evaluate the type of growth restriction (symmetric or asymmetric).

Structural congenital abnormalities are frequently present in chromosomally abnormal fetuses. As explained, we accounted for omphalocele and hydrops fetalis in the EV calculation. Holoprosencephaly, associated with trisomy 13 and 18, might have a small influence on EV. However, holoprosencephaly can be accompanied by both microcephaly and hydrocephaly, each contributing to EV in a different direction. Moreover, it is unlikely that a 30–40% smaller EV is caused by structural abnormalities exclusively. Abnormal EV in aneuploid fetuses can be explained by an increased duration of the cell-cycle, due to checkpoint control genes, resulting in a significantly reduced numerical cell count compared to euploid fetuses.²⁰

At present, it is only possible to speculate regarding the clinical importance of first-trimester growth restriction in aneuploid fetuses. It is as of yet unclear whether first-trimester growth restriction is helpful in identifying fetuses with chromosomal abnormalities during the first-trimester of pregnancy. It may, however, be hypothesized that markedly growth restricted aneuploid fetuses are more prone to intrauterine fetal death in the second and third trimester of pregnancy, and these pregnancies may be identified earlier by measuring EV. This hypothesis should be subject of further research on EV and pregnancy outcome.

Limitations of this study include the low number of cases for both trisomy 13 and monosomy X; the groups with the lowest incidence of the aneuploidies investigated in this study. However, the fact that we found a statistically significant difference in EV for trisomy 13 and an only marginally non-significant difference for monosomy X ($p=0.004$ and $p=0.055$, respectively) suggests that there is a strong relationship between aneuploidy and decreased EV. It seems likely that the analysis of additional cases in these groups would confirm the relationship. Another limitation of our study is that at this time the BARCO I-Space is too large (requiring a separate 40m²/400 sq. ft. room) and too expensive for 3D VR to become a routine diagnostic procedure, which limits its use in routine practice. However, a desktop version of this 3D VR system is currently being developed, which will make this new and innovative technique more accessible to hospitals in the near future. A prototype is already being evaluated at our outpatient clinic for use in both research and daily clinical practice.

In conclusion, evaluation of growth in the first-trimester is typically performed by measuring CRL using two-dimensional ultrasound. CRL can only be used as a reliable indicator of growth restriction in aneuploid fetuses in the first-trimester for pregnancies with trisomy 18. Using EV, growth restriction is also evident in trisomy 21, trisomy 13 and monosomy X. This study shows that in aneuploid fetuses, EV measurements can be used to diagnose abnormal first-trimester growth.

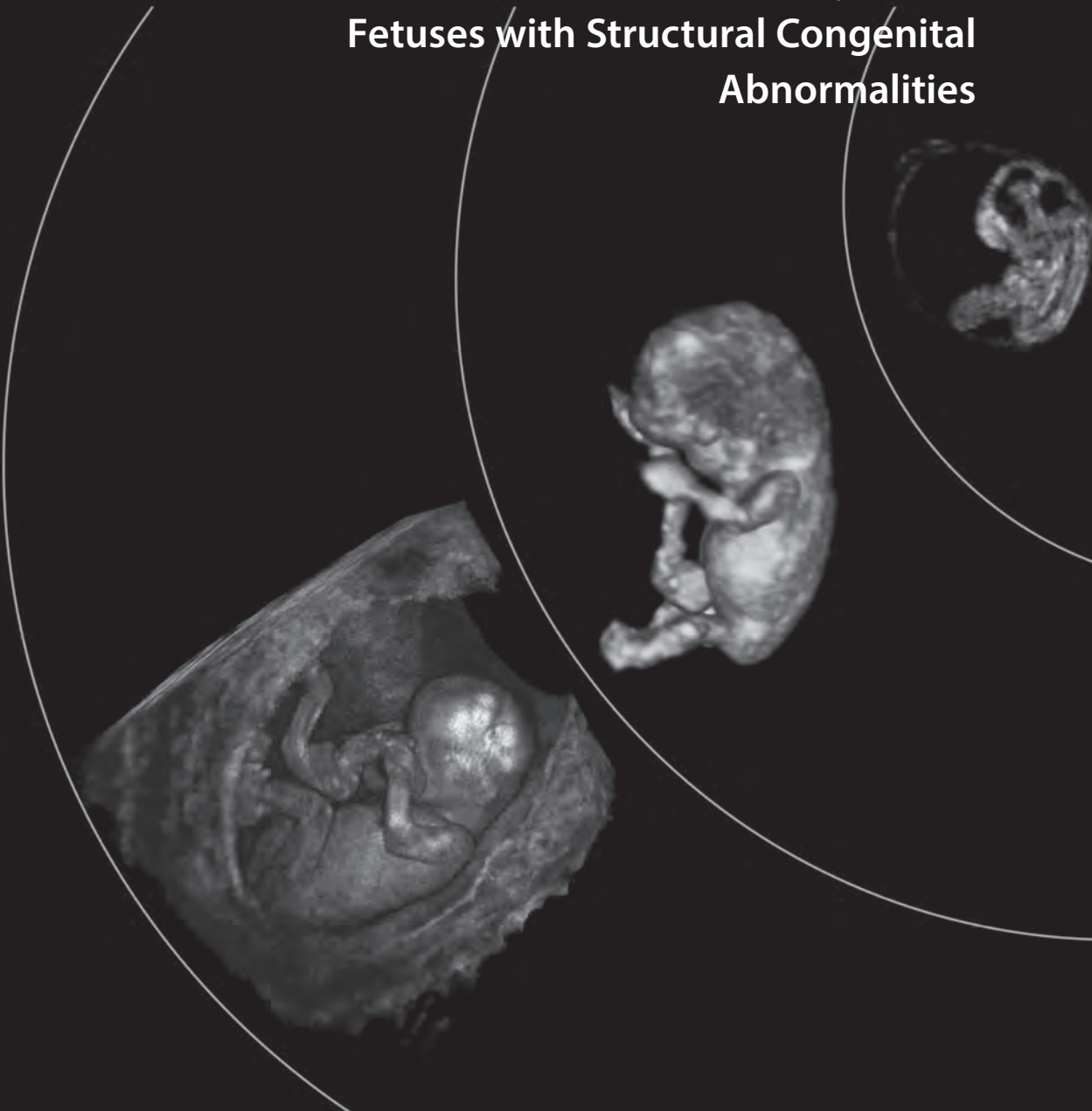
References

1. Schemmer G, Wapner RJ, Johnson A, Schemmer M, Norton HJ, Anderson WE. First-trimester growth patterns of aneuploid fetuses. *Prenat Diagn* 1997;17:155-159.
2. Nicolaides KH. Nuchal translucency and other first-trimester sonographic markers of chromosomal abnormalities. *Am J Obstet Gynecol* 2004;191:45-67.
3. Bahado-Singh RO, Lynch L, Deren O, Morroti R, Copel JA, Mahoney MJ, Williams J, 3rd. First-trimester growth restriction and fetal aneuploidy: the effect of type of aneuploidy and gestational age. *Am J Obstet Gynecol* 1997;176:976-980.
4. Rousian M, Koning AH, van Oppenraaij RH, Hop WC, Verwoerd-Dikkeboom CM, van der Spek PJ, Exalto N, Steegers EA. An innovative virtual reality technique for automated human embryonic volume measurements. *Hum Reprod* 2010;25:2210-2216.
5. Falcon O, Peralta CF, Cavoretto P, Auer M, Nicolaides KH. Fetal trunk and head volume in chromosomally abnormal fetuses at 11+0 to 13+6 weeks of gestation. *Ultrasound Obstet Gynecol* 2005;26:517-520.
6. Aviram R, Shpan DK, Markovitch O, Fishman A, Tepper R. Three-dimensional first-trimester fetal volumetry: comparison with crown rump length. *Early Hum Dev* 2004;80:1-5.
7. Blaas HG, Taipale P, Torp H, Eik-Nes SH. Three-dimensional ultrasound volume calculations of human embryos and young fetuses: a study on the volumetry of compound structures and its reproducibility. *Ultrasound Obstet Gynecol* 2006;27:640-646.
8. Bagratee JS, Regan L, Khullar V, Connolly C, Moodley J. Reference intervals of gestational sac, yolk sac and embryo volumes using three-dimensional ultrasound. *Ultrasound Obstet Gynecol* 2009;34:503-509.
9. Sur SD, Clewes JS, Campbell BK, Raine-Fenning NJ. Embryo volume measurement: an intraobserver, intermethod comparative study of semiautomated and manual three-dimensional ultrasound techniques. *Ultrasound Obstet Gynecol* 2011;38:516-523.
10. Ioannou C, Sarris I, Salomon LJ, Papageorgiou AT. A review of fetal volumetry: the need for standardization and definitions in measurement methodology. *Ultrasound Obstet Gynecol* 2011;38:613-619.
11. Cruz-Neira C, Sandin D, DeFanti T. Surround-screen projection-based virtual reality: the design and implementation of the CAVE (tm). *Proceedings of the 20th annual conference on computer graphics and interactive techniques*. New York: ACM Press 1993.
12. Koning AH, Rousian M, Verwoerd-Dikkeboom CM, Goedknegt L, Steegers EA, van der Spek PJ. V-scope: design and implementation of an immersive and desktop virtual reality volume visualization system. *Stud Health Technol Inform* 2009;142:136-138.
13. Verwoerd-Dikkeboom CM, Koning AH, Groenenberg IA, Smit BJ, Brezinka C, Van Der Spek PJ, Steegers EA. Using virtual reality for evaluation of fetal ambiguous genitalia. *Ultrasound Obstet Gynecol* 2008;32:510-514.
14. Groenenberg IA, Koning AH, Galjaard RJ, Steegers EA, Brezinka C, van der Spek PJ. A virtual reality rendition of a fetal meningomyelocele at 32 weeks of gestation. *Ultrasound Obstet Gynecol* 2005;26:799-801.
15. Verwoerd-Dikkeboom CM, van Heesch PN, Koning AH, Galjaard RJ, Exalto N, Steegers EA. Embryonic delay in growth and development related to confined placental trisomy 16 mosaicism, diagnosed by I-Space Virtual Reality. *Fertil Steril* 2008;90:2017 e2019-2022.

16. Rousian M, Verwoerd-Dikkeboom CM, Koning AH, Hop WC, van der Spek PJ, Exalto N, Steegers EA. Early pregnancy volume measurements: validation of ultrasound techniques and new perspectives. *BJOG* 2009;116:278-285.
17. Verwoerd-Dikkeboom CM, Koning AH, Hop WC, Rousian M, Van Der Spek PJ, Exalto N, Steegers EA. Reliability of three-dimensional sonographic measurements in early pregnancy using virtual reality. *Ultrasound Obstet Gynecol* 2008;32:910-916.
18. Verwoerd-Dikkeboom CM, Koning AH, Hop WC, van der Spek PJ, Exalto N, Steegers EA. Innovative virtual reality measurements for embryonic growth and development. *Hum Reprod* 2010;25:1404-1410.
19. Boghossian NS, Horbar JD, Murray JC, Carpenter JH. Anthropometric charts for infants with trisomies 21, 18, or 13 born between 22 weeks gestation and term: the VON charts. *Am J Med Genet A* 2012;158A:322-332.
20. Sheltzer JM, Torres EM, Dunham MJ, Amon A. Transcriptional consequences of aneuploidy. *Proc Natl Acad Sci USA* 2012;109:12644-12649.

CHAPTER 5

Diagnostic Applicability of the Third Dimension in Embryos and Fetuses with Structural Congenital Abnormalities

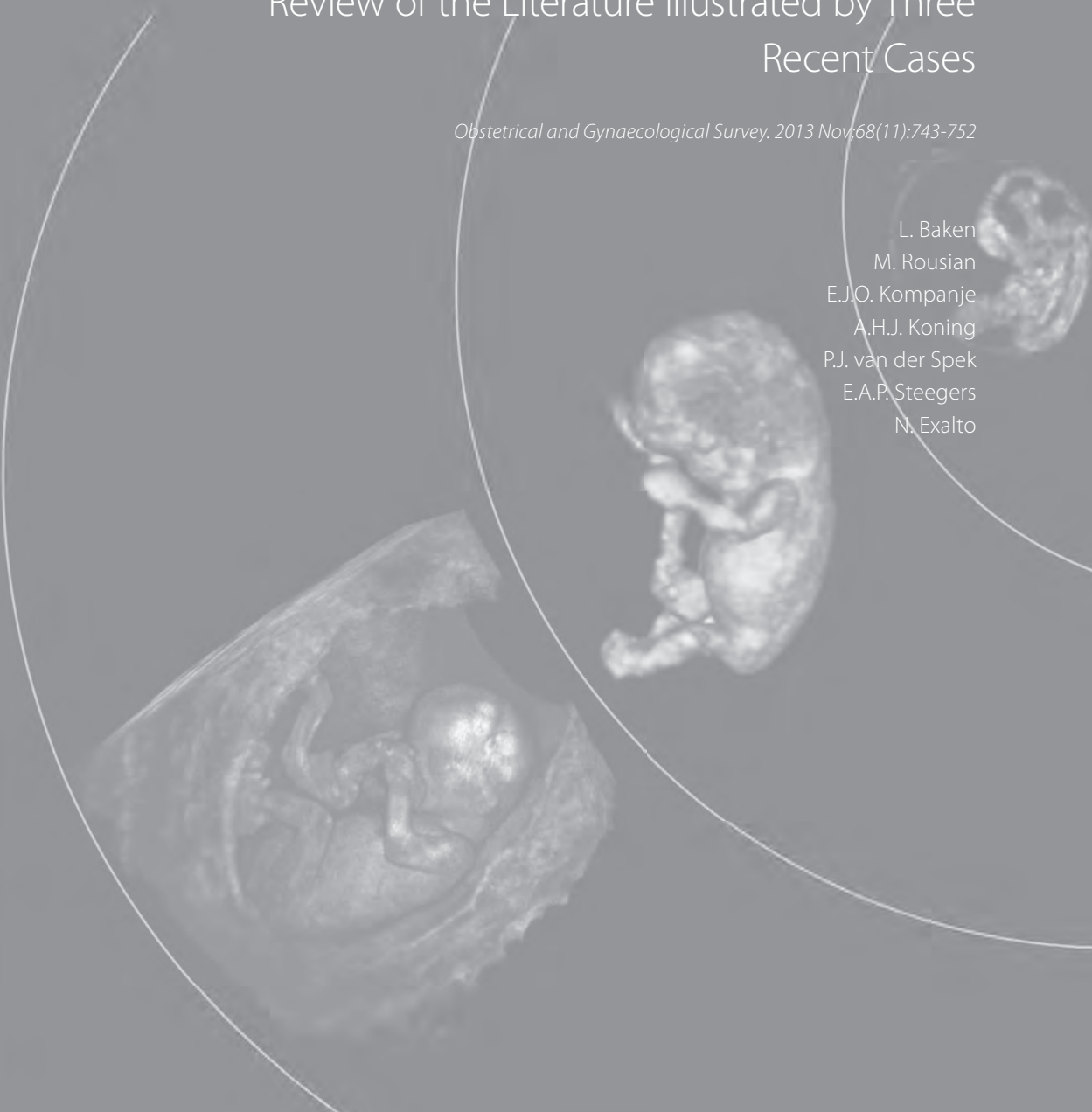


5.1

Diagnostic Techniques and Criteria for First-Trimester Conjoined Twin Documentation: a Review of the Literature illustrated by Three Recent Cases

Obstetrical and Gynaecological Survey. 2013 Nov;68(11):743-752

L. Baken
M. Rousian
E.J.O. Kompanje
A.H.J. Koning
P.J. van der Spek
E.A.P. Steegers
N. Exalto



Abstract

Objectives. Conjoined twins are rare. High-quality imaging techniques are essential for proper first-trimester diagnosis. Technological development leads to new imaging techniques such as three-dimensional (3D) virtual embryoscopy. The aim of this review was to explore imaging techniques used in the first-trimester diagnosis of conjoined twins and provide a systematic diagnostic table for making this diagnosis.

Design. A PubMed literature search was performed using the terms ultrasound, Doppler, MRI and CT combined with first-trimester and conjoined twins. Three recent cases at our department are reviewed and examined additionally using three-dimensional virtual embryoscopy.

Results. The different types of conjoined twins are summarized in a table for practical use during ultrasound examination. In evaluating conjoined twins, two-dimensional ultrasound is the criterion standard. Three-dimensional and Doppler ultrasound add anatomical and prognostic information. Virtual embryoscopy imaging reveals additional findings in our three cases not seen with routine two-dimensional ultrasound examination.

Conclusions. Each case of conjoined twins is unique and should be evaluated with the best possible imaging techniques. Three-dimensional and Doppler ultrasound should be added to the systematic diagnostic evaluation of conjoined twins. Virtual embryoscopy imaging may contribute to earlier, more appropriate counseling and management of these pregnancies.

Introduction

Conjoined twins are a rare phenomenon. These twins have fascinated people since old age; the oldest known printed illustration of a pair of conjoined twins is in the 1499 book by Jacob Locher¹, *Carmen heroicum de partu monstifero*. The prevalence of conjoined twins in live births is estimated to be around 1 in 250 000.² There is an unexplained female predominance (3:1).^{3,4}

Two hypotheses exist on the origin of conjoined twins; the fission theory in which a fertilized ovum divides incompletely and the fusion theory explaining secondary fusion of two originally distinct monovular embryos. Spencer⁵⁻⁸ argues that all types of conjoined twins can only be explained by secondary fusion. The recent finding of a monochorionic diamniotic conjoined twin pregnancy may further contribute to the fusion theory.⁹ Others are in favor of the fission theory, maintained by the observation that the incidence of mirror-imaging is higher in conjoined twins than in monozygotic twins.¹⁰ No matter what theory is correct, conjoined twinning is an infrequent and random event challenging physicians in making a proper diagnosis, which is essential for considering treatment options.

Nowadays, conjoined twins are frequently detected during first-trimester ultrasound examinations, challenging the use of sophisticated diagnostic imaging techniques.

Proper first-trimester diagnosis of conjoined twins is important for many different reasons: to avoid false positive diagnosis¹¹⁻¹³, detect related ultrasound abnormalities⁴, the possibility to offer early termination with less maternal morbidity and psychological impact^{14,15}, the possibility of selective fetocide, and the reduction of coexisting conjoined twins in a triplet pregnancy¹⁶⁻²² or even a quadruplet pregnancy²³, and to monitor the associated risks of a (conjoined) twin pregnancy.³

In this study we explore the first-trimester diagnosis and typing of conjoined twins. Imaging techniques used in the diagnostic process are described. We provide a systematic diagnostic table that might be helpful in the first-trimester diagnosis of a conjoined twin.

Methods

Literature search

Articles were identified through a PubMed database search retrieving articles on the first-trimester diagnosis of conjoined twins. The literature search was performed in January 2013 for all available articles written in English. The free-text search terms "ultrasound", "Doppler", "MRI", and "CT" in combination with "first-trimester", and "conjoined twins" were used. Articles on parasitic conjoined twins were excluded. References of all relevant articles were hand-searched for additional citations.

Diagnostic process of recent cases

In the past years, three cases of conjoined twins were diagnosed in the Erasmus MC University Medical Center Rotterdam in which informed consent for research was given by the parents. All three cases were initially examined using two-dimensional (2D) and three-dimensional (3D) ultrasound.

For consecutive analysis using virtual embryoscopy (VE), the transvaginal 3D images made on the GE Voluson 730 expert and E8 system (GE Medical Systems) were converted to cartesian volumes, using specialized 3D software (4D View, GE Medical Systems), and were transferred to the BARCO I-Space virtual reality system. The volumes were resized, turned, and clipped in different planes to obtain the best possible images for evaluation. The evaluation of the three cases with virtual reality was performed before termination of the pregnancy and evaluated by a different examiner who was blinded to the results of the previous performed 2D/3D ultrasound.

The diagnostic findings during 2D and 3D ultrasound were extrapolated from the medical records. All findings seen with the VE imaging technique were documented and compared to the 2D/3D ultrasound findings.

Results

Classification of conjoined twins

Each set of conjoined twins is unique with respect to the site and extent of union and their complex anatomy. The most complex anatomy is situated at the site of union.²⁴ Description of conjoined twins is made easier with a classification into eight types, advocated by Spencer.^{6,25} These eight types are named cephalopagus, thoracopagus, omphalopagus, ischiopagus, parapagus, craniopagus, rachipagus and pyopagus. The suffix “pagus” means fixed.

The first differentiation in this classification of conjoined twins is made in ventral versus dorsal union. Further differentiation is made by the site of union. The eight types of conjoined twins with their characteristics, incidence and vitality are summarized in Table 1.

(Supplemental material 1, <http://links.lww.com/OBGYNSURV/A12>)

The prognosis always depends on the specific type as described in Table 1. Surgical separation is very likely to fail with the loss of both children when a single heart is seen during first-trimester ultrasound.²⁴

Clues to the diagnosis

Suspicion of conjoined twinning should be raised in a twin pregnancy with a single placenta, when it is not possible to demonstrate a separating amniotic membrane or when there is only one yolk sac present. Signs of possible conjoined twins are also the following: more than three vessels in the umbilical cord, no change in relative positions of twins after movement or follow-up scans, fewer limbs than would be expected, hyperflexion of the spine, and bifid appearance of the fetal pole.^{2,26-28} Also increased nuchal translucency thickness can be seen in conjoined twins, especially in thoracopagus due to hemodynamic disturbances.²⁹ When fetal activity increases, at around eight weeks' gestational age (GA), it becomes easier to differentiate between monoamniotic twins and conjoined twins.³⁰

Imaging techniques

Ultrasound

Ultrasonography is widely used in the obstetrical field and is the most important and primary imaging technique in prenatal diagnosis of conjoined twins.² The first diagnosis of conjoined twins using transabdominal ultrasound was in 1976.³¹ The first diagnosis of conjoined twins in the first-trimester, at 12 weeks of gestational age, was reported by Schmidt *et al.*³² in 1981.

Most diagnoses of conjoined twins are established using 2D ultrasound, especially when fusion of body parts is obvious. Ultrasound is the preferred investigation modality since it is non-ionizing and non-invasive and has low costs and broad availability. It also permits real-time examination, useful as conjoined twins do not switch their relative position. Minimally conjoined omphalopagus twins can be an exception to this rule; changes in relative position have been reported.^{33,34}

The introduction of the transvaginal ultrasonography provided ultrasound images with high resolution and therefore made it possible to visualize the early pregnancy.³⁵ This has led to advances in first-trimester diagnosis of abnormalities in the fetal anatomy³⁶, like in evaluating the extent of fusion in conjoined twins.²⁶ The earliest reported diagnosis of conjoined twins was performed using transvaginal ultrasound at seven weeks of gestation.³⁷

Three-dimensional ultrasound









Three-dimensional ultrasound became available with the advances made in computer technology and has shown to be helpful in the detection of congenital abnormalities.^{38,39} In conjoined twins, 3D ultrasound is used to exactly define the extent of fusion and to obtain more precise anatomic information.⁴⁰⁻⁴² In many cases of conjoined twins, 3D ultrasound helped to confirm the presence of anomalies and improved diagnostic confidence.⁴¹⁻⁴⁸ Especially facial features, like in parapagus or cephalopagus conjoined twins, can be studied in detail better using 3D ultrasound.^{43,49} Three-dimensional surface rendered images may also help the future parents to understand the complex anomalies in their fetuses.^{41,42,48}

Doppler ultrasound

Doppler ultrasound has expanded its application in obstetrics including in the evaluation of conjoined twin pregnancies.^{16,42,50} The prognosis of conjoined twins largely depends on the conjunction of the cardiovascular system. Especially the differentiation between thoracopagus and omphalopagus, to correctly classify and determine the prognosis, can be facilitated by Doppler ultrasound of the heart.^{37,45,51,52} Doppler ultrasound is an excellent tool in the evaluation of the vasculature of conjoined vital organs, like the liver, to determine prognosis and separability.^{14,50,53}

Furthermore, Doppler ultrasound may reveal a characteristic "double layer" umbilical arterial velocity waveform due to two separate arterial supplies in a single umbilical cord.^{54,55} Such a distinctive Dop-

Table 1: Types of conjoined twins and their characteristics (**bold:** present in 100% of cases).

	Ventral					Dorsal		
	Cephalo pagus	Thoraco pagus	Omphalopagus	Ischio pagus	Parapagus	Cranio pagus	Rachi pagus	Pyo pagus
								
	rostral	rostral	rostral	lateral	caudal			
Incidence	11%	19%	18%	11%	28%	5%	<1%	6%
Extent of union	Head to umbilicus	Thorax to umbilicus	Umbilicus	Lower abdomen and pelvis	Lower abdomen and pelvis	Cranium (never foramen magnum/skull base)	Vertebral column	Sacrum and perineum
Varieties	Symmetrical/asymmetrical	-	Fusion from sternum to umbilicus	End-to-end fusion/twins facing each other	Dicephalus/di-prosopus	Orienta-tion in any position	Fusion into occiput	-
Head/face	Fused, 2 faces on opposite sides of head	2	2	2	1 or 2 heads, 2 faces	Fused skull, 2 faces	2 faces	2
CNS	2	-	-	-	Anencephaly	Fused meninges separate brains	2	Fused dura/spinal cords
Vertebral column	2	2	2	2	2	2	Fused spinal cords	2
Shoulders	4	4	4	4	2-3	4	4	4
Upper limbs	4	4	4	4	2-4	4	4	4
Thorax	Fused	Fused	Fused	2	Fused	2	2	2

Heart	2	1 con-joined/2 fused	2	2	1 or 2	2	2	2	2
Abdomen	1	Fused	Fused	2	1	2	2	2	2
Umbilicus	1	1	1	1	1	2	2	2	2
Liver	2	Shared	Shared	Minimal fusion	Shared	2	2	2	2
GI-tract	1 upper GI	2	Shared	1 lower GI	1 lower GI	2	2	2	2
Genitalia	2	2	2	Shared	2	2	Un-known	Fused	Fused
Pelvis	2	2	2	Fused	1	2	2	Fused	Fused
Lower limbs	4	4	4	3-4	2	4	4	3-4	3-4
Viability	No	Rare	Yes	Yes	Yes	Yes	Yes	Yes	Yes
Separate- bility	No	Not likely	Yes	Yes	Not likely	Not likely	Not repor- ted	Yes	Yes

pler ultrasound pattern can be used as an extra diagnostic sign in conjoined twins as is proposed by Woo *et al.*⁵⁴

Computed tomography Scan

Only two publications, published in 1984 and 1990, respectively, were found on the use of computed tomography for antenatal diagnosis of conjoined twins, both in the third trimester of pregnancy.^{56,57}

In case of conjoined twins, computed tomography can be used postpartum as a diagnostic tool to evaluate separability.⁵⁸

Magnetic resonance imaging

Fetal magnetic resonance imaging (MRI) has already proven to be complementary to conventional obstetrical ultrasound. Especially in case of complex anatomical anomalies, an MRI may provide additional information, like in evaluating conjoined twin pregnancies.⁵⁹⁻⁶²

The literature does not provide cases of conjoined twins diagnosed in the first-trimester with MRI. The earliest prenatally diagnosed conjoined twins using MRI was at 16 weeks of gestation.⁶⁰

When conjoined twins are presented late in pregnancy, MRI overcomes the limitations of ultrasound, like in the case of obesity and because of the decreasing amount of amniotic fluid. MRI provides overall assessment of the pregnancy during all three trimesters.

Virtual Embryoscopy

Virtual embryoscopy is a new imaging technique that enhances the 3D US modality using all three dimensions, in contrast to traditional 3D reconstructions viewed on a 2D screen. The Department of Bioinformatics of the Erasmus MC operates a fully immersive virtual reality system: the BARCO I-Space. It allows the viewers to perceive depth in and interact with 3D volumes in an intuitive manner. The V-Scope volume-rendering application creates a “hologram” of the 3D ultrasound volume in order to enable a so-called VE. Stereoscopic imaging allows discerning of fine details and understanding of complex relationships in the 3D volumes. We refer to previous articles for a detailed explanation of the BARCO I-Space and V-Scope.⁶³ The innovative VE technique has already successfully been applied in prenatal medicine.⁶⁴⁻⁷² Because of the improved depth perception and 3D interaction, the I-Space enables better assessment of embryonic and fetal structures.

As seen in our cases below VE provides additional diagnostic information in evaluating complex anatomical structures in conjoined twins.

Cases

Case 1

A 30-year-old gravida 4 para 2 was referred to the Erasmus MC University Medical Center Rotterdam at 10+6 weeks' GA because of conjoined twins detected with routine ultrasound. Two-dimensional

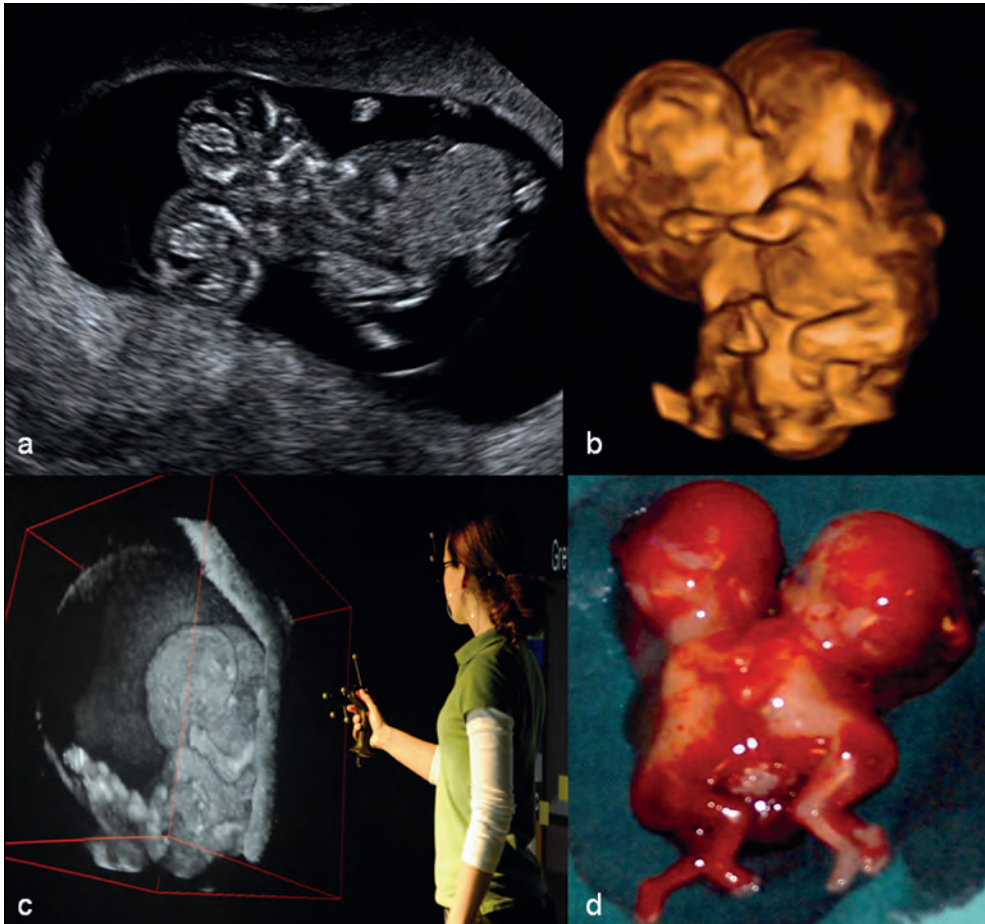


Figure 1: Case 1. Thoracopagus. A conventional 2D US image (A) clearly showing fusion of the thorax and abdomen. Because 1 heart was seen during 2D US, the diagnosis thoracopagus was made. A 3D US image (B) showing fetuses “embracing” each other. I-Space rendering of the conjoined twins (C). The operator is visible with the 3D volume of the twins. With VE, the fourth arm was discovered as well as an abdominal defect, abnormal ulnar deviation, and severe scoliosis, which were not seen during 2D/3D US. (It is important to remember that, on article, a photograph of an I-Space rendering is nothing more than a 2D picture, because depth cannot be put on article or on a computer screen. This Figure therefore does not capture the full potential of the I-Space.) Ex vivo photograph showing the union of both thorax and abdomen (D).

and 3D transabdominal and transvaginal ultrasound examination revealed a thoracopagus with fused thorax and abdomen, sharing one heart and liver (Table 2; Figure 1A, B). The conjoined twins appeared to have two separate heads, shoulder girdles, pelvises and four lower extremities. In both twins fetal hydrops was noticed. Only three upper extremities could be visualized using ultrasound. Fetal karyotype revealed a normal male genotype. The parents were informed about the prognosis and decided to terminate the pregnancy. Pregnancy was terminated at 11+5 weeks’GA using misoprostol.

Table 2: 2D/3D ultrasound and VR findings in presented cases (**bold**: only seen with VE).

Case	1			2			3		
Type	Thoracopagus			Cephalopagus			Parapagus		
GA	10w6d			13w1d			11w6d		
	Ref.	2D/3D	VE	Ref.	2D/3D	VE	Ref.	2D/3D	VE
Head	2	2	2	1	Fused	Fused	2	2	2
Frontal bossing	-	-	No	-	-	Yes	-	-	Yes R>L
Face	2	2	2	1/2	?	1	2	-	2
Vertebral column	2	-	2, scoliosis	2	-	2	2	2	2
Shoulders	4	4	4	4		4	2-4		3
Upper limbs	4	3	4	4	4	4	2-3	2	2
Hands			Ulnar deviation						
Thorax	Fused	Fused, hydro-thorax	Fused, hydro-thorax	Fused	Fused	Fused	Fused	Fused	Fused
Heart	1/2	1	1	2	2	?	1/2	1	?
Abdomen	Fused	Fused	Defect	Fused	Fused	Fused	Fused	Fused	Fused
Umbilicus	1	-	1	1	1	1	1	1	1
Omphalo-cele	-	-	No	-	-	Yes	Yes	Yes	Yes, small
Stomach	2	-	?	1	-	1	1/2	1	?
Liver	Shared	1	?	2	-	?	Shared	1	?
Pelvis	2	-	2	2	-	2	1	-	1
Lower limbs	4	4	4	4	4	4	2	2	2
General		Hydrops	Hydrops					Hydrops	Hydrops
Chromosomal		46, XX			46, XX			46, XY	
Viability		Rare			No			Yes	
Seperate-ability		Not likely			No			Not likely	

Intact conjoined twins were born and macroscopic examination confirmed the diagnosis thoracopagus (Figure 1D). The parents refused autopsy.

Using the I-Space VE system, the thoracopagus with fetal hydrops was confirmed (Figure 1C). In addition four arms and four legs could be distinguished easily as well as severe scoliosis in both fetuses, an abdominal wall defect and an abnormal ulnar deviation of one of the hands.

Case 2

A 28 year-old gravida 2 para 1 was referred to our center at 13+1 weeks' GA because of conjoined twins diagnosed with routine 2D ultrasound. Two-dimensional and 3D ultrasound examination revealed a cephalopagus with fusion of the heads, both thorax, and part of the abdomens (Table 2; Figure 2A,B). Two heartbeats, one stomach, four arms and four legs, and one shared umbilical cord were visualized. The fetal karyogram showed a normal female genotype.

The parents were informed about the lethal prognosis and they decided to terminate the pregnancy at 14 weeks' GA by induction. Intact conjoined twins were born, and the diagnosis of cephalopagus was confirmed by macroscopic examination (Figure 2D). The parents did not give permission for an autopsy.

A cephalopagus can either be symmetrical (two identical faces on opposite sides of the head) or asymmetrical (one "normal" face and one reduced face). The back of the head however could not be visualized with 2D and 3D ultrasound.

Intuitive orientation in the dataset with 3D VE allowed for detailed evaluation of anatomical structures (Figure 1C). Three-dimensional VE visualized only one face and also four shoulders and an omphalocele, making the definitive diagnosis of asymmetrical cephalopagus conjoined twins.

Case 3

A 22-years-old gravida 3 para 2 was presented at 11+6 weeks' GA to our department after detection of conjoined twins during routine ultrasound. Conjoined twins with fetal hydrops were revealed with 2D and 3D ultrasound (Figure 3A, B). Two separate heads and two separate spines were seen with fusion at the level of the thorax and the abdomen, sharing one heart, liver and stomach. Two arms and two legs could be visualized as well as a small omphalocele. The fetuses were diagnosed as a parapagus dicephalus (Table 2). Karyotyping by chorionic villus sampling revealed a normal male genotype.

After counseling, the parents decided to terminate the pregnancy at 14+4 weeks' GA using misoprostol. Autopsy findings correlated with the diagnosis parapagus dicephalus (Figure 3E). There were three lungs, one heart, one set of kidneys, a shared gastro-intestinal tract and two equally normal sized brains present. The internal genitalia were male.

During 3D VE examination two faces were seen with marked frontal bossing. There were three shoulders with two arms (Figure 3C, D).

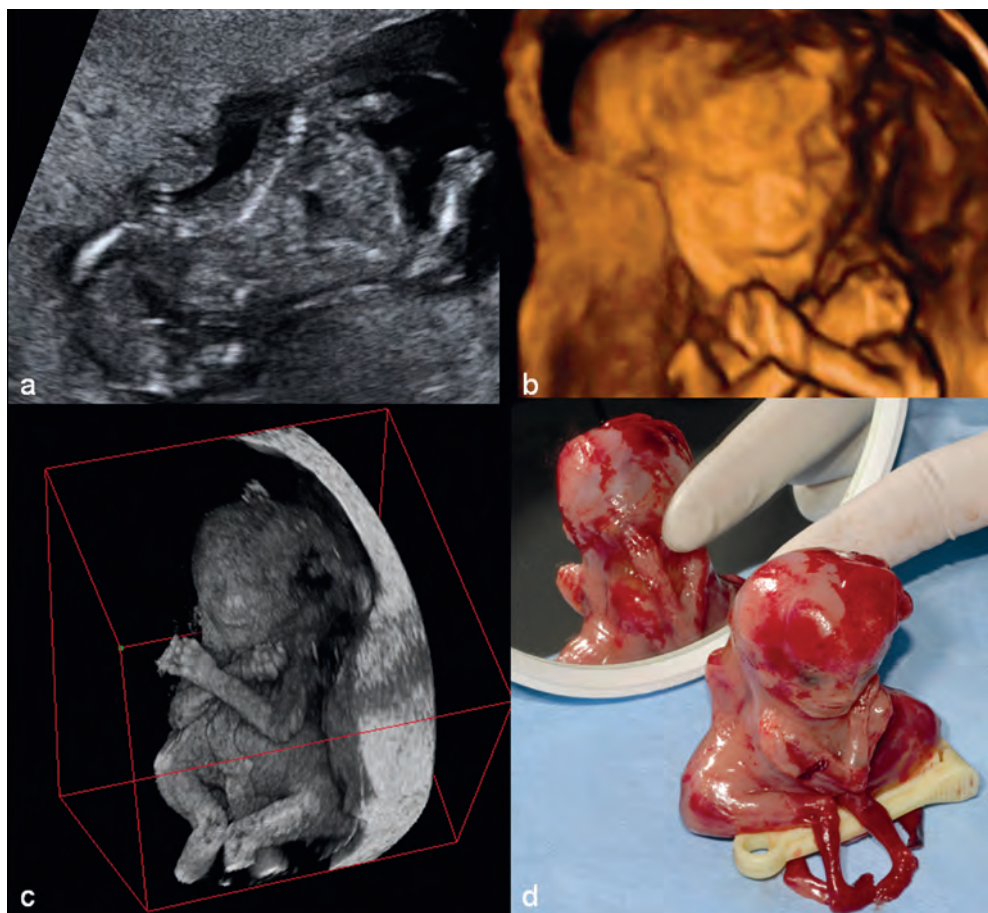


Figure 2: Case 2. Cephalopagus. Two-dimensional US image (A) showing 2 vertebral columns and 1 single head. Three-dimensional US image (B) showing the profile of the fused face. I-Space volume (C) clearly showing the 2 fetuses situated in front of each other (each arm belongs to one of the twins) with the faces fused laterally. With VE, it was possible to visualize the back of the head, indicating this as an asymmetrical cephalopagus. Ex vivo photograph (D) showing the 4 upper extremities. The absence of a second face, already seen in VE, was confirmed.

Discussion

Accurate prenatal imaging is crucial in diagnosing the rare cases of conjoined twins. Even though with the classification, each conjoined twins is unique with respect to the site and extent of union and their complex anatomy. Prognosis, especially vitality and separability, should therefore be evaluated individually for each case with the best possible imaging techniques.

Ultrasound is the main imaging modality used in diagnosing conjoined twins and will remain so in the foreseeable future, because of its favorable characteristics like accessibility and cost and the fact

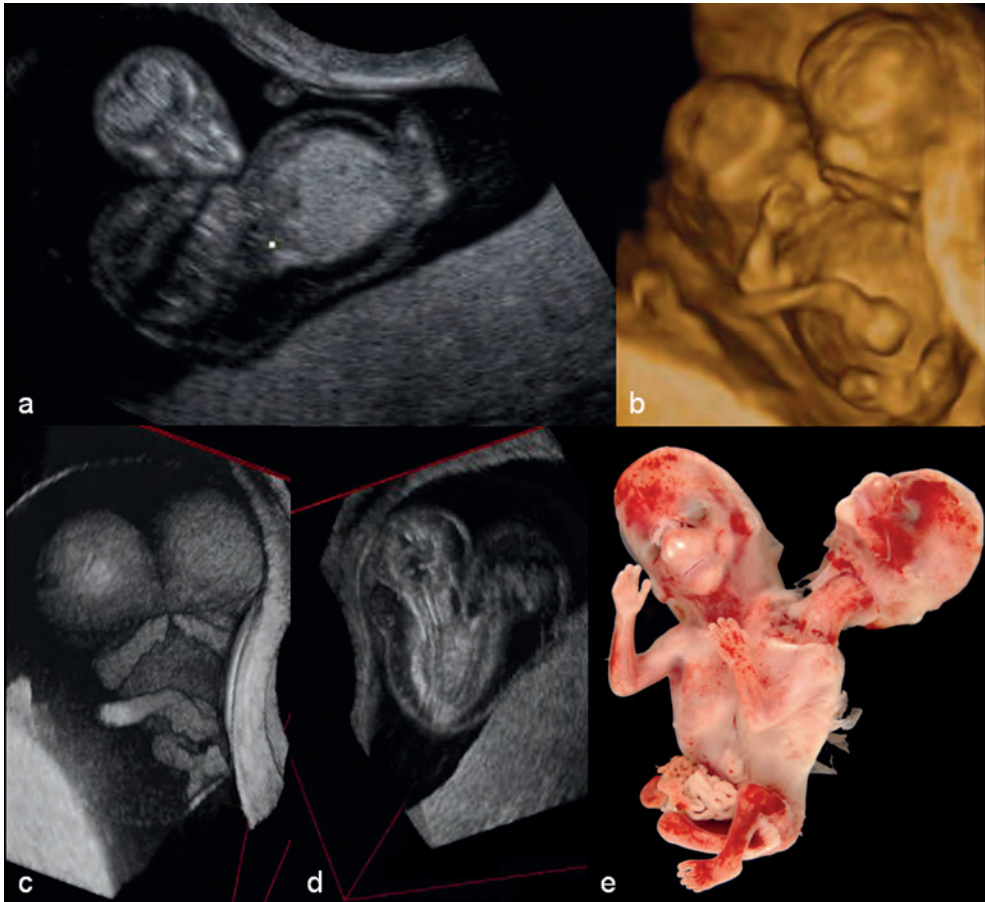


Figure 3: Case 3. Parapagus dicephalus. Two-dimensional US image (A) showing hydrops and 2 separate heads. Three-dimensional US image (B) showing fusion of thorax and abdomen and a single umbilical cord. I-Space volume (C) showing the fusion of thorax and abdomen. Virtual embryoscopy also showed the presence of only 1 pelvis. Furthermore, frontal bossing and a small omphalocele were visualized. I-Space volume showing hydrops (D). Two vertebral columns are visualized. Ex vivo photograph (e) confirming that only 2 upper and 2 lower extremities were present.

that in many cases the diagnosis can be made using conventional ultrasound, especially when the conjunction between the twins is obvious.

Three-dimensional ultrasound should always be included in the first-trimester evaluation of conjoined twins. Three-dimensional ultrasound can easily be performed and does not consume much extra time during the ultrasound examination. Because the spatial relationships in conjoined twins are complex and understanding them is essential for a proper diagnosis, 3D ultrasound will be of help in diagnosing these twins. Moreover, 3D ultrasound can provide extra anatomical information in

several cases of conjoined twins, especially regarding facial features. The surface rendered images of 3D ultrasound as well facilitate counseling of the parents.

Although 2D and 3D ultrasound are sufficient in most cases of conjoined twins, they are not always successful in providing all detailed information of the complex anatomy in conjoined twins. As these details may modify the viability and separability in selected cases, other imaging techniques should also be considered. Moreover, ensuring the lethal prognosis is essential for parents in deciding to ask for a termination of pregnancy and facilitates the mourning process.

Doppler ultrasound imaging is important for the determination of viability and separability by visualizing vascular communications and by determining the number of hearts. When the vascular anatomy cannot be clearly visualized with ultrasound, the clinician should resort to Doppler ultrasound.

The lack of publications on MRI in first-trimester conjoined twin pregnancies may indicate that there is no benefit of this imaging technique in these particular pregnancies. However, MRI has emerged to be a complementary imaging technique in conjoined twins after the first-trimester. The superiority of MRI as compared to ultrasound in the second and third trimester might also apply to the first 12 weeks of pregnancy, especially since imaging techniques are in constant development. The excellent resolution of tissue composition perceived with MRI makes it a potential useful complementary tool in first-trimester diagnosis of conjoined twins. A thorough evaluation of this possible diagnostic effect could change our view on the diagnostic process of congenital abnormalities like conjoined twins. Furthermore, the VE technique can also be applied to MRI to provide even more information.

In the three cases of conjoined twins referred to our clinic, we demonstrated that 3D VE provides additional and more precise anatomic information. A combination of 2D and 3D ultrasound examination and 3D VE improves the detailed morphological description and diagnosis.

We conclude that conventional 2D ultrasound in most cases is sufficient in the first-trimester diagnosis of conjoined twins. The diagnostic process can be easily expanded with 3D and Doppler ultrasound to gain extra and more precise information in an efficient way. Three-dimensional VE provides additional diagnostic information in evaluating complex anatomical structures, especially when depth perception is needed, as in case of conjoined twins. This may contribute to earlier, more appropriate counseling and management of these pregnancies. As this is the first article on VE in the diagnosis of conjoined twins, more research is needed to evaluate the implementation of VE in the diagnostic process of conjoined twins and congenital malformations in general.

References

1. Locher J. *Carmen heroicum de partu monstrihero*. Ingolstadt: Johann Kachelofen; 1499.
2. McHugh K, Kiely EM, Spitz L. Imaging of conjoined twins. *Pediatr Radiol*. 2006;36(9):899-910.
3. Machin GA, Keith LG, Bamforth F. *An atlas of multiple pregnancy: biology and pathology*. New York: CRC Press, Parthenon; 1999. 216 p.
4. Chen CP, Hsu CY, Su JW, Cindy Chen HE, Hwa-Ruey Hsieh A, Hwa-Jiun Hsieh A, et al. Conjoined twins detected in the first-trimester: a review. *Taiwan J Obstet Gynecol*. 2011;50(4):424-31.
5. Spencer R. Theoretical and analytical embryology of conjoined twins: part I: embryogenesis. *Clin Anat*. 2000;13(1):36-53.
6. Spencer R. *Conjoined Twins*. 1 ed. Baltimore: Johns Hopkins University Press; 2003 January 22, 2003. 496 p.
7. Spencer R. Theoretical and analytical embryology of conjoined twins: part II: adjustments to union. *Clin Anat*. 2000;13(2):97-120.
8. Spencer R. Conjoined twins: theoretical embryologic basis. *Teratology*. 1992;45(6):591-602.
9. Destephano CC, Meena M, Brown DL, Davies NP, Brost BC. Sonographic diagnosis of conjoined diamniotic monochorionic twins. *Am J Obstet Gynecol*. 2010;203(6):e4-6.
10. Kaufman MH. The embryology of conjoined twins. *Childs Nerv Syst*. 2004;20(8-9):508-25.
11. Usta IM, Awwad JT. A false positive diagnosis of conjoined twins in a triplet pregnancy: pitfalls of first-trimester ultrasonographic prenatal diagnosis. *Prenat Diagn*. 2000;20(2):169-70.
12. Weiss JL, Devine PC. False positive diagnosis of conjoined twins in the first-trimester. *Ultrasound Obstet Gynecol*. 2002;20(5):516-8.
13. Castro-Aragon I, Levine D. Ultrasound detection of first-trimester malformations: a pictorial essay. *Radiol Clin North Am*. 2003;41(4):681-93.
14. Hubinont C, Kollmann P, Malvaux V, Donnez J, Bernard P. First-trimester diagnosis of conjoined twins. *Fetal Diagn Ther*. 1997;12(3):185-7.
15. Fontanarosa M, Bagnoli G, Ciolini P, Spinelli G, Curiel P. First-trimester sonographic diagnosis of diprosopus twins with craniorachischisis. *J Clin Ultrasound*. 1992;20(1):69-71.
16. Lam YH, Lee CP, Tang MH, Lau E. Thermocoagulation for selective reduction of conjoined twins at 12 weeks of gestation. *Ultrasound Obstet Gynecol*. 2000;16(3):267-70.
17. Goldberg Y, Ben-Shlomo I, Weiner E, Shalev E. First-trimester diagnosis of conjoined twins in a triplet pregnancy after IVF and ICSI: case report. *Hum Reprod*. 2000;15(6):1413-5.
18. Sepulveda W, Munoz H, Alcalde JL. Conjoined twins in a triplet pregnancy: early prenatal diagnosis with three-dimensional ultrasound and review of the literature. *Ultrasound Obstet Gynecol*. 2003;22(2):199-204.
19. Suzumori N, Kaneko S, Nakanishi T, Yamamoto T, Tanemura M, Suzuki Y, et al. First-trimester diagnosis of conjoined twins in a triplet pregnancy. *Eur J Obstet Gynecol Reprod Biol*. 2006;126(1):132-3.
20. Boulot P, Deschamps F, Hedon B, Laffargue F, Viala JL. Conjoined twins associated with a normal singleton: very early diagnosis and successful selective termination. *J Perinat Med*. 1992;20(2):135-7.
21. Hill LM. The sonographic detection of early first-trimester conjoined twins. *Prenat Diagn*. 1997;17(10):961-3.

22. Solt I, Lowenstein L, Okopnik M, Sheinin O, Drugan A. Malformed pygopagus conjoined twins in a spontaneous triplet pregnancy. *Harefuah*. 2005;144(8):590-2, 6.
23. Rohilla S, Dahiya K, Rathee S, Yadav RK, Dhoulakhandi DB. Conjoined twins in a spontaneous trichorionic quadruplet pregnancy: a case report. *J Reprod Med*. 2011;56(7-8):351-5.
24. McMahon CJ, Spencer R. Congenital heart defects in conjoined twins: outcome after surgical separation of thoracopagus. *Pediatr Cardiol*. 2006;27(1):1-12.
25. Spencer R. Anatomic description of conjoined twins: a plea for standardized terminology. *J Pediatr Surg*. 1996;31(7):941-4.
26. Tongsong T, Chanprapaph P, Pongsatha S. First-trimester diagnosis of conjoined twins: a report of three cases. *Ultrasound Obstet Gynecol*. 1999;14(6):434-7.
27. Koontz WL, Herbert WN, Seeds JW, Cefalo RC. Ultrasonography in the antepartum diagnosis of conjoined twins. A report of two cases. *J Reprod Med*. 1983;28(9):627-30.
28. Maggio M, Callan NA, Hamod KA, Sanders RC. The first-trimester ultrasonographic diagnosis of conjoined twins. *Am J Obstet Gynecol*. 1985;152(7 Pt 1):833-5.
29. Maymon R, Mendelovic S, Schachter M, Ron-El R, Weinraub Z, Herman A. Diagnosis of conjoined twins before 16 weeks' gestation: the 4-year experience of one medical center. *Prenat Diagn*. 2005;25(9):839-43.
30. Luchinger AB, Hadders-Algra M, van Kan CM, de Vries JI. Fetal onset of general movements. *Pediatr Res*. 2008;63(2):191-5.
31. Wilson RL, Cetrulo CL, Shaub MS. The prepartum diagnosis of conjoined twins by the use of diagnostic ultrasound. *Am J Obstet Gynecol*. 1976;126(6):737.
32. Schmidt W, Heberling D, Kubli F. Antepartum ultrasonographic diagnosis of conjoined twins in early pregnancy. *Am J Obstet Gynecol*. 1981;139(8):961-3.
33. Huisman TA, Arulrajah S, Meuli M, Brehmer U, Beinder E. Fetal MRI of conjoined twins who switched their relative positions. *Pediatr Radiol*. 2010;40(3):353-7.
34. Neilson JP. Prenatal diagnosis in multiple pregnancies. *Curr Opin Obstet Gynecol*. 1992;4(2):280-5.
35. Timor-Tritsch IE, Farine D, Rosen MG. A close look at early embryonic development with the high-frequency transvaginal transducer. *Am J Obstet Gynecol*. 1988;159(3):676-81.
36. Dugoff L. Ultrasound diagnosis of structural abnormalities in the first-trimester. *Prenat Diagn*. 2002;22(4):316-20.
37. Sherer DM, Dalloul M, Kheyman M, Zigalo A, Nader I, Sokolovski M, et al. Transvaginal color Doppler imaging diagnosis of thoracopagus conjoined twins at 7 weeks' gestation. *J Ultrasound Med*. 2006;25(11):1485-7.
38. Merz E, Bahlmann F, Weber G. Volume scanning in the evaluation of fetal malformations: a new dimension in prenatal diagnosis. *Ultrasound Obstet Gynecol*. 1995;5(4):222-7.
39. Sladkevicius P, Campbell S. Advances in ultrasound assessment in the establishment and development of pregnancy. *Br Med Bull*. 2000;56(3):691-703.
40. Maymon R, Halperin R, Weinraub Z, Herman A, Schneider D. Three-dimensional transvaginal sonography of conjoined twins at 10 weeks: a case report. *Ultrasound Obstet Gynecol*. 1998;11(4):292-4.
41. Bega G, Wapner R, Lev-Toaff A, Kuhlman K. Diagnosis of conjoined twins at 10 weeks using three-dimensional ultrasound: a case report. *Ultrasound Obstet Gynecol*. 2000;16(4):388-90.

42. Fang KH, Wu JL, Yeh GP, Chou PH, Hsu JC, Hsieh CT. Ischiopagus conjoined twins at 9 weeks of gestation: three-dimensional ultrasound and power Doppler findings. *Ultrasound Obstet Gynecol.* 2005;25(3):309-10.
43. Kuroda K, Kamei Y, Kozuma S, Kikuchi A, Fujii T, Unno N, et al. Prenatal evaluation of cephalopagus conjoined twins by means of three-dimensional ultrasound at 13 weeks of pregnancy. *Ultrasound Obstet Gynecol.* 2000;16(3):264-6.
44. Suzumori N, Nakanishi T, Kaneko S, Yamamoto T, Tanemura M, Suzuki Y, et al. Three-dimensional ultrasound of dicephalus conjoined twins at 9 weeks of gestation. *Prenat Diagn.* 2005;25(11):1063-4.
45. Bonilla-Musoles F, Raga F, Bonilla F, Jr., Blanes J, Osborne NG. Early diagnosis of conjoined twins using two-dimensional color Doppler and three-dimensional ultrasound. *J Natl Med Assoc.* 1998;90(9):552-6.
46. Bornstein E, Santos R, Timor-Tritsch IE, Monteagudo A. "Brothers in arms": 3-dimensional sonographic findings in a first-trimester thoraco-omphalopagus conjoined twin pair. *J Ultrasound Med.* 2009;28(1):97-9.
47. Abu-Rustum RS, Adra AM. Three-dimensional sonographic diagnosis of conjoined twins with fetal death in the first-trimester. *J Ultrasound Med.* 2008;27(11):1662-3.
48. Ulker K, Akyer SP, Temur I, Tan T, Karaca M, Adiguzel E, et al. First-trimester diagnosis of parapagus diprosopus dibrachius dipus twins with cranirachischisis totalis by three-dimensional ultrasound. *J Obstet Gynaecol Res.* 2012;38(2):431-4.
49. Maruotti GM, Paladini D, Napolitano R, Mazzarelli LL, Russo T, Quarantelli M, et al. Prenatal 2D and 3D ultrasound diagnosis of diprosopus: case report with post-mortem magnetic resonance images (MRI) and review of the literature. *Prenat Diagn.* 2009;29(10):992-4.
50. Basgul A, Kavak ZN, Sezen D, Gokaslan H. Thoraco-omphalopagus conjoined twins detected at as early as 9 weeks of gestation: transvaginal two-dimensional ultrasound, color Doppler and fetoplacental Doppler velocity waveform findings. *Fetal Diagn Ther.* 2006;21(5):477-80.
51. Ohkuchi A, Minakami H, Sato I, Nakano T, Tateno M. First-trimester ultrasonographic investigation of cardiovascular anatomy in thoracoabdominally conjoined twins. *J Perinat Med.* 2001;29(1):77-80.
52. Varma SK, Waalwyk K, Menahem S, Meagher S. First-trimester diagnosis of conjoined twins aided by spatio-temporal image correlation. *J Clin Ultrasound.* 2011;39(9):527-9.
53. Sen C, Celik E, Vural A, Kepkep K. Antenatal diagnosis and prognosis of conjoined twins - a case report. *J Perinat Med.* 2003;31(5):427-30.
54. Woo JS, Liang ST, Lo R. Characteristic pattern of Doppler umbilical arterial velocity waveform in conjoint twins. *Gynecol Obstet Invest.* 1987;23(1):70-2.
55. Blickstein I, Keith LG. Multiple pregnancy: epidemiology, gestation & perinatal outcome. 2 ed. London: Informa UK Ltd; 2005.
56. Siegel HA, Seltzer SE, Miller S. Prenatal computed tomography: are there indications? *J Comput Assist Tomogr.* 1984;8(5):871-6.
57. Barth RA, Filly RA, Goldberg JD, Moore P, Silverman NH. Conjoined twins: prenatal diagnosis and assessment of associated malformations. *Radiology.* 1990;177(1):201-7.
58. Hockley AD, Gornall P, Walsh R, Nishikawa H, Lam H, MacPherson L, et al. Management of pyopagus conjoined twins. *Childs Nerv Syst.* 2004;20(8-9):635-9.
59. Unal O, Arslan H, Adali E, Bora A, Yildizhan R, Avcu S. MRI of omphalopagus conjoined twins with a Dandy-Walker malformation: prenatal true FISP and HASTE sequences. *Diagn Interv Radiol.* 2010;16(1):66-9.

60. Hu LS, Caire J, Twickler DM. MR findings of complicated multifetal gestations. *Pediatr Radiol*. 2006;36(1):76-81.
61. Turner RJ, Hankins GD, Weinreb JC, Ziaya PR, Davis TN, Lowe TW, et al. Magnetic resonance imaging and ultrasonography in the antenatal evaluation of conjoined twins. *Am J Obstet Gynecol*. 1986;155(3):645-9.
62. Spielmann AL, Freed KS, Spritzer CE. MRI of conjoined twins illustrating advances in fetal imaging. *J Comput Assist Tomogr*. 2001;25(1):88-90.
63. Koning AH, Rousian M, Verwoerd-Dikkeboom CM, Goedknegt L, Steegers EA, van der Spek PJ. V-scope: design and implementation of an immersive and desktop virtual reality volume visualization system. *Stud Health Technol Inform*. 2009;142:136-8.
64. Rousian M, Koning AH, van Oppenraaij RH, Hop WC, Verwoerd-Dikkeboom CM, van der Spek PJ, et al. An innovative virtual reality technique for automated human embryonic volume measurements. *Hum Reprod*. 2010;25(9):2210-6.
65. Rousian M, Verwoerd-Dikkeboom CM, Koning AH, Hop WC, van der Spek PJ, Exalto N, et al. Early pregnancy volume measurements: validation of ultrasound techniques and new perspectives. *BJOG*. 2009;116(2):278-85.
66. Rousian M, Verwoerd-Dikkeboom CM, Koning AH, van der Spek PJ, Exalto N, Steegers EA. [Innovative three-dimensional imaging: opportunities for virtual embryoscopy]. *Ned Tijdschr Geneesk*. 2010;154(25):A1606.
67. Verwoerd-Dikkeboom CM, Koning AH, Groenenberg IA, Smit BJ, Brezinka C, Van Der Spek PJ, et al. Using virtual reality for evaluation of fetal ambiguous genitalia. *Ultrasound Obstet Gynecol*. 2008;32(4):510-4.
68. Verwoerd-Dikkeboom CM, Koning AH, Hop WC, Rousian M, Van Der Spek PJ, Exalto N, et al. Reliability of three-dimensional sonographic measurements in early pregnancy using virtual reality. *Ultrasound Obstet Gynecol*. 2008;32(7):910-6.
69. Verwoerd-Dikkeboom CM, Koning AH, Hop WC, van der Spek PJ, Exalto N, Steegers EA. Innovative virtual reality measurements for embryonic growth and development. *Hum Reprod*. 2010;25(6):1404-10.
70. Verwoerd-Dikkeboom CM, Koning AH, van der Spek PJ, Exalto N, Steegers EA. Embryonic staging using a 3D virtual reality system. *Hum Reprod*. 2008;23(7):1479-84.
71. Verwoerd-Dikkeboom CM, van Heesch PN, Koning AH, Galjaard RJ, Exalto N, Steegers EA. Embryonic delay in growth and development related to confined placental trisomy 16 mosaicism, diagnosed by I-Space Virtual Reality. *Fertil Steril*. 2008;90(5):2017 e19-22.
72. Groenenberg IA, Koning AH, Galjaard RJ, Steegers EA, Brezinka C, van der Spek PJ. A virtual reality rendition of a fetal meningomyelocele at 32 weeks of gestation. *Ultrasound Obstet Gynecol*. 2005;26(7):799-801.

5.2

First-Trimester Diagnosis of Thrombocytopenia-Absent Radius Syndrome using Virtual Reality

Clinical Dysmorphology. 2014; Apr;23(2):71-73

L. Baken
I.A.L. Groenenberg
A.J.M. Hoogeboom
A.H.J. Koning
N. Exalto



Summary

The case presented here is, to the best of our knowledge, the earliest prenatal diagnosis of TAR syndrome reported to date and illustrates that very early first-trimester detection of TAR syndrome is feasible using 2D/3D ultrasound combined with virtual reality.

Introduction

Thrombocytopenia absent radius (TAR) syndrome is a rare condition characterized by hypomegakaryocytic thrombocytopenia and bilateral absence of the radius with presence of both thumbs. Thrombocytopenia is often symptomatic in the neonatal period and improves over time.¹ A micro-deletion of chromosome 1q21.1 is found in all investigated cases with TAR syndrome.² However, the recessive inheritance pattern of TAR syndrome requires an additional causative allele that until recently was unknown. A low-frequency SNP in the RBM8A gene is detected as the second causative allele in the origination of TAR syndrome.³

TAR syndrome can be accompanied by lower limb anomalies, renal anomalies (25% of cases; e.g. horseshoe kidney), cardiac anomalies (15%; e.g. septal defects), brain anomalies (less frequently reported; e.g. cerebellar dysgenesis) and agenesis of uterus, cervix and part of the vagina. A dysmorphic face is often described and individuals with TAR syndrome have a short stature.⁴ Mental retardation is reported in 7% of cases and is usually due to intracranial haemorrhage.

Only a limited number of cases of prenatally detected TAR syndrome have been reported in the literature. The first report demonstrating normal development of the radius and ulna in a pregnancy at increased risk for TAR syndrome was presented in 1973 by Omenn *et al.* using fetal radiography at a gestational age (GA) of 16 weeks, a normal fetus was correctly predicted.⁵ The first prenatal ultrasonographic diagnosis of TAR syndrome was reported in 1981 by Luthy *et al.*⁶

With careful examination of the long bones, TAR syndrome can be diagnosed in the first-trimester. O’Rahilly and Gardner⁷ reported that the initial ossification of the radius starts at Carnegie stage 22 (GA 7+5 – 8+0). The earliest visualisation and measurement of the radius and ulna was reported in 1994 by Zorzoli *et al.*⁸ at a GA of nine weeks (64-day GA). Only two reports on first-trimester diagnosis of TAR syndrome were found in the literature.^{9,10} The case presented here, to the best of our knowledge, is the earliest prenatal diagnosis of TAR syndrome reported to date and illustrates that very early first-trimester detection of TAR syndrome is feasible using two-dimensional/three-dimensional ultrasound scanning (2D/3D US) combined with virtual reality.

Case

We examined a 35-year-old woman, gravida 3 para 2 at 6+5 weeks GA (regular menstrual cycle of 28 days). Her first child was affected with TAR syndrome. Blood analysis at the time revealed the 1q21.1 deletion to be present in both the mother and the child. During her second pregnancy, TAR syndrome was ruled out at 10+6 weeks GA as normal upper extremities with bilateral radii were observed (Figure 1).

During the current pregnancy, she underwent 2D and 3D US weekly from six weeks GA. In addition, 3D datasets were evaluated off-line during the same week using the BARCO I-Space virtual reality system (Barco, Kortrijk, Belgium), which creates holograms of the 3D datasets. The users experience a true, binocular, depth perception and can intuitively interact with the volume using a joystick.

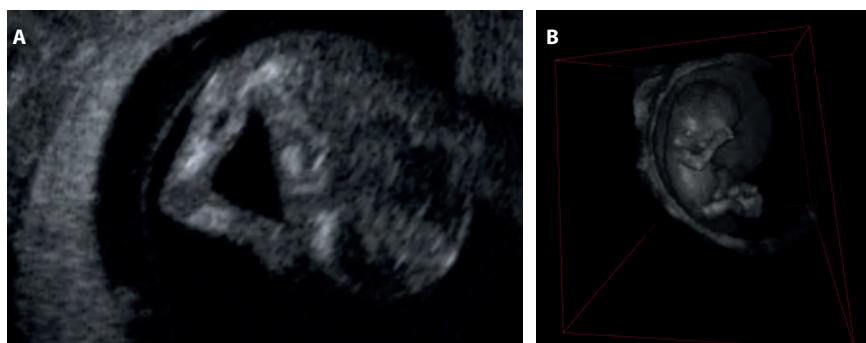


Figure 1: During the second pregnancy of the patient, at 10+6 weeks gestational normal upper extremities with presence of radii were visualized by (A) ultrasonography and (B) virtual reality. This excluded the diagnosis of thrombocytopenia-absent radius syndrome in this pregnancy.

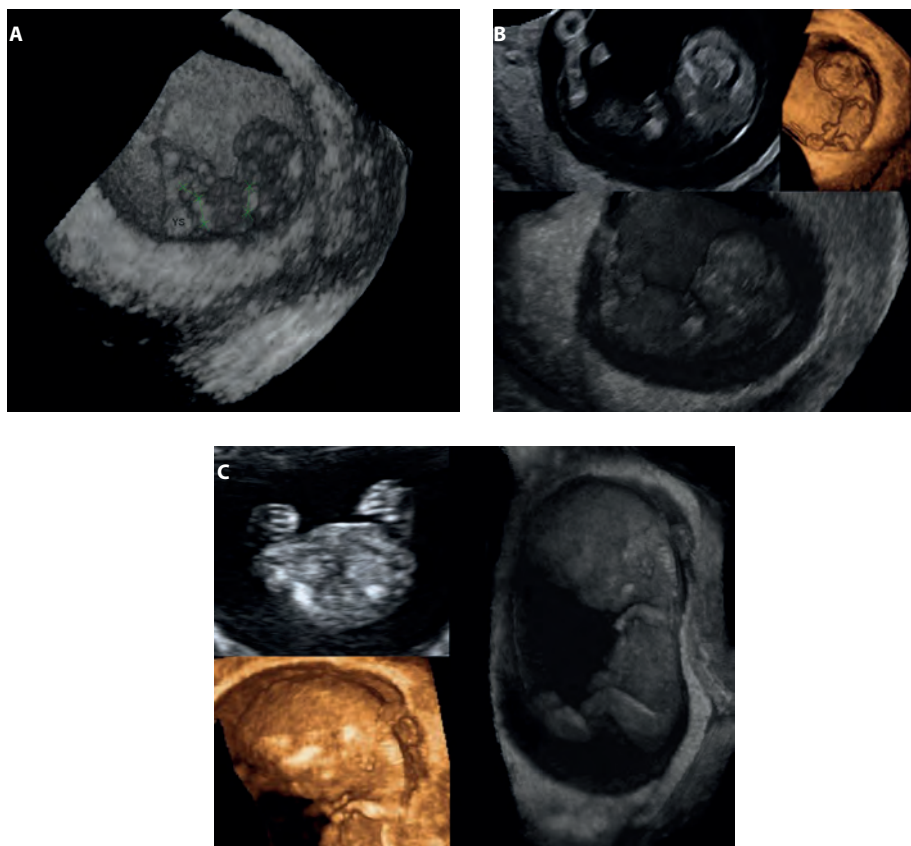


Figure 2: Patient with thrombocytopenia-absent radius syndrome showing (A) normal lower limbs and short upper limbs are seen using the I-Space virtual reality system at a gestational age (GA) of 9+1 weeks, (B) abnormal upper limbs with absent radius on two-dimensional and three-dimensional ultrasonography and using virtual reality at 10+1 weeks GA, and (C) the presence of both thumbs and abnormal ears at 11+1 weeks GA.

Between six and nine weeks GA the arms could not be evaluated using transvaginal 2D and 3D ultrasound because of the intermediate position of the uterus. At 9+1 weeks GA, during I-Space virtual reality (VR) evaluation, the left upper arm seemed to be short and the elbow was lacking. Normal lower extremities were observed. Because of low image quality, the radii could not be visualized (Figure 2A). At 10+1 weeks GA, the extremities were clearly visualized with both 2D and 3D US and VR, showing bilateral short upper and lower arms with absent radii (Figure 2B). Ultrasound examination of the thumbs was inconclusive. At 11+1 weeks GA both hands with thumbs were visualized (Figure 2C). All long bones, except for the femur, were shortened. Both elbows and wrists were fixed in flexion, as were the knees. Other findings were retrognathia and an abnormal position of the ears. Nuchal translucency was not increased. Fetal biometry, crown-rump length, and embryonic volume were consistent with GA (Figure 3A and B).

At 12+5 weeks of gestational age, after counseling the patient and her husband, the pregnancy was terminated. Unfortunately, because of poor quality of the pathological material no postmortem diagnosis could be made.

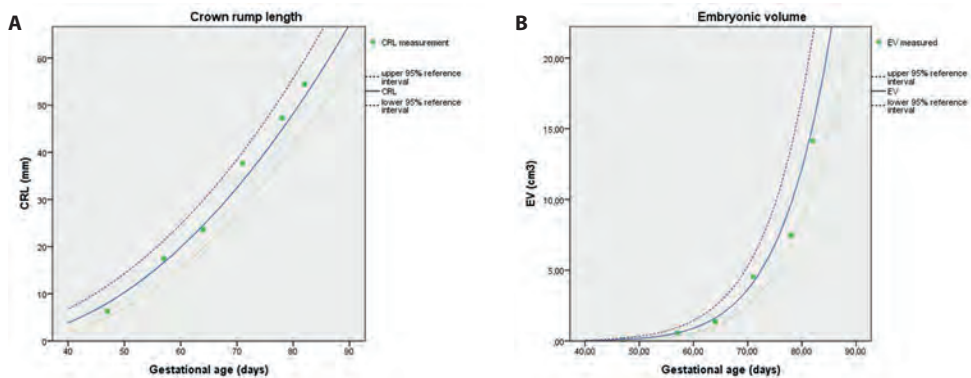


Figure 3: Biometric parameters, (A) crown-rump length (CRL), and (B) embryonic volume (EV), were measured using the I-Space virtual reality system from a gestational age of 6+5 to 11+5. The solid lines represent the expected crown-rump length or embryonic volume. The normal 5th and 95th percentiles are indicated by the dotted lines.

Discussion

The prenatal diagnosis of TAR syndrome is usually confirmed by the absence of the radii on US. In the present case the pregnancy was at an increased risk of 25% for TAR syndrome. The finding of abnormal, short upper extremities during the ninth week of pregnancy was highly indicative of TAR syndrome. Follow-up US showed the absence of radii and the presence of thumbs, establishing the diagnosis.

To the best of our knowledge this is the earliest reported prenatal diagnosis of TAR syndrome. A better impression of the developing extremities is established using the I-Space VR system, even

when image quality is too low for conventional 2D and 3D ultrasound evaluation. Binocular depth perception helped estimate the size and position of the upper extremities, which was not possible at the 2D and 3D ultrasound examination in this case.

Although most infants with TAR syndrome now survive, one has to bear in mind that it is a very serious functional handicap. After thorough counseling of parents about TAR syndrome, a substantial part will decide to terminate the pregnancy. With an earlier diagnosis, using VR, there is no longer the need to wait for and rely on chorionic villus sampling in the diagnosis of TAR syndrome. Second, an early first-trimester diagnosis provides the possibility of an early, and therefore safer, termination of pregnancy. Third, for those women who have a high recurrence risk re-assurance early in pregnancy is important which can be provided using the combination of 2D/3D US and VR.

Conclusion

First-trimester diagnosis of TAR syndrome is possible using conventional 2D and 3D ultrasound. VR techniques have the potential to facilitate and accelerate the diagnosis. VR may be used as a complementary tool in evaluating difficult congenital abnormalities, where depth perception improves visualization, as is the case in TAR syndrome.

References

1. Hall JG. Thrombocytopenia and absent radius (TAR) syndrome. *J Med Genet.* 1987;24(2):79-83.
2. Klopocki E, Schulze H, Strauss G, Ott CE, Hall J, Trotier F, et al. Complex inheritance pattern resembling autosomal recessive inheritance involving a microdeletion in thrombocytopenia-absent radius syndrome. *Am J Hum Genet.* 2007;80(2):232-40.
3. Albers CA, Paul DS, Schulze H, Freson K, Stephens JC, Smethurst PA, et al. Compound inheritance of a low-frequency regulatory SNP and a rare null mutation in exon-junction complex subunit RBM8A causes TAR syndrome. *Nat Genet.* 2012;44(4):435-9, S1-2.
4. Toriello HV. Thrombocytopenia-absent radius syndrome. *Semin Thromb Hemost.* 2011;37(6):707-12.
5. Omenn GS, Figley MM, Graham CB, Heinrichs WL. Prospects for radiographic intrauterine diagnosis—the syndrome of thrombocytopenia with absent radii. *N Engl J Med.* 1973;288(15):777-8.
6. Luthy DA, Mack L, Hirsch J, Cheng E. Prenatal ultrasound diagnosis of thrombocytopenia with absent radii. *Am J Obstet Gynecol.* 1981;141(3):350-1.
7. O’Rahilly R, Gardner E. The initial appearance of ossification in staged human embryos. *Am J Anat.* 1972;134(3):291-301.
8. Zorzoli A, Kustermann A, Caravelli E, Corso FE, Fogliani R, Aimi G, et al. Measurements of fetal limb bones in early pregnancy. *Ultrasound Obstet Gynecol.* 1994;4(1):29-33.
9. Bellver J, Lara C, Perez-Aytes A, Pellicer A, Remohi J, Serra V. First-trimester diagnosis of thrombocytopenia-absent radius (TAR) syndrome in a triplet pregnancy. *Prenat Diagn.* 2005;25(4):332-4.
10. Witters I, Claeihout P, Fryns JP. Increased nuchal translucency thickness in thrombocytopenia-absent-radius syndrome. *Ultrasound Obstet Gynecol.* 2005;26(5):581-2.

5.3

Differentiation of Early First-Trimester Cranial Neural Tube Defects

Ultrasound in Obstetrics and Gynecology. 2014 Jun;43(6):711-2.

doi: 10.1002/uog.13292.

Published as a letter to the editor

L. Baken

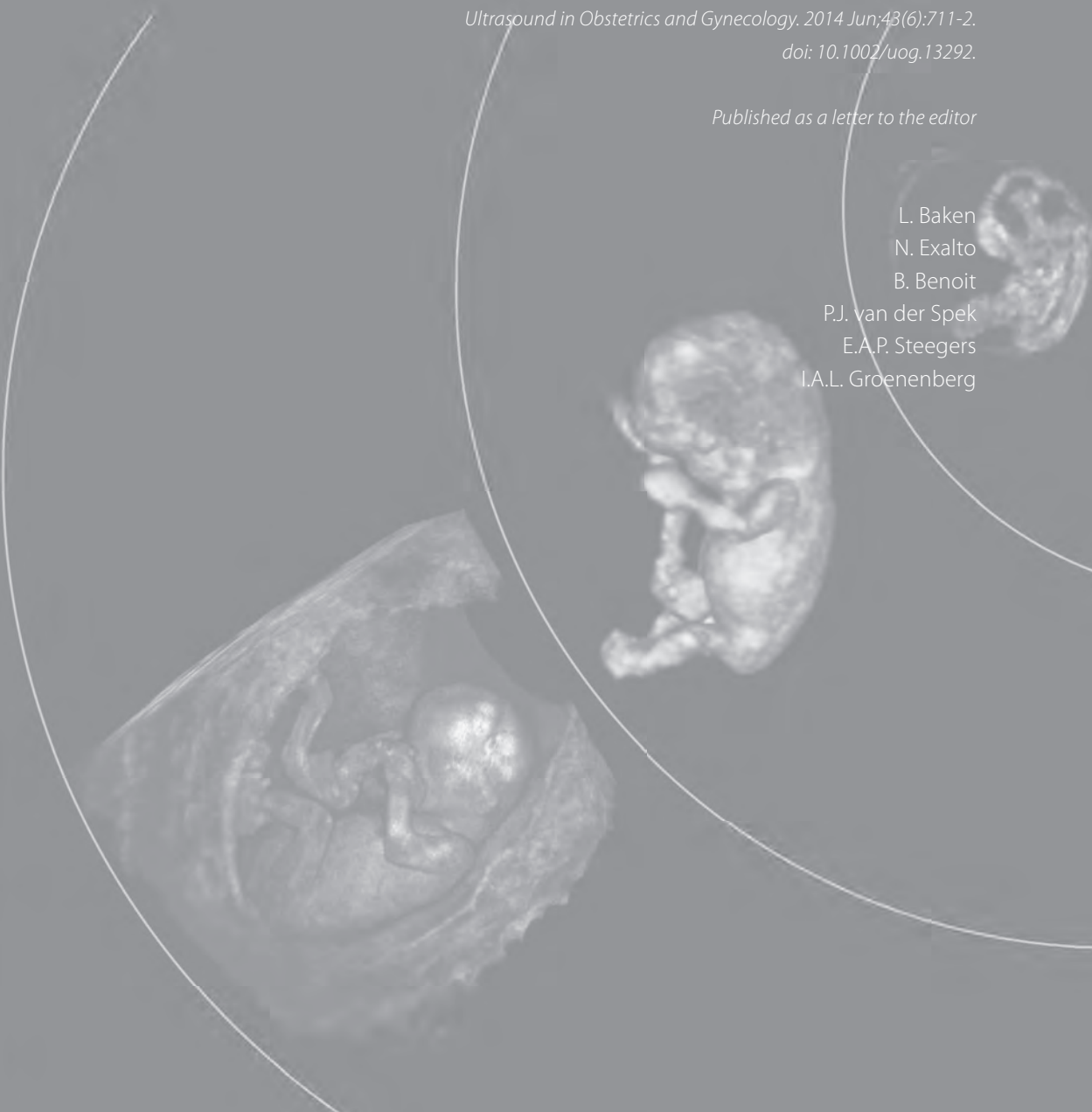
N. Exalto

B. Benoit

P.J. van der Spek

E.A.P. Steegers

I.A.L. Groenenberg



Abstract

Objective. To demonstrate the feasibility and the importance of the *in vivo* diagnosis of the different types of cranial neural tube defects (NTDs) in early first-trimester pregnancies using two- and three-dimensional (2D/3D) ultrasound.

Methods. Three early first-trimester embryo's with cranial NTDs were studied using transvaginal 2D and 3D ultrasound and compared to normal embryos of comparable gestational age (GA). Embryos were classified into one of the six types of cranial NTDs by two sonographers.

Results. The three cases showed an aberrant development of the cranial region in comparison to the normal embryo's. In two cases a defect was present from the mesencephalon through the rhombencephalon (type IV). This type is lethal very early, usually before the ninth week of pregnancy. The third case presented with an open neural tube over the parietal region of the head (type II) and can survive beyond 9 weeks GA.

Conclusion. Diagnosis of the different types of cranial NTDs is feasible using transvaginal ultrasound examination in early pregnancy. Differentiating between the types of cranial NTDs is of high importance in starting to understand etiology, developing prevention and intervention strategies, planning obstetrical management and initiating new research projects.

Introduction

Neural tube defects (NTDs) are one of the most commonly reported birth defects. Open NTDs, including anencephaly and spina bifida, are the result of failure of primary neurulation, the folding and fusion of the neural plate.¹ The variety of appearances of cranial NTDs at different gestational ages (GA) is well explained by the acrania-exencephaly-anencephaly sequence hypothesis.²⁻⁴ Exencephaly has been diagnosed as early as 9 weeks using transvaginal ultrasound^{5,6}, however it is usually detected around 11 weeks GA (Figure 1). Ultrasound characteristics of exencephaly are the 'Mickey Mouse' or 'Bart Simpson' appearance and protuberant eyes that result in a 'frog-like' appearance, all when viewed in a coronal plane.⁵

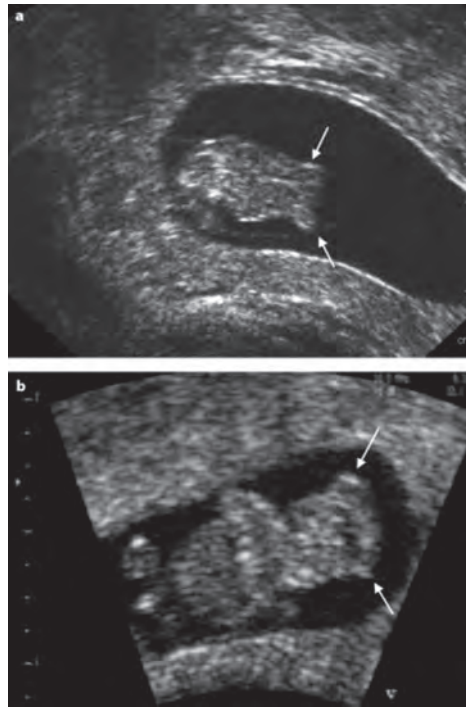


Figure 1: Sections through the heads of 'typical' exencephaly cases at CRL 22mm (A) and CRL 28 (B) visualized using two-dimensional transvaginal ultrasound. The irregular contours of the brain are indicated by the arrows. Reproduced with permission of John Wiley and Sons.

The prevalence of NTDs is reported to be approximately 1:1000 births. The vast majority of malformed embryo's however are lost in early pregnancy.⁷ The estimated incidence of NTDs in early pregnancy is therefore ten times higher. As we are moving towards earlier diagnosis of fetal abnormalities, including NTDs⁶, using high frequency transvaginal ultrasound, more abnormal pregnancies will be

detected which will spontaneously miscarry shortly after detection. The question arises whether these early non-viable NTDs can be detected by ultrasound and how these pregnancies present.

Previously, it was believed that the process of neural tube closure, primary neurulation, occurred in a 'zipper-like' fashion, starting at one point and proceeding in both cranial and caudal direction. From animal models a more complex model of neural tube closure was proposed. At least four different closure initiation sites have been described.⁸⁻¹¹ The closure of the neural tube is therefore a discontinuous process. In the literature there is general agreement that closure of the human neural tube also follows a multi-closure pattern. The different patterns in NTDs seen in second and/or third trimester anencephalic fetuses and neonates are better explained by a multi-closure model, however there is still a debate about the number and exact position of these closure sites.^{8, 12-16}

Data on neural tube closure in early human embryos is limited to two studies.^{12, 15} O'Rahilly *et al.* studied neural tube closure in histologically sectioned embryos, whereas Nakatsu *et al.* studied miscarried embryo's with and without cranial NTDs from the Kyoto Collection of Human Embryo's using a dissection microscope. According to Nakatsu *et al.* there are three closure initiation sites; one low at the future cervical region (closure 1), an intermediate closure site (closure 2) at the mesencephalic-rhombencephalic boundary and one high at the rostral end of the neural groove (closure 3).¹⁵ The

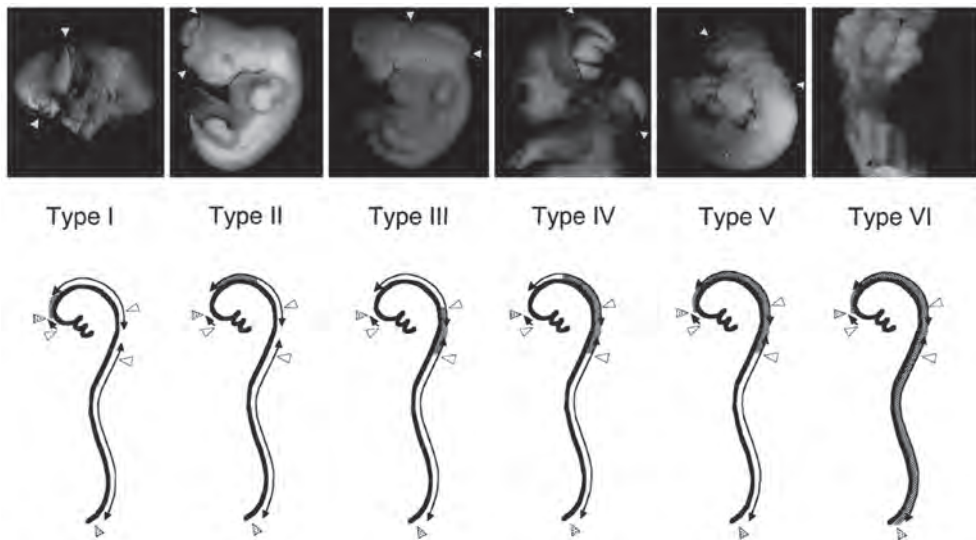


Figure 2: Different types of cranial neural tube defects (NTD) in human embryo's as reported by Nakatsu *et al.* In the upper row of the figure are representative cases of each type of cranial NTD. The arrowheads indicate the location of the defect. In the schematic pictures below the shaded area's indicate the location of the detected. The open triangles indicate the initiation site of neural tube (NT) closure. The dotted triangle indicate the anterior and posterior neuropores. Type I The NT is open at the frontal part of the head, type II The NT is open at the parietal region of the head, type III the NT is open over the fourth ventricle, type IV the NT is open over the mesencephalon through the rhombencephalon, type V the NT is open from the frontal part of the head through the cervical region, type VI total dysraphism. Reproduced with permission of John Wiley and Sons.

presence of closure site 2 could not be demonstrated by O'Rahilly *et al.*¹² The pictorial essay of embryos with cranial NTDs from the Kyoto collection provides a guide to what might possibly be seen during early pregnancy using transvaginal ultrasound.

Six different types of cranial NTDs, based on the location of the closure defect (Figure 2), are described by Nakatsu *et al.*¹⁷ The survival turned out to be significantly decreased if the rhombencephalon or fourth ventricle were involved in the defect (types III, IV and V) with two-third of cases not surviving beyond 7 weeks GA. Total dysraphism (type VI) was not compatible with life at an even earlier stage. These types will therefore not be detected during the 11-13 week scan. On the other hand, 70 percent of the embryos with a rostral defect of the cranial NTD (prosencephalon and/or mesencephalon, types I and II) did survive beyond 7 weeks GA. One may hypothesize that these types present as exencephaly during the first-trimester scan.

The aim of this pictorial essay is to demonstrate that the *in vivo* diagnosis of the different types of cranial NTD is feasible using two- and three-dimensional ultrasound. Our secondary aim is to emphasize the importance of distinguishing the classic exencephaly type from these "new" types of early cranial NTDs.

Methods

Cases for this study were derived from a prospective periconception cohort study from 2009 to 2012 at the department of Obstetrics and Gynaecology at the Erasmus MC, University Medical Center Rotterdam, the Netherlands. The participating women received weekly three-dimensional (3D) ultrasound scans from six to twelve weeks GA. First-trimester transvaginal ultrasound scans were performed using a 9-12 MHz transvaginal probe of the GE Voluson E8 Expert system (GE Medical Systems, Zipf, Austria). During first-trimester ultrasound scans 3D datasets were obtained and stored offline.

In ongoing pregnancies in this cohort no cases with cranial neural tube defects were reported. We retrospectively evaluated all pregnancies between 2009 and 2012 that resulted in a first-trimester miscarriage and where fetal heart action was seen at 6 or 7 weeks GA ($n=60$). These cases were reevaluated for the presence of cranial NTDs. Cases < 8 weeks GA with no fetal heart action present too dysmorphic and evaluation of cranial morphology was therefore not possible. A total of 148 3D ultrasound datasets were available of which 82 (55.4%) were of reasonable to good quality to be evaluated for the presence of cranial NTDs. Two embryo's with cranial NTDs were identified from this cohort. An additional case of the Princess Grace Hospital in Monaco was included, resulting in a total of three cases with early first-trimester cranial NTDs. All 3D datasets for each subject were examined and optimal images were selected for further analysis.

3D datasets of embryos diagnosed with cranial neural tube defects were re-evaluated to examine whether the defect could be classified as one of the six types reported by Nakatsu *et al.* (Figure 2). Two different sonographers agreed on the classification of the embryos. Two-dimensional (2D) and 3D ultrasound images of embryos with NTDs were compared to 2D and 3D ultrasound images of normally developing embryos of similar gestational age.

Results

In three cases a specific type of cranial NTD was assigned. Maternal characteristics are presented in Table 1A. One of the women had a previous pregnancy with a cranial NTD. During this pregnancy she did not use folic acid supplements. The defect was at the parietal region and extended to the frontal area. Due to the very early gestational age at diagnosis, and miscarriage a few days later, this cranial NTD could not be classified into one of the six types. Characteristics of the cases presented in this study are shown in Table 1B.

Figure 3 shows 2D and corresponding 3D ultrasound images of normally developing embryo's with CRLs of 16 and 20 mm. Figures 4 - 6 show 2D and 3D images of embryo's with cranial NTDs. 3D surface rendering allowed for evaluation of the abnormalities in the contour of the embryo and establishment of the diagnosis of the specific type of cranial NTD. In cases one and two (Figure 4 and 5) a cranial defect was detected from the mesencephalon through the rhombencephalon corresponding to a type IV cranial NTD. In case three (Figure 6) the neural tube did not close at the parietal region of the head leading to a type II cranial NTD. (See Figure 2 for illustrations of different types of cranial NTDs.)

Table 1: Characteristics of the presented cases: maternal characteristics (A) and case characteristics (B).

A						
Case	Age	Conception	G-P-A	Folic acid use	Smoking	Previous pregnancy with NTD
4	43	Spontaneous	G5P2A2	Yes	Yes	Yes
5	37	Spontaneous	G2P0A1	Yes	Yes	No
6	35	Spontaneous	G3P1A1	Yes	No	No

B						
Case	CRL (mm)	GA-CRL (wk+d)	GA-LMP (wk+d)	GA miscarriage	Ultrasound findings	Cranial NTD type
4	23	9+0	9+2	9+5 (TOP)	Cranial defect from the mesencephalon through the rhombencephalon	IV
5	13	7+5	8+1	9+1	Cranial defect from the mesencephalon through the rhombencephalon	IV
6	14	7+5	9+5	9+5	Cranial defect at the parietal region of the head	II

Case numbers correspond to the figures.
 CRL = crown-rump length
 GA-CRL = gestational age for crown-rump length
 GA-LMP = gestational age according to last menstrual period
 GA miscarriage = gestational age according to last menstrual period at which negative heart action was diagnosed
 TOP = termination of pregnancy
 Cranial NTD type = cranial neural tube defect according to the types defined by Nakatsu et al.

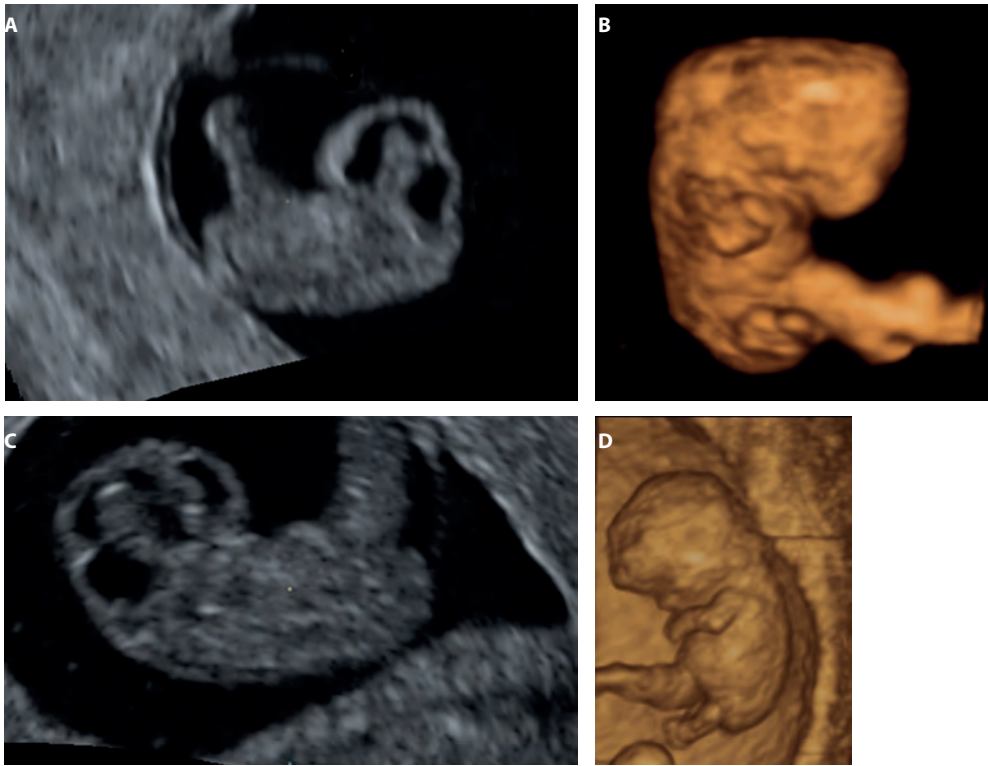


Figure 3: Two-dimensional (A) and corresponding three-dimensional (B) image of a normally developing embryo at 7+6 weeks GA (CRL 16mm). Two-dimensional (C) and corresponding three-dimensional (D) image of a normally developing embryo at 9+3 weeks GA (CRL 20 mm).

Discussion

Malformations of the brain such as holoprosencephaly and exencephaly are one of the first malformations that can be diagnosed using ultrasound.⁶ Cranial NTDs can be detected in the first-trimester of pregnancy. In this study it was shown that some of the different types of cranial NTD, as reported by Nakatsu *et al*, can be distinguished and detected *in vivo* using high frequency 2D and 3D transvaginal ultrasound during the early first-trimester.

NTDs in general are known as a multifactorial disorder caused by a complex interaction of genetic and environmental factors. An important and well studied factor in the etiology of NTDs is DNA methylation and the subsequent preventive actions of folic acid in reducing aberrant DNA methylation via the one-carbon metabolism pathway.^{18, 19} However, as about 30-50% of all NTDs are not prevented by folic acid treatment other mechanisms must be involved.¹⁹ In trying to understand these clinically relevant mechanisms extensive research is being performed on this topic.^{1, 20-22}

The first step in understanding etiology of congenital malformations such as cranial NTDs is being aware of the existence and subsequently the recognition of these malformations. Survival of exen-

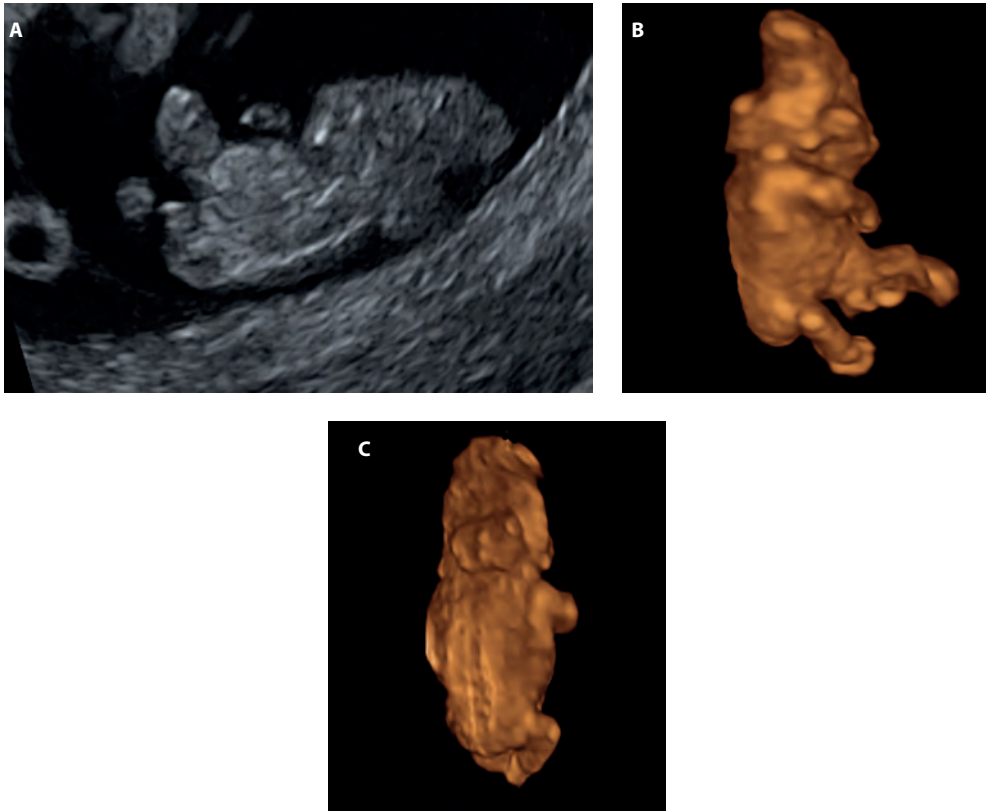


Figure 4: Case 1. Transvaginal two-dimensional (A) and three-dimensional (B,C) ultrasound images of an embryo with a cranial neural tube defect type IV (CRL 23 mm). Note the abnormal contour of the head. A neural tube defect is present from the mesencephalon through the rhombencephalon.

cephaly cases can be beyond the first-trimester or even up to term, in contrast the cranial NTDs in this study that do not age beyond ten weeks gestation¹⁵, indicating the severity of these cranial NTDs. As a consequence the opportunity to detect these cranial NTDs is limited to a short time frame. With ongoing development and innovation of our imaging technology detection rates of these subtle findings will improve. However diagnosis of total dysraphism (type VI) that does not survive beyond 7 weeks GA will remain a challenge as we were not able to assess images before 8 weeks GA. The fact that more ultrasound scans are being performed in early pregnancy will also contribute to this supposed increased detection.

We are aware that recognition of these early abnormal developing embryo's requires high end ultrasound equipment and highly experienced sonographers. This in combination with the low incidence of these defects means that many years of research are needed before questions concerning etiology and pathology can be answered. Collaboration of medical centers however will facilitate the research on cranial NTDs. Increasing awareness on the existence of different types of cranial NTDs is an

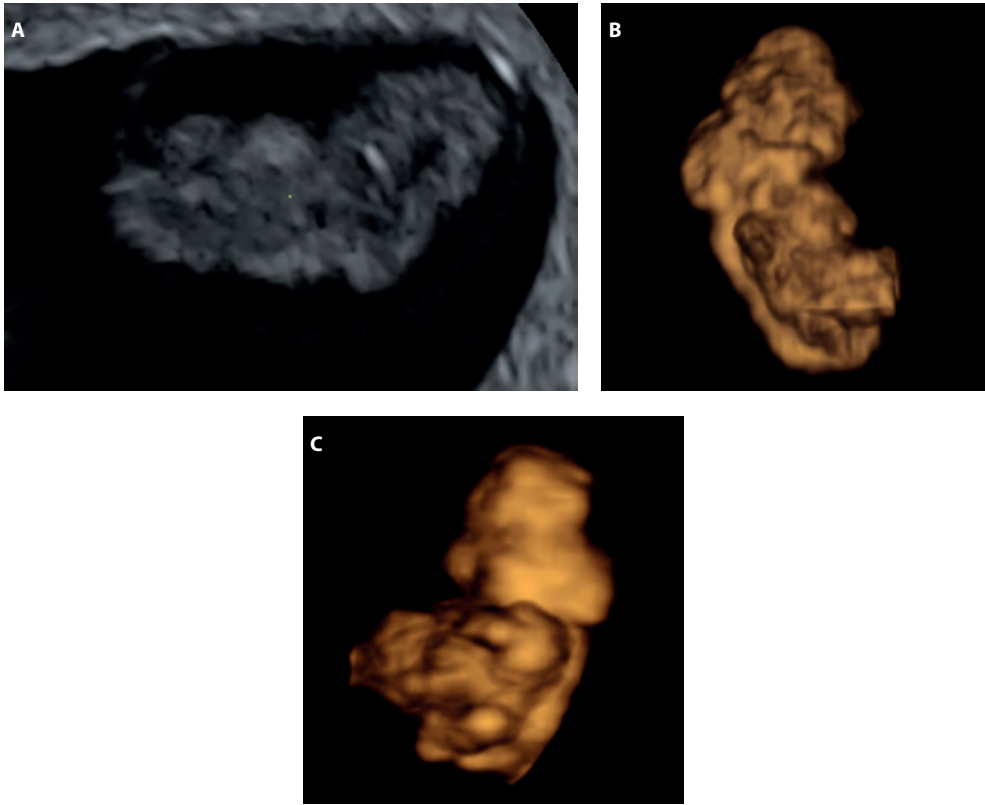


Figure 5: Case 2. Transvaginal two-dimensional (A) and three-dimensional (B) ultrasound images of an embryo with a cranial neural tube defect type IV (CRL 13 mm). In (C) the same embryo is presented at CRL 17. A neural tube defect is present from the mesencephalon through the rhombencephalon.

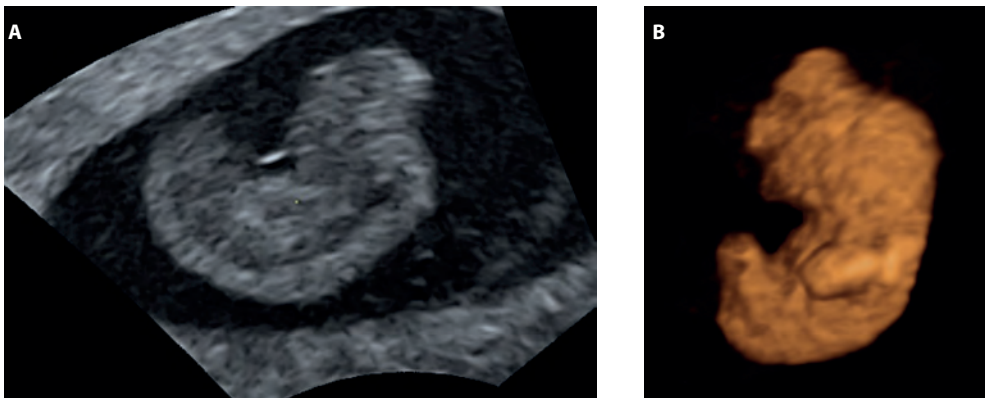


Figure 6: Case 3. Transvaginal two-dimensional (A) and three-dimensional (B) ultrasound images of an embryo with a cranial neural tube defect type II (CRL 14 mm). A neural tube defect is visible at the parietal region of the head.

important base to start unraveling the underlying process of the development of NTDs. Documentation of the different types of cranial NTDs is essential in studying etiology, especially as these cases miscarry early in pregnancy and would thus otherwise be missed. With good documentation the different types of cranial NTDs might be linked to different genetic pathways or environmental factors.²⁰

The existence of different types of cranial NTDs is a rather recent insight and the implications this has for obstetrical management are largely unknown. Understanding the cause of these malformations might contribute to the detection of high risk pregnancies and development of new intervention and prevention strategies. The *in vivo* detection of these cranial NTDs gives rise to the question whether these women are at an increased risk of recurrence of NTDs. If so, in a subsequent pregnancy, extra folic acid supplementation and additional ultrasound scans are recommended.

In conclusion, the different types of cranial NTDs can be diagnosed using transvaginal ultrasound examination in early pregnancy. Detection of these cranial NTDs is of particular importance in starting to understand etiology, developing prevention and intervention strategies, planning obstetrical management and initiating new research projects.

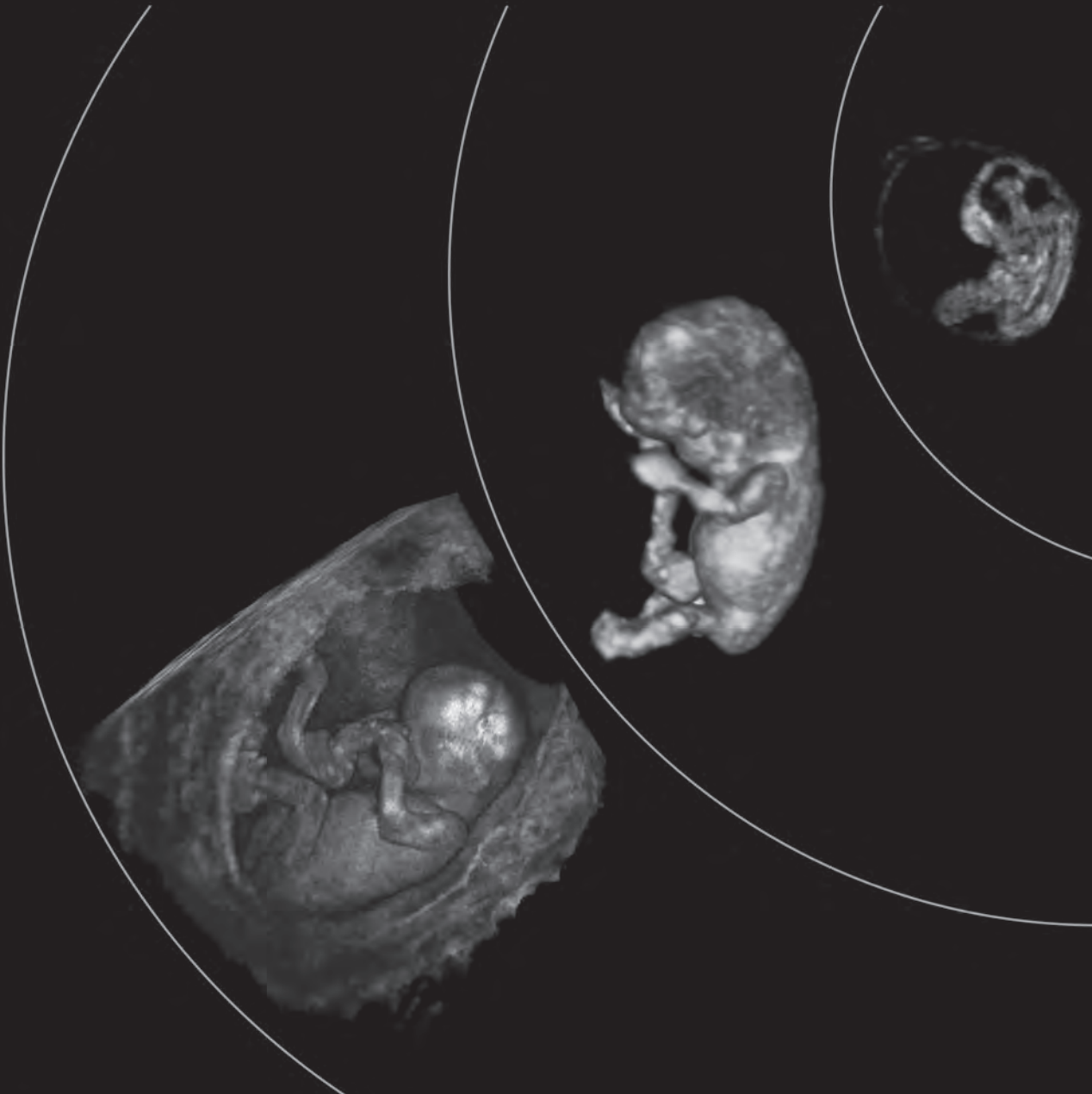
References

1. Copp AJ. Neurulation in the cranial region—normal and abnormal. *J Anat.* 2005;207(5):623-35.
2. Timor-Tritsch IE, Greenebaum E, Monteagudo A, Baxi L. Exencephaly-anencephaly sequence: proof by ultrasound imaging and amniotic fluid cytology. *J Matern Fetal Med.* 1996;5(4):182-5.
3. Matsumoto A, Hatta T, Moriyama K, Otani H. Sequential observations of exencephaly and subsequent morphological changes by mouse exo utero development system: analysis of the mechanism of transformation from exencephaly to anencephaly. *Anat Embryol (Berl).* 2002;205(1):7-18.
4. Gorgal R, Ramalho C, Brandao O, Matias A, Montenegro N. Revisiting acrania: same phenotype, different aetiologies. *Fetal Diagn Ther.* 2011;29(2):166-70.
5. Becker R, Mende B, Stierner B, Entezami M. Sonographic markers of exencephaly at 9 + 3 weeks of gestation. *Ultrasound Obstet Gynecol.* 2000;16(6):582-4.
6. Blaas HG, Eik-Nes SH. Sonoembryology and early prenatal diagnosis of neural anomalies. *Prenat Diagn.* 2009;29(4):312-25.
7. Roberts CJ, Lowe CR. Letter: Where have all the conceptions gone? *Lancet.* 1975;1(7907):636-7.
8. Greene ND, Copp AJ. Development of the vertebrate central nervous system: formation of the neural tube. *Prenat Diagn.* 2009;29(4):303-11.
9. Peeters MC, Viebahn C, Hekking JW, van Straaten HW. Neurulation in the rabbit embryo. *Anat Embryol (Berl).* 1998;197(3):167-75.
10. Van Straaten HW, Janssen HC, Peeters MC, Copp AJ, Hekking JW. Neural tube closure in the chick embryo is multiphasic. *Dev Dyn.* 1996;207(3):309-18.
11. Golden JA, Chernoff GF. Intermittent pattern of neural tube closure in two strains of mice. *Teratology.* 1993;47(1):73-80.
12. O'Rahilly R, Muller F. The two sites of fusion of the neural folds and the two neuropores in the human embryo. *Teratology.* 2002;65(4):162-70.
13. Van Allen MI, Kalousek DK, Chernoff GF, Juriloff D, Harris M, McGillivray BC, et al. Evidence for multi-site closure of the neural tube in humans. *Am J Med Genet.* 1993;47(5):723-43.
14. Golden JA, Chernoff GF. Multiple sites of anterior neural tube closure in humans: evidence from anterior neural tube defects (anencephaly). *Pediatrics.* 1995;95(4):506-10.
15. Nakatsu T, Uwabe C, Shiota K. Neural tube closure in humans initiates at multiple sites: evidence from human embryos and implications for the pathogenesis of neural tube defects. *Anat Embryol (Berl).* 2000;201(6):455-66.
16. Copp AJ, Stanier P, Greene ND. Neural tube defects: recent advances, unsolved questions, and controversies. *Lancet Neurol.* 2013.
17. Luthy DA, Mack L, Hirsch J, Cheng E. Prenatal ultrasound diagnosis of thrombocytopenia with absent radii. *Am J Obstet Gynecol.* 1981;141(3):350-1.
18. Wang L, Wang F, Guan J, Le J, Wu L, Zou J, et al. Relation between hypomethylation of long interspersed nucleotide elements and risk of neural tube defects. *Am J Clin Nutr.* 2010;91(5):1359-67.
19. Blom HJ, Shaw GM, den Heijer M, Finnell RH. Neural tube defects and folate: case far from closed. *Nat Rev Neurosci.* 2006;7(9):724-31.

20. Detrait ER, George TM, Etchevers HC, Gilbert JR, Vekemans M, Speer MC. Human neural tube defects: developmental biology, epidemiology, and genetics. *Neurotoxicol Teratol.* 2005;27(3):515-24.
21. Lemire RJ. Neural tube defects. *JAMA.* 1988;259(4):558-62.
22. Wallingford JB, Niswander LA, Shaw GM, Finnell RH. The continuing challenge of understanding, preventing, and treating neural tube defects. *Science.* 2013;339(6123):1222002.

CHAPTER 6

General Discussion



In this thesis the use of an innovative visualization technique, virtual reality (VR), is explored in the field of early prenatal diagnosis of abnormal embryonic development. The I-Space VR system is unique in its ability to allow optimal depth perception by immersing viewers in a virtual environment. In previous studies the reproducibility of I-Space measurements has already been established.^{1,2} However, the possibilities for analysis of first-trimester growth and development are numerous and new applications for the VR approach have been explored and developed. Before the introduction of new applications it has to be proven that these applications are performing at least as good as the gold standard.

The Erasmus MC is, as far as we know, the only center in the world that uses a CAVE-like VR system for early pregnancy evaluation. The development of a desktop VR system was an important step to make this promising technique more accessible. Its lower costs and limited desk space provide the opportunity to integrate a desktop VR system in daily clinical practice. In **chapter 2.1** it is demonstrated that such a desktop system can be put together with commercially available components at a fraction of the costs of the I-Space. Secondly, the accuracy of measurements on the desktop system was compared to the fully-immersive I-Space. The reproducibility was successfully established; length and volume measurements are at least as reliable as those performed in the I-Space. A desktop VR system in the consulting room will aid the obstetrician in the diagnostic process and counseling of the patient. In addition, the development of VR desktop systems provides opportunities for international research collaborations using VR. Following the introduction of the desktop VR system we foresee implementation of VR as an option in ultrasound machines in the near future.

As a second new application, the use of VR in detection of structural congenital abnormalities in early pregnancies was investigated. As VR provides powerful visualizations of early pregnancy, it is tempting to start using it immediately in the diagnosis of structural congenital abnormalities. Although new techniques have been introduced in this way without formal evaluation, e.g. three-dimensional ultrasound, we aim to provide evidence for a similar decision on VR by comparing it to the gold standard (**chapter 2.2**). In this case the gold standard is conventional two- and three-dimensional ultrasound. Detection rates for first-trimester structural congenital abnormalities proved to be at least as good using VR. In specific cases the spatial presentation of VR was able to provide extra diagnostic information. Depth perception appears especially useful in diagnosing malformations at the exterior of embryo. This is also supported by the case reports that are presented in **chapter 5**. On the other hand, some congenital abnormalities are still better diagnosed using conventional ultrasound, i.e. holoprosencephaly. Therefore, before VR can be implemented in the diagnostic process of congenital abnormalities a structured, research based list of abnormalities in which VR can be of diagnostic help should be available. Until then VR might be used as an additional diagnostic tool next to conventional ultrasound.

An important part of the V-Scope software used in the I-Space is its region-growing segmentation algorithm that semi-automatically calculates volumes of structures of interest.^{2,3} Since impaired embryonic growth is associated with adverse pregnancy outcomes and health in later life there is an increasing interest in more precise tools to quantify embryonic development. A better assessment

of embryonic growth was suggested by others by measuring embryonic volume (EV) rather than crown-rump length (CRL).^{4,5} In these studies embryonic volumes were estimated by delineating the contours of the embryo manually in several different planes, which is subject to individual variation. The semi-automatical approach of the I-Space and its true depth perception allow for more objective volume measurements and prevent incomplete segmentations. Normative growth charts of EV, both in relation to gestational age and to CRL, have been established by us using the I-Space VR system.³ These charts were used as a reference throughout this thesis (**chapter 3**).

In this thesis it is shown that EV measurements enable to differentiate between normal and abnormal human development in the first-trimester of pregnancy. Whereas the CRL is not significantly smaller than expected in most aneuploid pregnancies (i.e. trisomy 21, trisomy 13, and monosomy X), EV on the other hand on average is significantly smaller than expected in all these cases (**chapter 4.1**). A similar association was found in embryos and fetuses that were diagnosed with a structural congenital abnormality (**chapter 3.1**). EV has therefore proven to be more precise in quantifying impaired growth than CRL. EV measurements may therefore be implemented in routine clinical practice in the near future. However, our results were obtained by comparing our cases to previously established references curves. In order to analyze the actual predictive value of EV measurements, data should be obtained from large cohort studies. Prediction models, that include the most sensitive ultrasound characteristics, i.e. EV instead of CRL, and other non-ultrasound characteristics like maternal age, can be established from these larger studies. As miscarriage and the diagnosis of a chromosomal or structural abnormality are considered a life-event, more accurate prediction models based on large cohort studies are warranted.

EV also proved to be smaller than expected in pregnancies that will subsequently end in a miscarriage. However, in these cases EV did not improve the analysis of miscarriages as compared to CRL (**chapter 3.2**). Differences in growth pattern therefore seem to be present between miscarriage cases and cases with structural or chromosomal abnormalities. The results of our studies suggest that different subgroups of miscarriage cases exist; cases with and cases without marked growth restriction. Further research should look into if and how these different groups can be defined.

When using the I-Space VR system numerous non-standard measurements can be performed due to its wide range of tools, i.e. the tracing function and the algorithm for semi-automatical volume measurements. Most of these measurements are not performed during routine ultrasound scans because the structures of interest are too difficult to evaluate using two-dimensional media. Previously an *in vivo* study of the growth of the umbilical cord and the vitelline duct, facilitated by the I-Space, has been described.⁶ In this thesis we elaborate on the possibilities of non-standard biometric measurements and their use in the early recognition of abnormal growth and development (**chapter 4**).

Measurements of the hand are rarely performed during first-trimester ultrasound scans, even though it is well known that abnormalities of the hand are associated with several (genetic) syndromes. In **chapter 4.2 *in vivo*** growth charts of first-trimester hand are established, facilitated by the I-Space VR system. Its tracing function made it possible to easily measure the hand length regardless of the position of the hand and fingers. In this study it was found that hand abnormalities in aneuploid

pregnancies, well known in the second and third trimester of pregnancy, are already present in the first-trimester. Future studies should examine the discriminating ability of these new measurements in high-risk pregnancies. The etiology of different hand growth patterns in aneuploid pregnancies is unclear. When combining the results of **chapter 4.1** and **chapter 4.2** however, it can be seen that in general those pregnancies with chromosomal abnormalities that have a smaller EV than expected also show abnormal hand growth, e.g. broader hands in trisomy 21 (Figure 1).

Screening for structural and chromosomal abnormalities is an essential part of prenatal care.^{7,8} In the past decade second- and third-trimester prenatal diagnosis has shifted towards first-trimester analysis of pregnancy. Due to improvements in imaging techniques, a significant proportion of structural congenital abnormalities can nowadays be detected in the first-trimester of pregnancy.⁹⁻¹³ The third dimension offered by virtual reality systems proved to be useful in the detection of congenital abnormalities. This thesis describes how the depth perception and three-dimensional interaction offered by VR can be of great help in analyzing complex anatomical structures in case of conjoined twins (**chapter 5.1**) and in diagnosing the thrombocytopenia absent radius (TAR) syndrome (**chapter 5.2**). The use of three-dimensional ultrasound makes it possible to identify different types of cranial neural tube defects *in vivo* (**chapter 5.3**).

Most studies report on first-trimester screening for abnormalities between 11 and 14 weeks gestational age (GA). A distinction should be made between diagnosis of congenital abnormalities during this screening period (11-14 weeks GA) and the earlier diagnosis during the embryonic period. Logically, the size of the embryo partly determines whether structural congenital abnormalities can be detected. Despite the small size during the embryonic period, the diagnosis of specific abnormalities is frequently possible during this period as described in this thesis (**chapter 5**) and in the literature.¹⁴⁻¹⁶

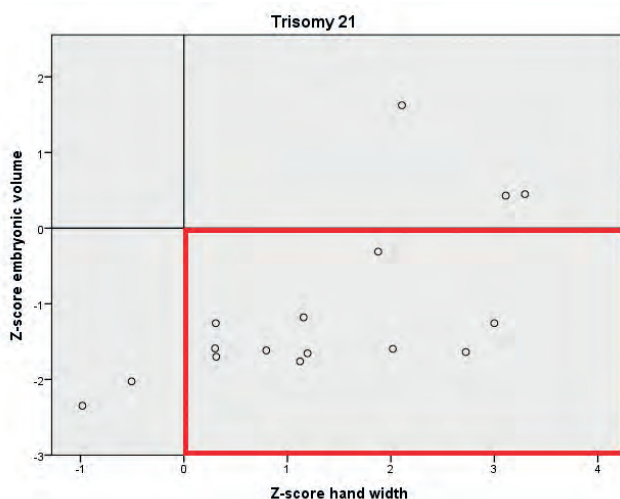


Figure 1: Z-score of embryonic volume (EV) versus z-score of hand width in trisomy 21 pregnancies.

In cases where the small embryonic size does limit the diagnosis, growth restriction i.e. a decreased EV, which is already present in the embryonic period, may be used as a marker for a congenital abnormality (**chapter 3.2**). One should be aware that pregnancy outcome cannot be changed by earlier diagnosis of a congenital abnormality in the majority of cases. However, it will improve obstetrical management, e.g. the number of follow-up scans.

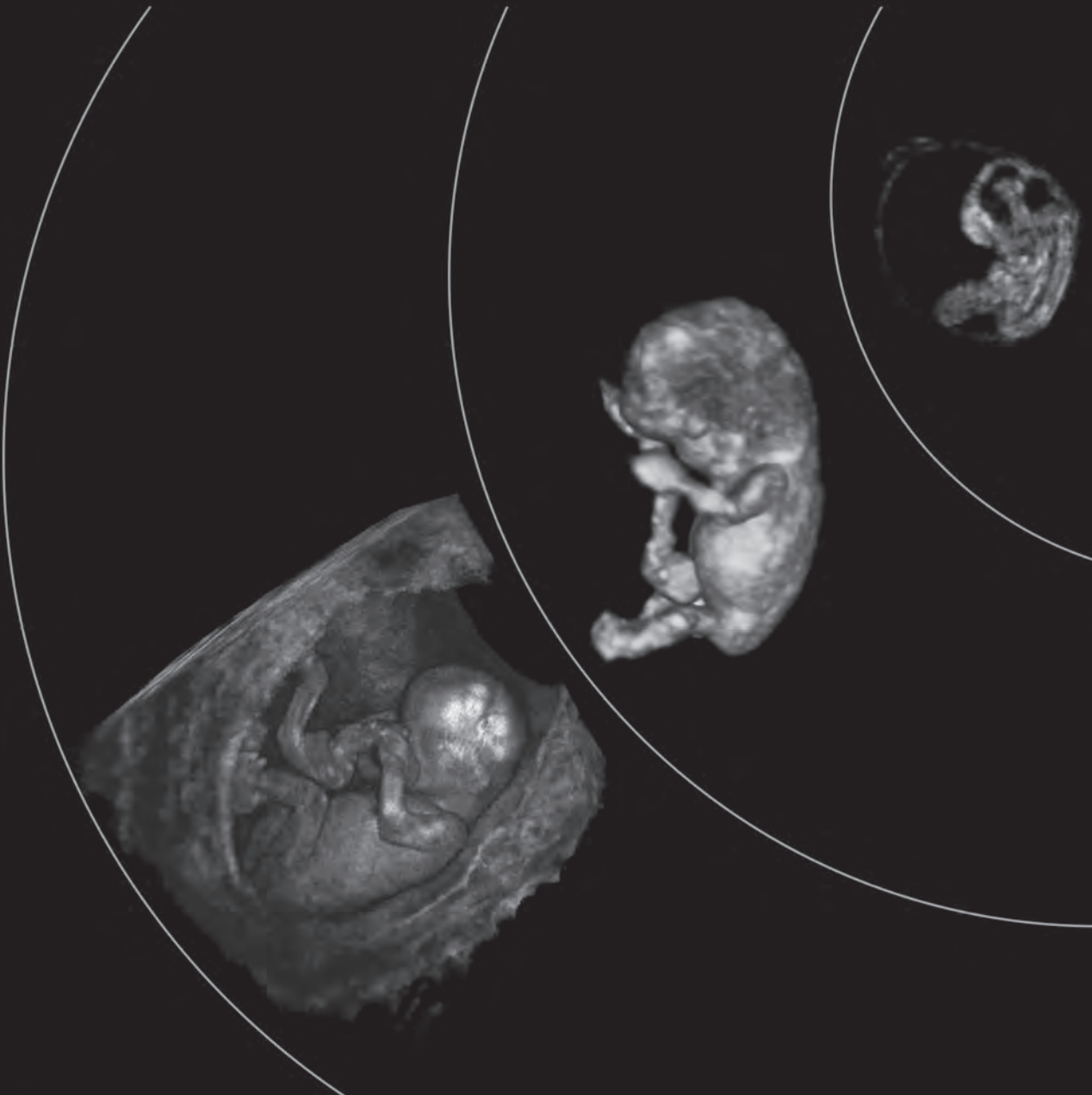
In conclusion, we can state that embryonic growth and development are highly associated with of pregnancy outcome. VR offers an impressive opportunity in analyzing early pregnancy in all its dimensions. The new applications of this VR approach and the new biometric and volume measurements will enable earlier and more accurate diagnosis of abnormal fetal growth and development. In order to improve perinatal outcome the focus of both research and clinical care should be on embryonic health. A better understanding of embryonic health will open the door to the field of embryonic medicine.

References

1. Verwoerd-Dikkeboom CM, Koning AH, Hop WC, *et al.* Innovative VR measurements for embryonic growth and development. *Hum Reprod* 2010; 25(6):1404-10.
2. Rousian M, Verwoerd-Dikkeboom CM, Koning AH, *et al.* Early pregnancy volume measurements: validation of ultrasound techniques and new perspectives. *BJOG* 2009; 116(2):278-85.
3. Rousian M, Koning AH, van Oppenraaij RH, *et al.* An innovative VR technique for automated human embryonic volume measurements. *Hum Reprod* 2010; 25(9):2210-6.
4. Aviram R, Shpan DK, Markovitch O, *et al.* Three-dimensional first-trimester fetal volumetry: comparison with crown rump length. *Early Hum Dev* 2004; 80(1):1-5.
5. Falcon O, Peralta CF, Cavoretto P, *et al.* Fetal trunk and head volume measured by three-dimensional ultrasound at 11 + 0 to 13 + 6 weeks of gestation in chromosomally normal pregnancies. *Ultrasound Obstet Gynecol* 2005; 26(3):263-6.
6. Rousian M, Verwoerd-Dikkeboom CM, Koning AH, *et al.* First-trimester umbilical cord and vitelline duct measurements using VR. *Early Hum Dev* 2011; 87(2):77-82.
7. Nicolaides KH. Screening for fetal aneuploidies at 11 to 13 weeks. *Prenat Diagn* 2011; 31(1):7-15.
8. Salomon LJ, Alfirevic Z, Berghella V, *et al.* Practice guidelines for performance of the routine mid-trimester fetal ultrasound scan. *Ultrasound Obstet Gynecol* 2011; 37(1):116-26.
9. Sonek J. First-trimester ultrasonography in screening and detection of fetal anomalies. *Am J Med Genet C Semin Med Genet* 2007; 145C(1):45-61.
10. Becker R, Wegner RD. Detailed screening for fetal anomalies and cardiac defects at the 11-13-week scan. *Ultrasound Obstet Gynecol* 2006; 27(6):613-8.
11. Donnelly JC, Malone FD. Early fetal anatomical sonography. *Best Pract Res Clin Obstet Gynaecol* 2012; 26(5):561-73.
12. Iliescu D, Tudorache S, Comanescu A, *et al.* Improved detection rate of structural abnormalities in the first-trimester using an extended examination protocol. *Ultrasound Obstet Gynecol* 2013; 42(3):300-9.
13. Katorza E, Achiron R. Early pregnancy scanning for fetal anomalies—the new standard? *Clin Obstet Gynecol* 2012; 55(1):199-216.
14. Becker R, Mende B, Stiemer B, *et al.* Sonographic markers of exencephaly at 9 + 3 weeks of gestation. *Ultrasound Obstet Gynecol* 2000; 16(6):582-4.
15. Sepulveda W, Lutz I, Be C. Holoprosencephaly at 9 weeks 6 days in a triploid fetus: two- and 3-dimensional sonographic findings. *J Ultrasound Med* 2007; 26(3):411-4.
16. Bonilla-Musoles FM, Raga F, Ballester MJ, *et al.* Early detection of embryonic malformations by transvaginal and color Doppler sonography. *J Ultrasound Med* 1994; 13(5):347-55.

CHAPTER 7

Summary / Samenvatting



Summary

Research of the past years indicates that the periconception period, the period including gametogenesis and embryogenesis, determines growth and development of the embryo and subsequent pregnancy outcome. Prenatal care starts to focus more on the first-trimester of pregnancy, where growth and development rates are the highest. The main aim of this thesis is to describe normal and abnormal development of embryonic and early fetal life using the innovative I-Space virtual reality (VR) system.

Chapter 1 is an introduction to the research performed in this thesis. **Chapter 1.1** comprises the general introduction of the research subject and provides the aims and the outline of this thesis. **Chapter 1.2** describes the technical details and the applications of the I-Space VR system in the early pregnancy.

In **chapter 2** new applications of the I-Space VR system are described. In **chapter 2.1** the design and validation of a desktop VR system is described. The desktop VR system is a new application that runs the same software, the V-Scope software, as the fully immersive I-Space. The development of a desktop system, due to its smaller size and its lower costs, is an important step towards the availability of VR in clinical practice. This study also demonstrates that length and volume measurements can be performed at least as reliable on the desktop system as in the I-Space. Future research can therefore as well be performed using the desktop VR system.

In **chapter 2.2** the I-Space VR technique is evaluated for the use of first-trimester diagnosis of structural congenital abnormalities. Detection rates of congenital abnormalities were compared between the I-Space and conventional two- and three-dimensional ultrasound. Five blinded observers scored abnormalities in 40 cases, once using the I-Space and once by means of conventional ultrasound. Furthermore, evaluation time was recorded and a questionnaire was filled out by the observers. The overall detection rates for both the I-Space and conventional ultrasound were comparable. However, abnormalities of skeleton and limbs were more often detected using the I-Space, whereas the detection rate for holoprosencephaly was higher using conventional ultrasound. The evaluation time was about two minutes longer for the I-Space. The reviewers reported a more clear presentation of the ultrasound images when VR is used as compared to conventional ultrasound. The results of this study show an additional value of VR in specific cases.

Chapter 3 describes the use of embryonic volume measurements in the quantification of growth restriction in embryo's and fetuses with structural congenital abnormalities (**chapter 3.1**), and in pregnancies that will subsequently end in a miscarriage (**chapter 3.2**). Embryonic volume (EV) measurements proved to be more informative than standard crown-rump length (CRL) measurements in the analysis of growth restriction in pregnancies diagnosed with first-trimester structural congenital abnormalities (**chapter 3.1**). EV measurements can therefore be used to diagnose abnormal first-trimester growth earlier and more accurately. In **chapter 3.2** we analyzed the use of EV measurements in pregnancies that will subsequently end in a miscarriage. In these cases EV does not improve the assessment of growth restriction when compared to CRL measurements. A different growth

pattern therefore seems to exist between miscarriage cases and pregnancies that are diagnosed with (chromosomal) congenital abnormalities.

In **chapter 4** both non-standard *in vivo* biometric measurements and volume measurements in first-trimester aneuploid pregnancies are described. **Chapter 4.1** provides unique normative data, related to gestational age and crown-rump length, on first-trimester hand growth. Different parameters of hand growth are measured; wrist width, hand width, and hand length. The depth perception of the I-Space enabled us to measure these structures. The newly developed growth charts were used to analyze hand growth in aneuploid pregnancies. It was shown that hand growth is significantly different in trisomy 21 (Down syndrome) and trisomy 18 (Edwards syndrome) already in the first-trimester of pregnancy. In **chapter 4.2** it was demonstrated that also in case of aneuploid pregnancies EV measurements is a better indicator of growth restriction when compared to conventional CRL measurements. Only in cases with trisomy 18 a smaller than expected CRL was seen, whereas EV was significantly smaller in trisomy 21, trisomy 18, and trisomy 13.

In **chapter 5** the use of VR in the diagnosis of first-trimester structural congenital abnormalities is evaluated. **Chapter 5.1** describes the applicability of VR in the diagnosis of conjoined twins. In this review all imaging techniques used in the diagnosis of conjoined twins are evaluated. The review is illustrated by three cases of conjoined twins that were diagnosed using two- and three-dimensional ultrasound and that were additionally evaluated using VR. As VR provided extra diagnostic clues to all three cases, VR can contribute to earlier and more appropriate diagnosis of these rare cases. In **chapter 5.2** VR facilitated the earliest diagnosis of thrombocytopenia-absent radius (TAR) syndrome reported in the literature. We believe that the application of VR can be useful in evaluating complex anatomical relationships requiring depth perception.

In **chapter 5.3** it was demonstrated that different types of cranial neural tube defects can be distinguished *in vivo* using three-dimensional ultrasound. The third dimension aided in relating our cases to previously published *ex vivo* documentation on cranial neural tube defects. Different types of cranial neural tube defects differ in their prognosis. Discerning the different types is of particular importance in understanding etiology and developing prevention strategies.

In **chapter 6**, the general discussion, the results of all studies presented in this thesis are discussed and put in a broader perspective. The I-Space VR technique provides true depth perception and allows for intuitive visualization of the early pregnancy in detail. Structures that cannot be analyzed or measured in two-dimensions were studied in this thesis using VR. In conclusion we can say that first-trimester growth is associated with pregnancy outcome. The new applications of this VR technique and the new biometric and volume measurements enable earlier and more accurate diagnosis of abnormal embryonic growth and development. Since developmental problems early in pregnancy have major implications for pregnancy outcome, the embryonic period should be monitored very precisely. Diagnosis of congenital malformations or the detections of markers that indicate abnormal embryonic development may lead to a better understanding of embryonic health and adjustments in obstetrical management.

Samenvatting

Uit wetenschappelijk onderzoek van de afgelopen jaren is gebleken dat de periconceptieperiode, de periode van gametogenese tot en met de embryogenese, bepalend is voor de ontwikkeling van het embryo en voor een deel ook voor de uiteindelijke zwangerschapsuitkomst. De prenatale geneeskunde concentreert zich daarom steeds meer op het eerste trimester van de zwangerschap waarin de groei en ontwikkeling uitermate snel en complex verlopen. Dit proefschrift heeft als doel om de normale en abnormale embryonale en vroeg foetale ontwikkeling te beschrijven zoals onderzocht met behulp van een innovatief 'virtual reality' (VR) systeem.

Hoofdstuk 1 is een introductie waarin het onderzoek dat is uitgevoerd in dit proefschrift wordt beschreven. **Hoofdstuk 1.1** betreft de algemene introductie van het proefschrift en geeft inzicht in de indeling en de doelstellingen van het proefschrift. **Hoofdstuk 1.2** beschrijft de technische details van het I-Space VR systeem.

In **hoofdstuk 2** worden de nieuwe applicaties van de I-Space besproken. In **hoofdstuk 2.1** wordt beschreven hoe de zogenaamde desktop versie van de I-Space is ontwikkeld en gevalideerd. Het desktop VR systeem is een nieuwe applicatie welke dezelfde software, namelijk V-Scope, gebruikt als de I-Space. De ontwikkeling van een desktop systeem is, vanwege de kleinere afmetingen en de lagere aanschaffkosten, een belangrijke stap voorwaarts in het beschikbaar maken van de VR techniek voor klinische toepassing. Deze studie toont ook aan dat lengte- en volumemetingen even betrouwbaar kunnen worden uitgevoerd met behulp van de desktop als in de I-Space. Toekomstig onderzoek kan daarom ook uitgevoerd worden met behulp van het desktop VR systeem.

In **hoofdstuk 2.2** is de I-Space VR techniek geëvalueerd voor het diagnosticeren van eerste trimester structurele aangeboren afwijkingen. De percentages van gedetecteerde afwijkingen werden vergeleken tussen de I-Space en conventionele twee- en driedimensionale (2D/3D) echografie. Vijf geblindeerde onderzoekers beoordelen 40 casussen op de aanwezigheid van aangeboren afwijkingen, zowel in de I-Space als met behulp van conventionele echografie. Ook werd de evaluatietijd per casus bijgehouden en vulden de vijf onderzoekers een vragenlijst in. De detectiepercentages voor de I-Space en conventionele echografie waren vergelijkbaar.

Afwijkingen aan het skelet en/of ledematen daarentegen werden vaker correct gediagnosticeerd met behulp van de I-Space, terwijl holoprosencephalie vaker werd gedetecteerd met behulp van conventionele echografie. The evaluatietijd was ongeveer twee minuten langer voor de I-Space. The onderzoekers rapporteerden een meer duidelijke presentatie van de echobeelden in de I-Space in vergelijking tot conventionele presentatie in 2D media. De resultaten van deze studie laten zien dat er een toegevoegde waarde is van de I-Space in specifieke gevallen.

In **hoofdstuk 3** wordt het gebruik van embryonale volume (EV) metingen beschreven voor het kwantificeren van groeiachterstand in embryo's en foetussen met structurele congenitale afwijkingen (**hoofdstuk 3.1**) en in zwangerschappen die uiteindelijk zullen eindigen in een miskraam (**hoofdstuk 3.2**). EV metingen blijken informatiever te zijn dan het meten van de kop-stuit lengte (CRL) in de analyse van groeiachterstand in het geval van eerste trimester structurele congenitale afwijkingen

(**hoofdstuk 3.2**). EV metingen kunnen daarom gebruikt worden ten behoeve van het vroeger en nauwkeuriger diagnosticeren van abnormale eerste trimester groei. In **hoofdstuk 3.2** werd de waarde van EV metingen geanalyseerd in zwangerschappen die uiteindelijk eindigden in een miskraam. In vergelijking tot het meten van de standaard CRL had het meten van EV in deze categorie abnormale ontwikkeling geen toegevoegde waarde. Er lijkt derhalve een verschil in groeipatroon te bestaan tussen miskraam zwangerschappen en zwangerschappen met een aangeboren afwijking.

Hoofdstuk 4 beschrijft zowel niet-standaard biometrische *in vivo* metingen als volume metingen in eerste trimester aneuploïde zwangerschappen. In **hoofdstuk 4.1** zijn unieke eerste trimester groeicurves, gerelateerd aan zowel de zwangerschapsduur als aan de CRL, voor de ontwikkeling van de hand opgesteld. Verschillende parameters die de groei van de hand reflecteren zijn gemeten: de breedte van de pols, de breedte van de hand en de lengte van de hand. De diepte perceptie in de I-Space maakte het mogelijk om deze structuren te meten. De nieuw ontwikkelde groeicurves werden gebruikt om de groei van de hand in aneuploïde zwangerschappen te analyseren. Er werd aangetoond dat de groei van de hand al in het eerste trimester van de zwangerschap significant anders is in casussen met trisomie 21 (syndroom van Down) en trisomie 18 (syndroom van Edwards). In **hoofdstuk 4.2** wordt aangetoond dat ook in het geval van aneuploïde zwangerschappen het EV een betere indicator van groeirestrictie is ten opzichte van de conventionele CRL meting. Alleen in casussen met trisomie 18 wordt een kleinere CRL dan verwacht gezien, terwijl in trisomie 21, trisomie 18 en in trisomie 13 het EV significant kleiner is dan op basis van de zwangerschapsduur zou worden verwacht.

In **hoofdstuk 5** word het gebruik van VR in het diagnosticeren van eerste trimester structurele congenitale afwijkingen geëvalueerd. In **hoofdstuk 5.1** wordt VR toegepast in het diagnosticeren van Siamese tweelingen. In deze review worden alle afbeeldingstechnieken die gebruikt worden in de diagnostiek van Siamese tweelingen besproken. De review word geïllustreerd aan de hand van een drietal casus die werden gediagnosticeerd met 2D en 3D echografie en aanvullend onderzoek met VR. Aangezien VR in alle drie de casussen een bijdrage leverde aan de diagnose, kan VR bijdragen aan een eerdere en accurate diagnose van deze zeldzame gevallen.

In **hoofdstuk 5.2** wordt gerapporteerd over de vroegst beschreven diagnose van het 'trombocytopenie met afwezige radius' (TAR) syndroom welke gefaciliteerd werd door VR. Wij zijn van mening dat VR een essentiële bijdrage kan leveren bij de evaluatie van complexe anatomische structuren

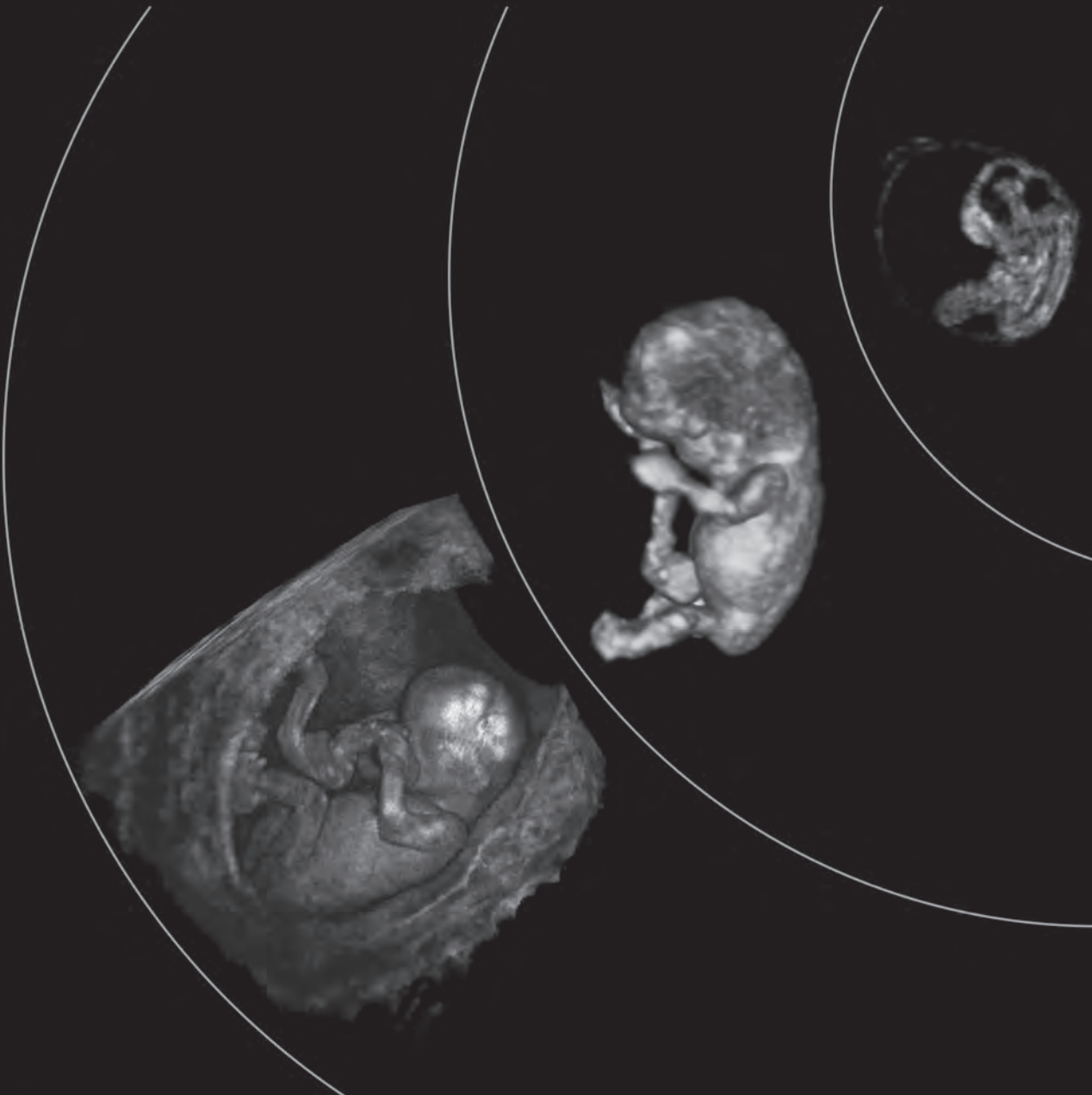
In **hoofdstuk 5.3** werd gedemonstreerd dat het mogelijk is om verschillende typen craniale neuraalbuisdefecten te diagnosticeren *in-vivo* met behulp van driedimensionale echografie. De derde dimensie hielp in het relateren van de casussen aan eerder gepubliceerde *ex vivo* documentatie over craniale neuraalbuisdefecten. De diverse typen craniale neuraalbuisdefecten verschillen in hun prognose. Het onderscheiden van de verschillende typen is van bijzonder belang in het leren begrijpen van de etiologie en het ontwikkelen van preventie strategieën.

In **hoofdstuk 6**, de discussie, worden de resultaten van alle studies bediscussieerd en in een breder perspectief geplaatst. De I-Space VR techniek zorgt voor werkelijke diepteperceptie en biedt de mogelijkheid om de vroege zwangerschap op een intuïtieve manier in detail te bestuderen. Structuren die

niet geanalyseerd of gemeten konden worden met behulp van 2D echografie werden in dit proefschrift bestudeerd door middel van VR. Concluderend kan gezegd worden dat groei in het eerste trimester van de zwangerschap geassocieerd is met zwangerschap uitkomst. De nieuwe VR applicaties en de nieuwe biometrische en volume metingen bieden de mogelijkheid tot vroegere en meer accurate diagnose van abnormale embryonale groei en ontwikkeling. Aangezien ontwikkelingsproblemen vroeg in de zwangerschap grote gevolgen kunnen hebben voor de zwangerschapsuitkomst, moet de embryonale periode zeer precies worden gevolgd. De diagnostiek van aangeboren afwijkingen en het detecteren van markers die geassocieerd zijn met abnormale embryonale ontwikkeling zullen leiden tot een beter begrip van embryonale gezondheid en tot aanpassingen in het obstetrische beleid.

CHAPTER 8

Addendum



Authors and Affiliations

B. Benoit	Department of Obstetrics and Gynecology, Princess Grace Hospital, Monaco
E. Birnie	Department of Biostatistics, Erasmus MC, University Medical Center Rotterdam, The Netherlands. Institute of Health Policy and Management, Erasmus University Rotterdam, The Netherlands
G.J. Bonsel	Department of Obstetrics and Gynaecology, Erasmus MC, University Medical Center Rotterdam, The Netherlands.
J.M.J. Cornette	Department of Obstetrics and Gynaecology, Erasmus MC, University Medical Center Rotterdam, The Netherlands.
A.J. Eggink	Department of Obstetrics and Gynaecology, Erasmus MC, University Medical Center Rotterdam, The Netherlands.
N. Exalto	Department of Obstetrics and Gynaecology, Erasmus MC, University Medical Center Rotterdam, The Netherlands.
I.A.L. Groenenberg	Department of Obstetrics and Gynaecology, Erasmus MC, University Medical Center Rotterdam, The Netherlands.
I.M.A. van Gruting	Department of Obstetrics and Gynaecology, Erasmus MC, University Medical Center Rotterdam, The Netherlands.
P.N.A.C.M. van Heesch	Department of Obstetrics and Gynaecology, Erasmus MC, University Medical Center Rotterdam, The Netherlands.
A.J.M. Hoogeboom	Department of Clinical Genetics, Erasmus MC, University Medical Center Rotterdam, The Netherlands
M. Husen-Ebbinge	Department of Obstetrics and Gynaecology, Erasmus MC, University Medical Center Rotterdam, The Netherlands.
E.J.O. Kompanje	Department of Intensive Care, Erasmus MC, University Medical Center Rotterdam, The Netherlands Natural History Museum Rotterdam, The Netherlands. Curator collection Human and Non-Human Dysmorphology
A.H.J. Koning	Department of Bioinformatics, Erasmus MC, University Medical Center Rotterdam, The Netherlands.
M. Rousian	Department of Obstetrics and Gynaecology, Erasmus MC, University Medical Center Rotterdam, The Netherlands.
E.M.S. Schoonderwaldt	Department of Obstetrics and Gynaecology, Erasmus MC, University Medical Center Rotterdam, The Netherlands.
P.J. van der Spek	Department of Bioinformatics, Erasmus MC, University Medical Center Rotterdam, The Netherlands.

E.A.P. Steegers	Department of Obstetrics and Gynaecology, Erasmus MC, University Medical Center Rotterdam, The Netherlands.
R.P.M. Steegers-Theunissen	Department of Obstetrics and Gynaecology, Erasmus MC, University Medical Center Rotterdam, The Netherlands.
A.K.K. Teunissen	Department of Obstetrics and Gynaecology, Leiden University Medical Center, Leiden, The Netherlands.
H.I.J. Wildschut	Department of Obstetrics and Gynaecology, Erasmus MC, University Medical Center Rotterdam, The Netherlands.
S.P. Willemsen	Department of Biostatistics, Erasmus MC, University Medical Center Rotterdam, The Netherlands.

List of Abbreviations

2D	two-dimensional
2D/3D US	two- and three-dimensional ultrasound
3D	three-dimensional
3D VR US	three-dimensional virtual reality ultrasound
4D	four-dimensional
6DOF	six degrees-of-freedom
CI	confidence interval
CNS	central nervous system
COTS	commercially-of-the-shelf
CRL	crown-rump length
CT	computed tomography
EEC syndrome	electrodactyly ectodermal dysplasia-cleft syndrome
EV	embryonic volume
GA	gestational age
ICC	intraclass correlation coefficient
ICSI	intra-cytoplasmic sperm injection
IVF	<i>in vitro</i> fertilization
LMP	last menstrual period
LoA	limits of agreement
LR-	negative likelihood ratio
LR+	positive likelihood ratio
MRI	magnetic resonance imaging
<i>n</i>	number
NT	nuchal translucency
NTD	neural tube defect
<i>p</i>	<i>p</i> -value
SD	standard deviation
Sens.	sensitivity
Spec.	specificity
TAR syndrome	thrombocytopenia absent radius
TOP	termination of pregnancy
US	ultrasound
USD	United States dollar
VE	virtual embryoscopy
VR	virtual reality

PhD Portfolio

Name PhD student:	Leonie Baken	PhD period:	2011-2014
Erasmus MC Department:	Department of Obstetrics and Gynaecology, subdivision of Prenatal Medicine	Promotors:	Prof.dr. E.A.P. Steegers and Prof.dr. P.J. van der Spek
Research School:	NIHES	Supervisors:	Dr. N. Exalto and Dr. A.J.H. Koning

	Year	Workload (ECTS)
1. PhD training		
General courses		
Systematic literature retrieval & Endnote	2013	2
Biomedical English Writing and Communication	2013	4
BROK ('Basiscursus Regelgeving Klinisch Onderzoek')	2013	1
In-depth courses		
Master of Science in Health Sciences, Netherlands Institute of Health Sciences, Rotterdam, The Netherlands (NIHES)	2010-2012	60
Presentations at national and international conferences		
Symposium Jonge zwangerschap, Spaarne Ziekenhuis, Hoofddorp, The Netherlands <i>Oral presentation</i>	2011	1
International Society of Ultrasound in Obstetrics and Gynecology (ISUOG) congress, Los Angeles, United States. <i>Oral poster</i>	2011	1
Wim Schellekens symposium, Westeinde Ziekenhuis, Den Haag, The Netherlands <i>Oral presentation</i>	2012	1
International Society of Ultrasound in Obstetrics and Gynecology (ISUOG) congress, Copenhagen, Denmark. <i>Oral poster and poster presentation</i>	2012	1
Symposium Jonge Zwangerschap, Erasmus MC, Rotterdam, The Netherlands <i>Oral presentation</i>	2013	1
Wladimiroff award, Erasmus MC, Rotterdam, The Netherlands <i>Oral presentation</i>	2013	1
International Society of Ultrasound in Obstetrics and Gynecology (ISUOG) congress, Sydney, Australia. <i>Oral poster</i>	2013	1
Conference of Association of Early Pregnancy Units, Leeds, United Kingdom <i>Oral communication</i>	2013	1
Seminars and workshops		
Attending weekly and quarterly research meetings of the Department of Obstetrics and Gynaecology, including two oral presentations	2010-2013	5
EUR PhD day	2013	0.2
Erasmus MC PhD day	2013	0.2
AAV wetenschapsmiddag	2013	0.2

	Year	Workload (ECTS)
2. Teaching		
Supervising practicals		
Course 'Embryologie en Praktische Gynaecologische Chirurgie'	2013	0.5
Supervising students		
Sanne Buijs, Psychology student, Leiden University	2012	1
Isabelle van Gruting, ANIOS Spaarne ziekenhuis	2012-2013	1
Other teaching activities		
'IMC Weekendschool, Kindergeneeskunde dag', Erasmus MC, Rotterdam, The Netherlands (2011-2013)	2011- 2013	1
Open day department of Obstetrics and Gynaecology	2012	0.5

Word of Thanks / Dankwoord

Dat ik hier vandaag mag staan was niet gelukt zonder de steun, motivatie en het enthousiasme van velen. Ik stapte als jonge, onervaren student in het onderzoekswereldje en beëindig deze periode vandaag met een grote dosis aan persoonlijke en wetenschappelijke wijsheid rijker. Ik ben blij en dankbaar dat ik deze stap heb kunnen nemen. Mijn dank gaat uit naar al die mensen die op welke manier dan ook hebben bijgedragen aan het tot stand komen van dit proefschrift. Een aantal van hen wil ik hier in het bijzonder vermelden.

Ik wil beginnen de mensen te noemen die in directe zin hebben bijgedragen aan het tot stand komen van dit proefschrift. In het bijzonder mijn promotoren professor Steegers en professor van der Spek.

Beste professor Steegers, beste Eric, als jonge studente ontving u mij om eens te praten over de mogelijkheden voor mijn master-onderzoek. Ik was aangenaam verrast dat u aan mij de keuze liet in welk van de voorgestelde projecten ik zou willen participeren. Het onderzoek naar de jonge zwangerschap met behulp van Virtual Reality fascineerde mij direct en ik ben vol enthousiasme aan de slag gegaan. Ik wil u bedanken voor het vertrouwen dat u vervolgens in mij stelde door mij te vragen om na mijn master-onderzoek verder te gaan met een promotie-traject.

Beste professor van der Spek, beste Peter, allereerst hartelijk dank voor alle mogelijkheden en ondersteuning die de afdeling Bioinformatica geboden heeft in het draaiend houden van dit onderzoek. Ook al spraken we elkaar niet zo frequent, het andere perspectief dat u mij liet zien vond ik inspirerend. U zag altijd wel bruggetjes tussen de beide afdelingen en hun projecten.

Beste Dr. Exalto, beste Niek, ik ben dankbaar dat u mijn co-promotor bent geweest. Uw positivisme en ervaring maakte dat we de revisies steeds weer inkopte. Aan elk commentaar van de reviewers wist u een positieve draai te geven. Het komt altijd goed, dat heb ik inmiddels wel geleerd! Uw stroom aan nieuwe ideeën maakt dat er nog vele promovendi na mij aan dit project kunnen doorwerken.

Beste Dr. Koning, beste Anton, hartelijk dank voor het zijn van mijn redder in nood in geval van technische problemen met de I-Space, een enkele keer zelfs in het weekend, waardoor mijn planning in de soep dreigde te lopen. Ook veel dank voor de snelle commentaren op mijn manuscripten. De nauwkeurige correcties hebben ervoor gezorgd dat mijn Engels een stuk verbeterd is!

Graag wil ik in dit nawoord ook professor Tibboel, professor Hofstra en professor Oepkes bedanken voor de snelle beoordeling van het proefschrift. Tezamen met de overige commissieleden, professor Bilardo, professor Reiss en Dr. Kompanje, wil ik u allen bedanken voor het plaatsnemen in de oppositie.

Alle deelnemers aan de Predict studie wil ik hartelijk danken voor het gestelde vertrouwen ten tijde van de spannende en kwetsbare periode die de vroege zwangerschap is. Zonder hen was dit onderzoek niet mogelijk geweest.

Collega's van de 'prenatale', dank voor het geduld tijdens het leren echoën, de mogelijkheid om mee te draaien in de kliniek in de vorm van het intake spreekuur, de deelname aan de 'vergelijkingsstudie' en de gezelligheid in de kantoortuin en tijdens congressen.

Natuurlijk wil ik alle (oud)-collega-promovendi van de afdeling Verloskunde & Gynaecologie bedanken voor het getoonde interesse en de gezelligheid in vorm van de kopjes koffie na de wetenschapsbespreking, de lunches op woensdag en de etentjes. Veel succes met jullie carrières!

Wat is een promotie zonder paranimfen? Lieve Vera, lieve Jenny, bedankt dat jullie vandaag naast mij willen staan. Vera, sinds de middelbare school vormen wij, samen met Iris en Quirine, een hecht vriendinnenclubje. Er gaan liters thee doorheen, maar we raken nooit uitgepraat. Ook al zijn we allemaal druk, jij nu met jouw promotietraject, laten we de regelmatige dates er in houden! Jenny, we kwamen elkaar op dag één van de studie tegen. Daarna is er geen college geweest dat we niet op dezelfde rij zaten (te kletsen). Inmiddels ben je een heuse dokter, super gedaan! Over niet al te lange tijd zijn we niet alleen vriendinnen, maar ook collega's! Meiden, ik hoop bij de bijzondere momenten die de toekomst voor jullie heeft weggelegd naast jullie te staan.

Lieve pap en mam, jullie hebben ons altijd laten weten dat als je iets echt wilt, je je door niets moet laten tegenhouden. Dit, samen met jullie onvoorwaardelijke geloof ik mijn kunnen, heeft mij vaak die laatste stap over de drempel doen nemen. Ik ben oneindig dankbaar voor jullie liefde, steun, goede raad en bovenal de vrijheid die jullie ons altijd hebben gelaten in onze keuzes. Pap, het wordt nu wel oppassen geblazen met die titels... ;-)

Lieve Arjan, grote kleine broer, ook al zijn we broer en zus, we zijn twee heel verschillende persoonlijkheden. Een studiebol als zus is misschien niet altijd even makkelijk. Studeren was niet je grootste hobby, maar je hebt de volle 100% genoten van het studentenleven! Ik ben trots dat je dit jaar je diploma Commerciële Economie hebt behaald. Ik bewonder je om je humor en je harde werken. Maak er wat moois van in dit leven!

Lieve Michael, het lijkt onmogelijk jou in een paar regels te laten weten hoe belangrijk jij bent geweest in het tot stand komen van dit proefschrift. Jij hebt als geen ander ervaren dat een promotie gepaard gaat met 'ups' en 'downs'. Lange gesprekken in het donker maakte dat ik de volgende dag met goede moed weer aan de slag ging. Bedankt dat je er altijd voor me bent en dat we alles tegen elkaar kunnen zeggen. Weet dat ik ook altijd naast jou sta! Ik kan niet wachten de rest van mijn leven met jou te delen.

About the Author



Leonie Baken was born on a sunny day in Delft, the 13th of October, 1988. She passed secondary school at the Alberdingk Thijm College in Hilversum and graduated with high grades only 17 years old. For years she had the ambition to study medicine at university, but unfortunately she was 'uitgeloot'. For this reason she studied Biology for one year at Utrecht University and managed to acquire a propedeuse diploma. In September 2007 she could finally start her medical study at Erasmus University in Rotterdam.

During the second year of her study she was invited to participate in an honours program for excellent medical students, offered by the Netherlands Institute of Health Sciences (NIHES). She passed for her doctoraal in Medicine and acquired a Master of Science in Health Science within five years. She decided to first continue her path in scientific research and in 2012 she started her PhD project at the department of Obstetrics and Gynaecology and the department of Bioinformatics at the Erasmus MC University Medical Center Rotterdam under the supervision of Prof.dr. Steegers and Prof.dr. van der Spek. In this period she presented results of her research at several international symposia, amongst others at the International Society of Ultrasound in Obstetrics and Gynecology (ISUOG) World Congress 2013 in Sydney. In march 2014 she resumed her studies and started her medical internships. She is expected to obtain her medical degree in 2016.

John Baken